2024

Developing a PBPK model for intranasal naloxone and opioid displacement from brain receptors

Jasmin Akther Hossain

DEVELOPING A PBPK MODEL FOR INTRANASAL NALOXONE AND OPIOID DISPLACEMENT FROM BRAIN RECEPTORS

A DISSERTATION SUBMITTED IN PARTIAL FULFILLMENT OF THE REQUIREMENTS FOR THE DEGREE OF

DOCTOR OF PHILOSOPHY IN PHARMACEUTICAL SCIENCES WITH SPECIALIZATION IN PHARMACEUTICS

LONG ISLAND UNIVERSITY, BROOKLYN, NEW YORK

MAY 16, 2024

BY

JASMIN AKTHER HOSSAIN

SPONSORING COMMITTEE

David R. Taft, Ph.D. (Committee Chair)

Robert A. Bellantone, Ph.D. (Committee member)

Kevin R. Sweeney, Ph.D. (Committee member)

Akm Khairuzzaman, Ph.D. (Committee member)

Joseph J. Bova (Vice Dean, Academic Affairs)

ABSTRACT

The therapeutic and nontherapeutic use of potent opioid agonists has increased dramatically over the past 20 years, with overdose trends following suit. Currently, naloxone is the primary drug used for treating emergency rescue from an opioid overdose. Naloxone works by displacing opioid agonists that are bound to receptors such as the μ-opioid receptor (MOR) in the brain, which are thought to be the sites of action responsible for symptoms due to overdosing, such as respiratory depression.

Intranasal (IN) administration of naloxone is an excellent alternative to the invasiveness of injections and poorly bioavailable oral formulation. However, the exact mechanism of how the drug enters the brain and how it produces its pharmacological response is not well-studied. While pharmacokinetic (PK) and pharmacodynamic (PD) data are available regarding the efficacy of naloxone in the reversal of prescription opioid overdose, their detailed mechanism in humans is not quantitatively fully understood. Also, there is very little research on IN naloxone PK and its application to the reversal of illicit high-potency synthetic opioids.

Taking advantage of drug transport to the brain by the IN route of administration requires a quantitative understanding of the general mechanisms and underlying processes for drug delivery to the brain. Modeling and studying IN naloxone administration can play an important role in future research by identifying appropriate dosing regimens for reversing different opioids and understanding the time course of respiratory depression recovery, as

well as overcoming other side effects of opioids. It can also help to refine dosage regimens for special populations such as children and babies.

This project aims to build a physiologically based pharmacokinetic (PBPK) model describing naloxone disposition by IN and IV (intravenous) administration and evaluate the effects on displacement of opioid agonists. The goals were:

- Evaluate the physiological factors affecting naloxone deposition from IV bolus (intravenous) and IN administration, and review and analyze published literature data for relevant pharmacokinetic information.
- Develop a PBPK model for IV and IN naloxone delivery and disposition and numerically evaluate the systems of equations using the R programming language. The model included: 1) all relevant physiological compartments and processes; 2) pH, solubility, and partitioning considerations for naloxone (a weak base); and 3) interactions with MORs, including the rates and extents of binding and release.
- Extend the naloxone PBPK model to simultaneously account for the disposition and displacement kinetics of an opioid agonist that is initially bound to the MORs, which would model naloxone rescue from an opioid overdose.
- Simulate the effects of naloxone administration and deposition on the ensuing opioid agonist displacement and the resulting time course of pharmacological response vs. the agonist displacement time profile.
- Simulate results for a target patient population using physiologically relevant parameter values.

DEDICATION

Bismillahir Rahmanur Raheem

This dissertation is dedicated to my family, my advisors, my friends, and all my well-wishers.

My work is dedicated to my late father, Mohammad Hossain, and my mother, who have given me unconditional love and trust throughout my life. My father always supported me in gaining knowledge and dreamt of me reaching high; I have done it, Abbu! I know how happy you would be for me. I miss you so much!

I must dedicate my work to my loving husband, Mohammed Billah, for supporting me in all my decisions. He has been a strong pillar in helping me mentally and financially throughout my graduate studies and every aspect of my life. I am indeed fortunate to have him as my life partner.

I also dedicate it to my father-in-law and mother-in-law for their encouragement and extraordinary support in completing my studies. They have always prayed for my success and helped me in all circumstances.

I must mention my little charming kids Meher and Mishraq for the innocent words, bearing with their mom not being able to spend time with them, and pure love to see their mom succeed!

This project is also dedicated to my dearest Professor, Dr. Bellantone, for his exciting ideas, constant advice, teaching new essential things, supervising this work, and motivating discussions, and to Dr. Taft for advising me and believing in me to keep up with my studies. Their support and step-by-step guidance made it possible for me to complete this work successfully.

Finally, I dedicate this to all my family members, especially Shamsul, Asfara, Tahora, Morshed and all my dearest friends, for all their love, overwhelming support, and well wishes for me.

ACKNOWLEDGEMENTS

First and foremost, praises and thanks to the Almighty Allah for His showers of blessings throughout my research work and for enabling me to complete the project successfully.

My days at Long Island University as a graduate student have been wonderful, and working on this project has been an incredible journey. Many people have provided me with priceless support, encouragement, and motivation.

Words cannot express my gratitude to my Professor and committee chair, Dr. David Taft, for his invaluable patience and advice throughout my Ph.D. study. He is an excellent professor who made teaching and learning enjoyable. He has always shared positive opinions even when things were not working for me. He sparked my interest in PK/PD studies and modeling.

I would like to express my deepest appreciation to my co-supervisor, Dr. Robert Bellantone, for being my project leader and guidance throughout this research. His dynamism, vision, sincerity, and motivation have deeply encouraged me. He has taught me the methodology to carry out the research and to present the work as clearly as possible. His ideas, wisdom and experience were instrumental in shaping this work. I would like to thank him for his compassion and good humor, which made our conversations enjoyable, as well as his invaluable assistance in completing this work within a challenging deadline.

I am also extremely grateful to my committee members, Dr. Kevin R. Sweeney and Dr. AKM Khairuzzaman, for their encouragement, insightful comments, valuable advice, and feedback to improve my research work.

I would like to extend my sincere thanks to Dr. Rutesh H. Dave and Dr. Jane Shtaynberg for providing me with a graduate assistantship, which has been a great financial support during my Ph.D. Also, I sincerely thank all my teachers, friends, and faculty members of the Pharmaceutical Science department for their unwavering support and guidance during my academic journey.

A special thanks to all my family. I cannot describe how grateful I am to my father-in-law, mother-in-law, my mother, brother, brothers-in-law and my sisters-in-law for their immeasurable support and well wishes for me. Your sacrifices and prayers for me were what sustained me thus far. I am also grateful to my caring, loving, and supportive husband, Billah, for trusting my choice to pursue the Ph.D. degree and my cheering kids, Meher and Mishraq. Their love and trust have kept my spirits and motivation high during this process and carried me through all the difficulties in my limited but wonderful life experience.

Finally, I thank all my friends and well-wishers who always encouraged me to keep up with my work.

TABLE OF CONTENTS

ABSTRACT i

DEDICATION iii

ACKNOWLEDGEMENTS v

LIST OF FIGURES x

LIST OF TABLES xii

CHAPTER 1.INTRODUCTION 1

CHAPTER 2.BACKGROUND AND LITERATURE SURVEY 5

2.1. Naloxone and fentanyl 5

2.1.1. Naloxone 5

2.1.2. Fentanyl 8

2.2. Nose-to-brain drug delivery 12

2.3. Nasal anatomy and physiology 15

2.4. Brain physiology and anatomy 16

2.5. Nasal Absorption 17

2.6. PBPK modeling 18

2.7. Literature survey 19

2.7.1. Naloxone PKPD 19

2.7.2. Fentanyl PKPD 21

2.7.3. Nose-to-brain drug delivery 24

2.7.4. Binding and displacement kinetics at the MOR 26

2.7.5. Where the literature leaves off 27

CHAPTER 3.OBJECTIVES OF THIS RESEARCH 28

3.1. Statement of the problem 28

3.2. Specific aims 29

3.3. Justification and significance 33

CHAPTER 4.MODELING AND SIMULATION METHODS 35
4.1. Introduction to modeling and its general purpose 35
4.2. Steps in constructing the model.....36
4.3. Writing the equations 38
4.3.1. Transport representation versus PK representation..... 38
4.3.2 Equations for binding and release kinetics at the MORs 42
4.3.3. Mass balance considerations 45
4.3.4. Modeling the clinical response..... 46
4.3.5. Include physicochemical and physiological parameters 47
4.4. Using R as a numerical platform for solving the differential equation 47
4.4.1. General approach..... 47
4.4.2. Verification of the R Code 49
CHAPTER 5.ESTIMATING PHYSIOLOGICAL PARAMETER VALUES..... 50
5.1. Approach to obtain "typical" physiological parameter values 51
5.2. 2-compartment model for naloxone IV and IN and fentanyl IV 53
5.4 3-compartment model with binding in the brain at MORs..... 61
5.4.1. MOR expression in the brain..... 64
5.4.2. Naloxone parameters associated with the brain compartment 66
5.4.3. Ventilation suppression by fentanyl 68
CHAPTER 6.THE NALOXONE RESCUE MODEL..... 72
6.1. Combining the individual models to construct the naloxone rescue model.....72
6.2. Verification of the rescue model 78
6.3. Simulations using the naloxone rescue model.....80
CHAPTER 7.PATIENT POPULATION SIMULATIONS 84
7.1. Generating a hypothetical patient population.....84
7.2. Initial simulation of fentanyl 500 μg IV and naloxone 4 mg after 5 minutes 90
7.3. Rescue simulations for other fentanyl doses and naloxone rescue regimens 101
7.3.1. Simulations for IV fentanyl 500μg and 1000μg IV, no naloxone..... 102

7.3.2. Simulation for 300μg IV fentanyl overdose and one dose of 4 mg IN naloxone given after 5 minutes..... 104
7.3.3. Simulations for 500μg IV fentanyl overdose and multiple IN doses of naloxone 4 mg 105
7.3.4. Simulations for 1000μg IV fentanyl and multiple 4 mg IN doses. 106
7.3.5. Simulations for 2000μg and 4000 μg IV fentanyl and naloxone 4mg at 5, 8 and 11 minutes..... 109
7.3.6. Simulations for 1000μg IV fentanyl and naloxone 8 mg at 5 and 8 minutes... 111
7.4. Parameter sensitivity analyses on the population simulations 112
CHAPTER 8.DISCUSSION AND SUMMARY 116
REFERENCES 119
APPENDIX 1. Notation and Glossary of Terms 127
APPENDIX 2. R-code for fentanyl and naloxone model 130
RESUME 137

LIST OF FIGURES

Figure 2-1. Flowchart for nose-to-brain delivery. 13
Figure 2-2. Diagram of the nasal structure. 15
Figure 4-1. 2-compartment model in the PK representation..... 39
Figure 5-1. 2-compartment model for IV naloxone and fentanyl and IN naloxone. 55
Figure 5-2. Naloxone plasma profiles following IV, IM, and IN administration. 56
Figure 5-3. Naloxone plasma profiles following IV, IM, and IN administration. 57
Figure 5-4. Naloxone plasma data and the fit for 2 mg IV. 58
Figure 5-5. IN naloxone plasma data and the fit profile for 2 mg IN. 59
Figure 5-6. Fentanyl plasma profiles following 0.5 mg IV administration. 60
Figure 5-7. Fentanyl digitized plasma data and the fit for 0.5 mg IV. 61
Figure 5-8. 3-compartment model with MOR binding in the brain. 62
Figure 5-9. Digitized MOR fraction occupied by naloxone and the fit for 2 mg IN... 67
Figure 5-10. Ventilation vs. time after fentanyl 0.3mg/70kg IV. 68
Figure 5-11. Digitized data and fits for ventilation suppression vs. the MOR occupancy by fentanyl. 70
Figure 6-1. IN naloxone and IV fentanyl model with MOR binding and release 72
Figure 6-2. Hypothetical naloxone administered at 5, 8 and 11 minutes using the UIF function. 76
Figure 6-3. UIF function for three naloxone doses..... 77
Figure 6-4. Concentration-time plot for IV 500μg fentanyl and no naloxone. 79
Figure 6-5. Concentration-time plot for 2000 μg naloxone IN and no fentanyl. 79
Figure 6-6. Fentanyl 500 μg IV and no naloxone IN dose at 5 minutes. 81
Figure 6-7. Fentanyl IV 500 μg followed by 4 mg naloxone IN at 5 minutes. 82
Figure 6-8. Fentanyl 500 μg IV followed by naloxone 8mg IN at 5 minutes. 83
Figure 7-1. Fentanyl mass in the central and peripheral compartments. 91

Figure 7-2. Fentanyl free and bound mass in the brain. 92
Figure 7-3. Fentanyl mass concentrations in the central and peripheral compartments. 93
Figure 7-4. Fentanyl free and bound molar concentrations in the brain. 94
Figure 7-5. Naloxone mass in the central and peripheral compartments. 95
Figure 7-6. Naloxone free and bound mass in the brain. 96
Figure 7-7. Naloxone mass concentration in the central and peripheral compartments. 97
Figure 7-8. Naloxone free and bound mass in the brain. 98
Figure 7-9. Percent of full ventilation when IN naloxone is given at 5 minutes. 100
Figure 7-10. Ventilation after 500 IV fentanyl and no naloxone rescue. 102
Figure 7-11. Ventilation after 1000µg IV fentanyl and no naloxone rescue. 103
Figure 7-12. Ventilation after 300µg IV fentanyl and single naloxone 4mg IN dose after 5 minutes 104
Figure 7-13. Ventilation after 500µg IV fentanyl and naloxone 4mg at 5 and 8 minutes. 105
Figure 7-14. Ventilation after 500 µg IV fentanyl and naloxone 4mg at 5, 8 and 11 minutes. 106
Figure 7-15. Ventilation after 1000 µg IV fentanyl and naloxone 4mg at 5 minutes. 107
Figure 7-16. Ventilation after 1000 µg IV fentanyl and naloxone 4mg at 5 and 8 minutes. 107
Figure 7-17. Ventilation after 1000 µg IV fentanyl and naloxone 4mg at 5, 8 and 11 minutes. 108
Figure 7-18. Ventilation after 2000 µg IV fentanyl and naloxone 4mg at 5, 8 and 11 minutes. 109
Figure 7-19. Ventilation after 4000 µg IV fentanyl and naloxone 4mg at 5, 8 and 11 minutes. 110

Figure 7-20. Ventilation after 1000 µg IV fentanyl and naloxone 8mg at 5 and 8 minutes. 111

LIST OF TABLES

Table 2-1. MOR binding and release rate constants for opioid agonists *in vitro.* 27
Table 5-1. Naloxone IV parameter estimates from fits shown in Figure 5-4. 58
Table 5-2. Additional naloxone IN parameter estimates from Figure 5-5. 60
Table 5-3. Fentanyl IV parameter estimates from fits shown in Figure 5-7. 61
Table 5-4. MOR expression in the brain. 65
Table 5-5. Naloxone parameter estimates from fits shown in Figure 5-9. 67
Table 5-6. F_{sup} vs. time calculated from the data in Figure 5-10. 69
Table 5-7. Parameter estimates from fits shown in Figure 5-11. 71
Table 7-1. Target parameters for the hypothetical patient population. 85
Table 7-2. Average parameters for the population generated from Table 7-1. 87
Table 7-3. Parameter sensitivities for the minimum fraction of full ventilation. 114
Table 7-4. Parameter sensitivities for the rescue times. 115

CHAPTER 1. INTRODUCTION

Opioids are a class of drugs that have anesthetic, analgesic and sedative effects. They interact with the opioid receptors in the brain, spinal cord, and other areas of the body to reduce pain perception. Opioid drugs such as morphine, fentanyl, hydromorphone, oxycodone, etc., are commonly prescribed for severe pain management, while codeine is used to manage coughs and diarrhea. Other opioids, such as methadone and buprenorphine, are used for maintenance treatment of opioid dependence. However, all can cause euphoria, which is one of the main reasons they are taken for recreational use. This leads to tolerance, increasing intake of opioid drugs and addiction. In 2011, an estimated 4 million people in the United States used opioids recreationally or were dependent on them. Opioids have more toxic side effects, such as respiratory depression and difficulty with breathing, and opioid overdose can lead to death. Thus, regular use of opioids can lead to numerous health problems associated with opioid dependence. [1]

According to the World Health Organization (WHO), approximately 125,000 people died from an opioid overdose in 2019. In the United States (USA), the number of people dying from drug overdoses amounted to 70,630 in 2019, and approximately 70.6% of these deaths involved opioids. [2] The number of opioid overdoses has increased in recent years in several countries, in part because of the increased availability of opioids used in the management of chronic pain and because of the increasing use of highly potent opioids appearing on the illicit drug market. [1]

One of the most potent synthetic opioid drugs available on the market is fentanyl. It is prescribed for pain management in cancer patients or those recovering from surgery. However, because of its high potency, the drug is hazardous even in small amounts. It has a high risk of addiction, and potential overdose can cause respiratory depression in minutes and, consequently, death. At present, fentanyl and its analogs are also widely available in the illicit market for recreational use, as well as mixed with other recreational opioids such as heroine for profits by the black market. Fentanyl continues to fuel an epidemic of synthetic opioid drug overdose deaths in the United States. Since 2018, fentanyl and its analogs have been responsible for most drug overdose deaths in the United States, causing over 71,238 deaths in 2021. Fentanyl is now responsible for most of all drug overdose deaths in the United States, surpassing heroin in 2018.[3]

Currently, the most readily available emergency treatment for reversing the negative effects of opioid overdose is naloxone, which is the first opioid antagonist with no agonistic activity. [2] It was approved for opioid use disorder treatment in the United States in 1971. To combat opioid overdose and mortality, naloxone is increasingly used in pre-hospital settings by emergency personnel and prescribed to laypersons for out-of-hospital administration. Initially, naloxone was administered by intravenous (IV) injection, but formulations have recently become available for intranasal (IN) and intramuscular (IM) administration. The US Food and Drug Administration (FDA) approved 2 and 4 mg doses of IN naloxone for the emergency treatment of known or suspected opioid overdose in 2015. Because of its ease of administration, laypersons widely use this form. However, the effectiveness of naloxone, particularly after an opioid

overdose, varies depending on the binding interaction with the opioid, the pharmacokinetics and pharmacological response of the opioids that were overdosed, and the availability of naloxone at the site of opioid receptors. [2,4,5]

Naloxone administration has been found to produce a rescue response rapidly in opioid overdose within a few minutes.[5] The drug's pharmacokinetic properties regarding IV administration are well studied. However, naloxone is now most commonly used by intranasal (IN) administration in the field because of its ease of use. Still, the mechanism of how it causes the physiological effects after administration through the nasal route is not well studied. There is no detailed study on how the drug enters through the nasal route and reaches the brain to bind with opioid receptors (specifically, μ-opioid receptors, or MORs) and the rate and extent of absorption through the nasal cavity. So, this study focuses on this route of naloxone administration and how it produces its effects and rescues a patient from adverse effects due to fentanyl overdose.

This project focused on PBPK modeling of the pharmacokinetics of naloxone and the opioid drug fentanyl by developing a model based on the physiological characteristics and pharmacological response of IN naloxone and fentanyl overdose and modeling naloxone rescue from an overdose situation. The model was then used to simulate fentanyl overdose situations, and rescue by various IN naloxone administration regimens was simulated in a hypothetical patient population. The modeling involved 1) modeling naloxone alone, 2) modeling fentanyl alone, and 3) putting both drugs together to model and simulate naloxone rescue from opioid overdose.

The PBPK model captures the processes involved in drug pharmacokinetics and pharmacodynamics, describes each step mathematically and helps to understand the process involved and the factors affecting the process. It also quantitively makes predictions, evaluates the system of equations, and explores the outcomes. In addition, by performing simulations with ranges of parameters and comparing the results with literature data, the PBPK model and parameter values are adjusted if necessary.

The PBPK model improves understanding of naloxone and fentanyl disposition and binding and displacement kinetics with MORs. The model and its numerical implementation in the R programming language provided a platform to explain the pharmacokinetics of naloxone rescue from fentanyl overdose based on interactions with the MORs.

CHAPTER 2. BACKGROUND AND LITERATURE SURVEY

This project aims to examine the pharmacokinetics of naloxone and develop a model based on the physical characteristics and pharmacological response of IN naloxone with relevant opioid agonists. It also aims to characterize the pharmacokinetics of the opioid agonist fentanyl and its pharmacodynamics resulting from binding to μ-opioid receptors (MORs) in the brain, specifically regarding respiratory depression as the pharmacological marker. Finally, it aims to model the interaction of naloxone and fentanyl at the MORs to quantitatively predict the time course of naloxone rescue from fentanyl overdose situations.

2.1. Naloxone and fentanyl

2.1.1. Naloxone

Naloxone is an opiate antagonist that is used intravenously in emergencies to reverse the respiratory depression caused by opioid overdoses. It is a nonselective, competitive antagonist that binds with μ-opioid, κ-opioid, and δ-opioid receptors (MORs, KORs, and DORs) in the central nervous system (CNS). It has its greatest affinity for MORs and works by displacing opioid agonists that are bound to these receptors to cause a reversal of adverse effects resulting from an opioid overdose. [6]

Naloxone hydrochloride is approved for administration by a variety of routes, including intravenous (IV), intramuscular (IM), subcutaneous (SQ), and intranasal (IN). It is also administered via inhalation following nebulization or endotracheal tube in intubated

patients. It is available as a nasal spray (Narcan® 4mg, Kloxxado 8mg) or an injection (Zimhi® 5 mg/0.5 mL). The FDA approved Narcan® nasal spray in March 2023 as an over-the-counter (OTC) medicine that is available without a prescription.

Naloxone is administered at doses of 0.4-2 mg IV, IM or SQ, and 4 or 8 mg IN. The dose is repeated until the desired response is reached. Overall, naloxone is safe and is not known to cause harm when administered in typical doses to opioid-naïve patients. Despite the long-standing use of naloxone to reverse the symptoms of opioid overdose or toxicity, proper dosing remains controversial, with various regimens recommended in the literature. [4,7]

Naloxone is a competitive antagonist at opioid receptors, with the highest binding affinity for the μ-opioid receptor (MOR), followed by the δ-opioid receptor (DOR) and the κ-opioid receptor (KOR). Naloxone has negligible affinity for the nociception receptor. These receptors are widely distributed in the central nervous system, and their activation, which occurs when occupied by an opioid agonist, triggers many of the analgesic and respiratory depression effects associated with opioid agonist drugs. By binding to these receptors, naloxone effectively displaces opioid agonists from the receptors and blocks their ability to activate the receptors. As a result, naloxone rapidly reverses the opioid-induced effects. If naloxone is administered in the absence of concomitant opioid use, no functional pharmacological activity occurs, except the inability of the body to combat pain naturally. [5]

When administered parenterally, naloxone is rapidly distributed throughout the body, and its onset of action is 1-2 minutes. The mean half-life ranges from ~30-81 minutes and varies with the dose and route of administration, which is shorter than the half-lives of some opioid agonists, such as morphine (half-life of 1.5-2 hours) and fentanyl (half-life of 90 minutes). [8] Thus, repeat dosing of naloxone may be needed if the opioid receptors must be stopped from triggering for an extended period.

Naloxone is primarily metabolized by the liver and exhibits low systemic bioavailability when taken by mouth because of hepatic first-pass metabolism. Its major metabolite is naloxone-3-glucuronide, which is excreted in the urine. [9] Intranasal administration of naloxone bypasses hepatic first-pass metabolism and can potentially target brain delivery, bypassing the blood-brain barrier. [10]

The physical properties of naloxone are of considerable potential importance because it is a weak base with a pKa of 7.94 in water, so it is present in both the ionized (water soluble) and unionized (lipid soluble) forms at physiological pH. The molecular weight of naloxone is 327.4 g/mol, and its partition coefficient is log P ~ 2.09. [11] Its unionized form is highly lipophilic, so naloxone can rapidly penetrate the blood-brain barrier and achieve a much greater brain-to-serum ratio than morphine (the reference did not state if that is total or ionized naloxone). [5] Based on its pKa, it is estimated from the Henderson-Hasselbalch equation [12] that naloxone in the plasma is ~20% neutral and 80% ionized, which provides a balance between forms with good solubility in water and the ability to permeate lipid barriers and ionized and neutral forms are assumed to rapidly

inter-convert in response to absorption, distribution or change in pH. This is important because naloxone base (lipophilic) is assumed to be the form that crosses the blood-brain barrier, but commercial products are aqueous-based and at pH well below its pKa, so the naloxone is in its water-soluble form. For instance, the pH of injectable naloxone is 3-4.5, and the pH of the Narcan Nasal Spray is 3.5-5.5. [13,14]

With IV administration, naloxone enters the bloodstream in the ionized form, then partially converts to the neutral form in the plasma before crossing the blood-brain barrier. On the other hand, when administered IN, naloxone may enter both the ionized and neutral forms because IN bypasses the blood-brain barrier. This has formulation implications, making naloxone a good candidate for IN administration because it can be administered with a substantial dose in the formulation and achieves good delivery into the brain.

2.1.2. Fentanyl

Fentanyl is a potent opioid agonist that was synthesized by Dr. Paul Janssen in 1959. It is used as an analgesic and anesthetic drug in the medical setting. Initially, it was approved for medical use in the US by 1968 only as a combination with droperidol because of concerns about its high potency and a greater tendency to produce muscle rigidity in comparison to other opioids. It is 50-100 times more potent than heroin and morphine and showed faster onset and shorter duration of action in animal and human studies. The clinical use of fentanyl was restricted to anesthesia until the 1990s, when non-injectable formulations were developed and available for patient administration. Currently, in

addition to injectable formulations, many fentanyl products are approved for use in the US, including oral transmucosal lozenges and lollipops, effervescent buccal tablets, sublingual tablets and sprays, nasal sprays, and transdermal patches. [15-17]

Fentanyl is used as an anesthetic and analgesic agent in surgical settings and postoperative pain management. It is frequently used in palliative care to manage moderate to severe pain in cancer patients experiencing chronic pain or breakthrough pain. Fentanyl is sometimes used in emergency medicine settings, such as in the management of severe pain and trauma or during rapid sequence intubation (RSI) for sedation and analgesia. Fentanyl may be used in labor analgesia, often administered via patient-controlled analgesia (PCA) systems or epidural infusion to provide pain relief during labor. Fentanyl is sold under numerous brand names, including Sublimaze® (fentanyl citrate injectable for anesthesia and post-operative pain, now discontinued); Actiq® (fentanyl citrate, as an oral lollipop); Fentora® (fentanyl citrate buccal tablet) and Onsolis® (fentanyl citrate buccal film); Duragesic® and Matrifen® (fentanyl base transdermal patches); Instanyl® and Lazanda® (fentanyl citrate nasal spray).[3,18]

Fentanyl poses an exceptionally high overdose risk in humans since the amount required to cause toxicity is unpredictable, and the most dangerous adverse effect of fentanyl is respiratory depression, which can lead to anoxic brain injury or death. In its pharmaceutical form, most overdose deaths attributed solely to fentanyl occur at serum concentrations at a mean of 0.025 µg/mL, with a range of 0.005–0.027 µg/mL. A two mg

dose of fentanyl powder is a lethal amount for most people. In the US, fentanyl and fentanyl analogs have reportedly caused over 29,000 deaths in 2017.[3]

The increase in fentanyl deaths is not necessarily due to prescribed fentanyl but is also related to illicitly made fentanyl that is being mixed with or sold as heroin. The illicit use of pharmaceutical fentanyl and its analogs first appeared in the mid-1970s in the medical community and continues in the present. These analogs may be hundreds of times more potent and can lead to overdose. Recreational use of fentanyl is increasing day by day and is often taken orally, smoked, snorted, or injected. Fentanyl is sometimes sold on the black market in the form of transdermal fentanyl patches (such as Duragesic®) and lollipops (such as Actiq®) that are diverted from legitimate medical supplies. The gel taken from inside transdermal patches is sometimes ingested or injected. [3]

Fentanyl overdose is a medical emergency and requires prompt intervention. Currently, the drug used for fentanyl overdose is naloxone, and it can require multiple doses depending on the degree of overdose.

Fentanyl has a high affinity for MORs and produces its pharmacological effect by activating the receptor. When it binds with MORs, downstream signaling changes the perception of pain, resulting in analgesic effects. Fentanyl has a lower affinity for DORs and KORs, being ~600-2500 times lower than its affinity for MORs. [3]

Fentanyl is a small molecule drug with a molecular weight of 336.47g/mol and is a weak base with a pKa of 8.99. Its neutral form is highly lipophilic (log P ~ 4.1), allowing it to

penetrate the blood-brain barrier easily, bind with the MORs, and produce a rapid onset of action. Fentanyl is also ~85-90% bound to plasma proteins, and this increases with increasing ionization of the drug. [18,19]

IV fentanyl can produce an onset of action within 5-6 minutes. It has a rapid distribution of 1.7 minutes and an elimination half-life of 7 hours. The intravenous volume of distribution is 4L/kg (3-8L/kg). The oral volume of distribution is 25.4 L/kg. The usual duration of action for the analgesic effect is 30-60 minutes after a single IV dose of up to 100 μg. Fentanyl is primarily metabolized in the liver to several inactive metabolites and demonstrates a high first-pass clearance, with 75% of an IV dose excreted in the urine and ~9% of the dose in feces primarily as metabolites. Total plasma clearance of fentanyl can vary for different types of dosages, with 0.5 L/hr/kg (0.3-0.7 L/hr/kg) for transmucosal lozenges or 42 L/hr for buccal tablets. Following an intravenous dose, surgical patients displayed a clearance of 27-75 L/h. [18,19]

Fentanyl is a very potent drug. A dose of 100 μg is approximately equivalent in analgesic activity to 10mg of morphine. Although the principal therapeutic actions are analgesia and sedation, there remains the adverse effect of respiratory depression. Alterations in the respiration rate and alveolar ventilation associated with therapeutic doses may last longer than the analgesic effect. They can increase with an increase in dose, and larger doses can produce apnea. The peak respiratory depressant effect of a single IV dose of fentanyl is observed within 5 to 15 minutes. [19]

When fentanyl overdose occurs, in addition to ventilation support, naloxone is used to rescue respiratory depression. Naloxone can be administered intravenously, intramuscularly, or intranasally. Multiple doses may be required, especially if the individual has ingested large amounts of fentanyl or if other opioids are also present.

The reasons for multiple dosage requirements are not clearly understood. [16] Thus, there is a clear need for clinical studies to assess the effectiveness of naloxone in reversing respiratory depression induced by fentanyl. Studies are desperately needed to elucidate the physiological mechanisms underlying fentanyl overdose and naloxone rescue so that effective treatments can be developed to reduce the risk of death.

2.2. Nose-to-brain drug delivery

Conventionally, the nasal route has been used to deliver drugs to treat local diseases like nasal allergy, sinusitis, nasal infections, and nasal congestion. It has also been utilized for the systemic delivery of small molecular weight polar drugs, peptides, and proteins that are not easily administered via routes other than by injection or where a rapid onset of action is needed. [20] IN administration is an effective route to deliver drugs into the systemic circulation, resulting in rapid onset and higher drug bioavailability than classical administration routes for many drugs. More recently, it has gained attention as a potential delivery route to the brain because of the unique connection between the central nervous system and the olfactory nasal neuroepithelium. [21]

The nasal route is highly suitable for minimally invasive drug delivery for the following reasons. The epithelium of nasal mucosa is highly vascularized and has an impressively

large surface area for rapid drug absorption. It also has lower metabolizing enzyme levels than the gastrointestinal tract and liver, high total blood flow per mL, and direct drug transport to the systemic circulation and the brain, thereby avoiding first-pass hepatic metabolism and enhancing bioavailability. [22] A schematic of nose-to-brain delivery is shown in Figure 2-1.

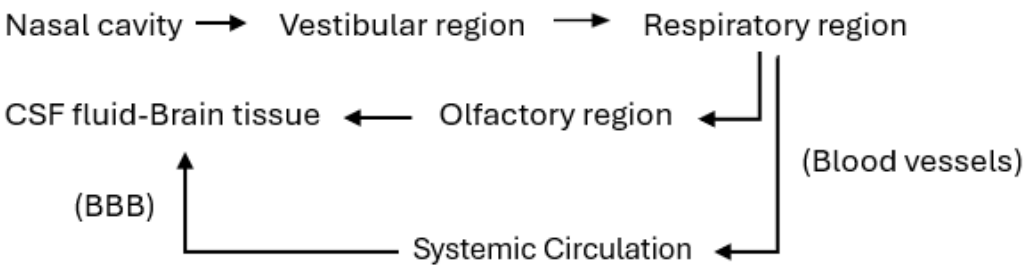

Figure 2-1. Flowchart for nose-to-brain delivery.

Nose-to-brain drug delivery provides important advantages over other routes of administration that can be significant for rescue use in the field. For instance, drugs can enter the brain and cerebrospinal fluid (CSF) more readily than when given IV since they effectively bypass the blood-brain barrier, and the large surface area of the nasal mucosa can also facilitate a rapid onset of therapeutic effect. [23,24] In addition, IN administration is a non-invasive method that is easily administered in emergencies in the field by first responders and self-administered by patients. Also, though perhaps less significant for naloxone, is that IN administration avoids hepatic first-pass metabolism.

While the mechanisms underlying intranasal drug delivery to the CNS are not entirely understood, an accumulating body of evidence suggests that pathways involving nerves connecting the nasal passages to the brain and spinal cord may be important for some, but likely not all, drugs. In addition, pathways involving the vasculature, cerebrospinal fluid, and lymphatic system have been implicated in the transport of molecules from the nasal cavity to the CNS. A combination of these pathways is likely responsible, although one pathway may predominate, depending on the properties of the drug and formulation and the delivery device used. [24] Because 1) IV administration rapidly brings about effective concentrations of naloxone in the brain, and 2) naloxone is fully dissolved in nasal formulations, which are at pH below 6, there is no evidence in the literature to suggest that any absorption pathway other than into the vasculature or cerebral spinal fluid is significant.

When the drug is administered in the nasal cavity, it encounters nasal mucosa that is highly vascularized and supplied with trigeminal nerve endings. The drug is rapidly absorbed into the CSF and systemic circulation, while some fraction enters the olfactory region or is eliminated by mucociliary clearance. Once it enters the CSF or the nerve region, it is directly transported into the brain, bypassing the blood-brain barrier, which can lower the dose required to achieve appropriate drug levels in the CNS and reduce the side effects.

2.3. Nasal anatomy and physiology

The nose is a complex structure, as shown in [25]. The nasal cavity is divided into three main regions: the vestibule, respiratory, and olfactory regions. The vestibule region is the anterior external region opening to the nasal cavity and is not involved in drug absorption. The respiratory epithelium consists of ciliated and non-ciliated columnar cells, mucus-secreting goblet cells, and basal cells, and has a surface area of ~160 cm^2 in humans and is involved in drug absorption. The third region is an olfactory region consisting of olfactory receptor cells and basal and sustentacular cells. The olfactory region has a surface area of ~10 cm^2. The respiratory region has superior permeability and vascularization compared to the other nasal sites. The drug can enter the CSF and olfactory bulb from the olfactory nerves. Subsequently, the drug can be distributed from the CSF to the brain by mixing with interstitial fluid in the brain.

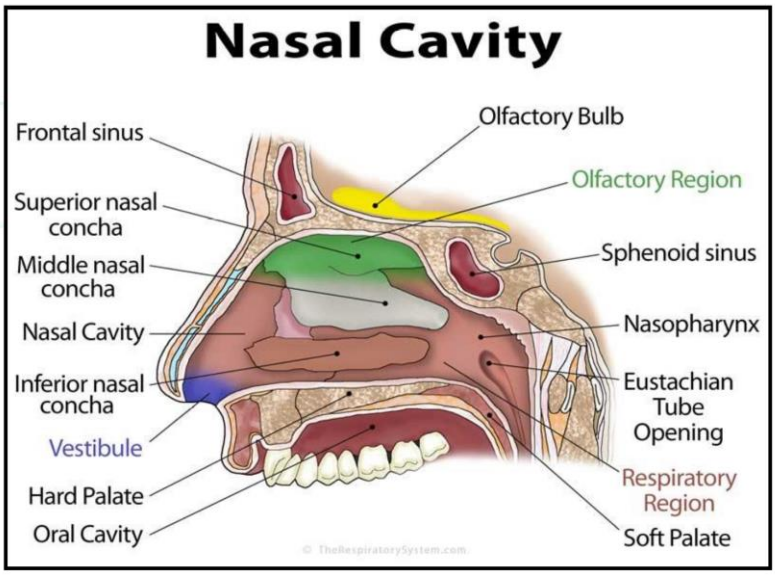

Figure 2-2. Diagram of the nasal structure.
Taken from [**25**].

The nasal cavity has a total volume of 16-19 mL, and it is slightly acidic pH (5.5–6-5) and contains enzymes that may catalyze the degradation of some drugs [26]. However, they do not significantly affect naloxone, which is primarily metabolized in the liver. [5] The time between a particle being captured by the mucus layer and removed from the nose is 12-15 minutes. [23] Once the drug is administered IN, it takes only a few minutes to reach the brain via olfactory transport. [26]

2.4. Brain physiology and anatomy

The human brain has no lymphatic system but produces more than 500 mL of CSF daily. CSF is secreted at the choroid plexus and occupies the four ventricles' cavities, as well as the cranial and spinal subarachnoid space. The cerebrospinal fluid moves over the surfaces of the brain and spinal cord and is rapidly absorbed into the general circulation. The choroid plexus forms the blood-cerebrospinal fluid barrier, and this barrier is functionally distinct from the brain microvascular endothelium, which forms the blood-brain barrier. Virtually all non-cellular substances in blood are distributed into cerebrospinal fluid. There is ~140 mL of CSF in the human brain, which fills the four ventricles (20 mL), spinal sub-arachnoid space (30 mL), and cranial subarachnoid space (90 mL). In the human brain, the entire CSF volume is produced and excreted to blood every 4-5 hours or 4-5 times daily. [27] The CSF acts as a second compartment where the effects of enzymes, receptors, and transporters can be studied.

2.5. Nasal Absorption

Drug transport across the olfactory and respiratory epithelial barriers occurs through extracellular or intracellular mechanisms. The paracellular route involves passive diffusion through an aqueous route of transport. There is an inverse log-log correlation between intranasal absorption and the molecular weight of water-soluble compounds. The log molecular weight correlates linearly with the log percent intranasally absorbed. The transcellular process involves transport through a lipoidal route. [24,28]

Absorption of a drug from the nasal region can occur by several mechanisms. A drug can enter the bloodstream via transport through the nasal mucosa into the cerebral spinal fluid (CSF), from which it can enter the blood by crossing the blood-CSF barrier (BCSFB). The drug can also enter the bloodstream from the nasal region through blood vessels in the nasal mucosa region. A drug can enter the brain region directly from the CSF or systemic circulation by crossing the blood-brain barrier. These are the most likely pathways for naloxone delivery to the brain and the tissues where the μ-opioid receptors (MORs) are located. [20]

Other ways in which a drug can enter the brain include absorption into lymphatic vessels reaching neck cervical lymph nodes and extracellular diffusion or convection in perineural or perivascular nerve bundle spaces, leading to access to the cranial site. [29] However, these are not postulated to be as relevant for naloxone delivery because these areas do not contain the MORs that are involved in opioid-induced toxicities such as respiratory depression. [30]

For nasal absorption of naloxone, specific pathways likely dominate absorption into the central compartment and the brain. In particular, naloxone is administered in a water-soluble form due to the acidic pH of marketed formulations. Absorption through the nasal mucosa into the CSF and systemic circulation is rapid and is postulated in this work to be the dominant pathway to naloxone entering the brain regions containing the MORs.

Factors affecting the IN drug absorption include 1) the physiochemical properties of the drug, such as the drug molecular weight, lipophilicity-hydrophilicity, and weak acid/base vs. neutral form; 2) nasal effects due to membrane permeability, environmental pH, mucociliary clearance (cold and rhinitis), and enzymatic degradation in the nasal cavity; and 3) formulation properties such as the drug concentration, pH, osmolarity, drug distribution in the formulation, viscosity, and delivery mechanisms.[28]

2.6. PBPK modeling

Physiologically based pharmacokinetic (PBPK) modeling has become useful in drug discovery and development. It can be used to explore the effects of various physiological parameters such as age, ethnicity, or disease status on human pharmacokinetics, study the interaction of drugs, and guide dosing decisions. Pharmacokinetic (PK) modeling mathematically characterizes our understanding of drug behavior. It involves studying how a drug is absorbed, distributed, metabolized, and excreted by the body (ADME processes) over time. Pharmacodynamic (PD) modeling focuses on the relationship between drug concentration at the site of action and the magnitude of pharmacological response. PKPD modeling combines PK and PD modeling and attempts to describe and

quantify the relationship between dose/drug concentration and its effect on pharmacological response. [31,32]

PKPD models can be empirical or mechanistic. A mechanistic PKPD model for IN drug delivery was used to create a realistic model from a physiological point of view. To develop the model, a large body of information was gathered from systems biology, and differential equations were utilized to characterize the relationship between the dose of naloxone and different opioids and the obtained pharmacological response.

2.7. Literature survey

2.7.1. Naloxone PKPD

Pharmacokinetic and pharmacodynamic studies of naloxone, dosing regimens, and previous patient study outcomes have been previously reviewed. [4] Naloxone is a safe medication that is not known to cause any adverse effects when administered in typical doses to opioid-naïve or non-opioid-dependent patients in doses up to 1 mg/kg. After IV administration of naloxone, approximately 60-65% of the drug is excreted through the kidney as conjugated metabolites. The serum half-life of the drug is approximately 60 min, and the volume of distribution and metabolic clearance following an IV bolus of naloxone are about 200 L and 2500 L/d, respectively.

Naloxone transfers equilibrates rapidly between the plasma and the brain and has a blood effect-site equilibration half-life of 6.5 minutes. Despite the relatively low bioavailability of IN naloxone, there are reports of its clinical efficacy being equal to or surpassing that of IV administration. [4] The IN administration of naloxone has been increasingly utilized

due to ease of administration by laypersons and improved safety for EMS personnel, which has resulted in the avoidance of potential needlestick injuries when treating a patient population at high risk for blood-borne illnesses. [33]

One study found that 2mg of a standard 0.4 mg/mL concentration of IN naloxone has poor bioavailability yet a shorter time to peak concentration by about 5 minutes for IN compared to 0.8mg IM naloxone. This study was limited by the small number of patients and the large volume of liquid (5 mL) administered. Because large portions of the dose pooled in the nasopharynx before being swallowed, the naloxone was measured only in 2 subjects. [34] In contrast, another study found that IN administration of 0.2 mL of 20ng/mL or 40ng/mL dose displayed a bioavailability of ~25%. [35] Other efficacy studies done in pre-hospital settings have shown IN naloxone to be effective in reversing opioid toxicity in about 75% -84% of patients [36-38].

It was also found that following IN administration of 2–8 mg of naloxone in low volumes via an FDA-approved device, plasma naloxone concentrations rose faster, reached a higher maximum (C_{max}), and remained elevated longer than after a typical 0.4 mg IM dose. [39] Similarly, it was found that IN naloxone is a viable alternative to IV naloxone while reducing the risk of needle stick injury. [40]

Following IV administration, naloxone is rapidly distributed in the body. In one study, the mean serum half-life in adults was 4.7 minutes for the distribution phase and 64 minutes for the elimination phase. [41] Still, IN naloxone administration is useful because of the drug's rapid entry into the CSF, systemic circulation, and the CNS.

Pharmacokinetic investigations of novel IN formulations of naloxone indicate that the drug is rapidly absorbed into the bloodstream from the nasal mucosa, with peak plasma concentrations in plasma reached in 20–30 minutes. [42]

The US FDA has approved two naloxone non-prescription products for use by laypersons for emergency treatment of known or suspected opioid overdose: an intranasal spray with a concentrated naloxone dose of 2 or 4 mg in 0.1 mL and an auto-injector for intramuscular (IM) or subcutaneous (SC) use with a naloxone dose of 0.4 or 2 mg. [43]

Another published study demonstrated that the mean unconjugated naloxone plasma concentrations after administration of the two IN test formulations were higher than those observed after the administration of the IM dose at all experimental time points beginning at two minutes post-dosing and maintained high levels above the C_{max} of 0.4 mg IM for two hours. [44] In another study, a population pharmacokinetic model analysis of naloxone was performed using a 2-compartment model. Typical model parameter estimates were clearance of 3.5 L/min (in a 70-kg individual) and apparent volume of distributions V_1 of 12.1L and V_2 of 102 L. [45]

2.7.2. Fentanyl PKPD

Most fentanyl PKPD studies have been done in animals, and compared to other drugs, very few studies have been performed on humans, most of them in a small number of subjects. This is because fentanyl is a potent drug, and the side effects of respiratory depression and cardiac arrest can be life-threatening. [46] These studies have shown wide

variation in the reported mean pharmacokinetic constants for fentanyl in adults, healthy volunteers, or patients.

Recently, many semi-physiological approaches and mechanism-based PK/PD models have been developed to study better the effects of fentanyl and its pharmacokinetics characteristics in different populations. [46-48]

An early study conducted by Singleton et al. on fentanyl pharmacokinetics in elderly and young adults found that when fentanyl was administered as a 2-min IV infusion at a dose of 15-20 μg/kg, the fentanyl concentrations were higher in elderly subjects than in young adults. Non-compartment analysis showed a volume distribution of 1.36-2.27 L/kg and clearance of 13.1-14 mL/kg/min.[49]

In another study, Hengstmann et al. studied the pharmacokinetic properties of 0.5mg IV bolus injection in six patients to develop an IV infusion model for fentanyl. The study reported that after the 0.5 mg IV bolus dose, fentanyl plasma concentration decreased within 10 minutes from 50ng/ml to 5ng/ml. The average volume of distribution was 80L, and the total plasma clearance was 500ml/min. The biological half-life averaged 140 ± 60 minutes. [50]

Reilly et al. found a wide discrepancy between seven previous studies that reported calculated pharmacokinetic parameters for fentanyl. Those studies showed that fentanyl disposition was described using two or three-compartment models. The reported volume of distribution ranged from 4.4 to 59.7 L, the estimated terminal elimination half-life

ranged from 141 to 853 minutes, and the total body clearance ranged from 160 to 1530 mL/min. Following a 500 μg IV bolus dose of fentanyl, the peak concentration was 8.4-113.6ng/mL, declining to 0.5 ng/mL within 2.9-18.9 hours. [51]

In a recent study conducted on adults undergoing third-molar extraction, intravenous and intranasal fentanyl was administered to evaluate the pharmacokinetics, efficacy and tolerability of fentanyl using a randomized cross-over study design.[52] Both forms of the drug were well tolerated, and the onset and duration of action were quite similar. Using non-compartmental analysis, the estimated volume of distribution was ~250 L, and the clearance was ~1.3L/min for a 100 μg IV bolus dose. [52]

Oral fentanyl has low bioavailability due to high first-pass metabolism. However, because of its high lipophilicity, fentanyl is administered through various other non-invasive routes. Transmucosal and transdermal fentanyl formulations are widely used in clinical settings, in breakthrough cancer patients, in emergencies and in pediatric populations. Oral transmucosal fentanyl is available in 200, 400, 600, 800, 1200 and 1600 μg doses as sweetened lozenges. These formulations are 40-50% bioavailable depending on the patient's swallowing and the amount of the drug. They have a rapid onset of action and short duration of effect and take about 15-20 minutes to reach maximum fentanyl plasma concentrations. Intranasal transmucosal and spray fentanyl formulations (Instanyl®, Subsys®) are also available with 50, 100 and 200 μg of fentanyl dissolved in 100 μl per spray. These can be up to 90% bioavailable, and the drug can cross the blood-brain barrier (BBB) and enter the brain via nasal mucosa. The onset of action is rapid (7

min) and its duration is ~ 2 h. Transdermal fentanyl patches release fentanyl at a constant zero-order rate for 2-3 days, making them suitable for chronic pain management. These patches (Duragesic®) are available in 12, 25, 50, 75 or 100µg/h concentrations. Therapeutic serum fentanyl levels are achieved 12-16h after applications and can have a bioavailability of 92%. The transdermal patches, however, carry a risk of abuse and overdose due to the high fentanyl concentration present in the reservoir, which could be easily extracted. There are many new fentanyl formulations approved for use in non-perioperative settings and widely used for pain management. [53]

2.7.3. Nose-to-brain drug delivery

Intranasal (IN) drug delivery is a non-invasive and effective route for administering drugs to the brain at pharmacologically relevant concentrations, bypassing the blood-brain barrier and minimizing adverse side effects. IN drug delivery can be particularly promising for the treatment of diseases that are associated with brain receptors. The drug delivery mechanism involves the initial drug penetration through the nasal epithelial barrier, followed by drug diffusion in the perivascular or perineural spaces along the olfactory or trigeminal nerves and extracellular diffusion throughout the brain. Some drug may be lost by drainage through the lymphatic system, while a part may even enter the systemic circulation and reach the brain by crossing the blood-brain barrier. [30]

The nasal route circumvents hepatic first-pass elimination associated with oral delivery: it is easily accessible and suitable for self-medication. The large surface area of the nasal mucosa affords a rapid onset of therapeutic effect, potential for direct-to-central nervous

system delivery, no first-pass metabolism, and non-invasiveness, all of which may maximize patient convenience, comfort, and compliance. [24]

IN administration has limitations, which limits its usefulness for many drugs. For naloxone, the most important considerations are formulation-related and include limitations on the volume of the dose administered (typically less than 0.2 mL per spray) and mucociliary clearance. Also, nasal enzymatic barriers can reduce drug efficacy. There are also formulation limitations, such as limiting the use of surfactants, which can function as solubilizers for the neutral form of naloxone, because they may damage or irritate the nasal membranes.

Intranasal naloxone is also thought to be absorbed through nasal mucosa directly into the CNS as well as through systemic circulation, crossing the blood-brain barrier and entering the brain tissue. IN naloxone was found to be as effective as IV naloxone in reversing both respiratory depression and depressive effects on the central nervous system caused by opioid overdose. This could be possible because of the direct transport of naloxone to the central nervous system across the olfactory mucosa in addition to the systemic absorption of naloxone through the highly vascular respiratory region. [54]

Drug absorption via the nasal route appears to be a reliable way of getting drugs into systemic circulation. The nasal route has easy access, a large surface area, is well vascularized and circumvents first-pass metabolism. [55]

2.7.4. Binding and displacement kinetics at the MOR

Kaufman and colleagues showed that 1.55 μg/kg of naloxone is needed to reduce the effect of a 12mg morphine dose by half. [56] However, predicting an adequate dose in a clinical setting is challenging, as effective antagonism of opioid toxicity depends upon the amount of opioid present and its potency, as well as interactions with the opioid receptor. The former is dependent not only upon the specific opioids and the dose administered but also on the route of administration and the patient's ability to clear the drug. Moreover, the affinity and binding/release kinetics of an opioid antagonist with MORs critically affect its reversal by naloxone. [45]

Data and information found in the literature for binding characteristics include the following [57]:

- The rate and extent of opioid agonist effect reversal are dictated by binding and release (association and dissociation) kinetics with MORs, which are characterized by binding and release rate constants k_b and k_r, respectively.

The receptor dissociation constant K_d (reciprocal of the equilibrium binding constant K_e) equals the free drug concentration at which 50% of the receptors are occupied at equilibrium.

- Table 2-1 lists *in vitro* values of K_i and k_r for MORs for some opioids and naloxone and the *in vivo* values for naloxone. [58,59]

Table 2-1. MOR binding and release rate constants for opioid agonists *in vitro*.

Drug	Dissociation constant K_d (μM)	Release rate constant k_r (h^{-1})
Fentanyl	0.00135	14.4
Morphine	0.00117	7.2
Buprenorphine	0.00022	0.72
Sufentanil	0.00014	3.6
Carfentanil	0.00005	0.9
Naloxone	0.0011	144.0
Naloxone (*in vivo*)	0.018	50.4

2.7.5. Where the literature leaves off

Overall, the available literature provided much of the background, but there is limited application of mechanistic models for opioid toxicity rescue by naloxone. Specifically, while some PK modeling has been done, there are no attempts to mechanistically account for the effects of MOR expression, binding kinetics, and characterization of opioid concentrations in the brain vs. pharmacological responses (alone or vs. time). Importantly, studies to date have not modeled naloxone rescue from opioid overdose emergencies and do not quantitatively explain naloxone rescue by IN administration.

Thus, there is a need to advance the previous work to model and quantitatively understand factors affecting naloxone rescues and make physiologically reasonable predictions.

CHAPTER 3. OBJECTIVES OF THIS RESEARCH

3.1. Statement of the problem

Intranasal drug delivery of naloxone is highly utilized for opioid antagonism. Still, as discussed in Section 2.7.5, there are knowledge gaps regarding the nose-to-brain delivery of naloxone and naloxone rescue from opioid-induced emergencies, particularly as related to respiratory depression. Addressing these gaps will provide a greater understanding that may be essential for developing more effective and targeted naloxone treatment systems.

Some fundamental problems include:

- Drug transport mechanisms for naloxone: While there is a general understanding of the potential routes by which naloxone can travel from the nasal cavity to the brain (e.g., olfactory pathways), the precise mechanisms of drug transport and the quantitative effects of factors that influence it are not fully elucidated. Research is needed to understand better these transport mechanisms, which are essential for naloxone.
- Drug formulation optimization: Developing drug formulations for optimal nasal delivery to the brain is an ongoing challenge. Research is needed to identify the best delivery systems and formulations to enhance naloxone IN delivery and optimize the delivery to the proper sites in the CNS.
- Bioavailability and pharmacokinetics: Even though IN naloxone has good efficacy, the bioavailability of drugs delivered via the nasal route is relatively low, and different studies have reported different bioavailability values. Thus, a comprehensive

study of the pharmacokinetics and bioavailability of naloxone would likely provide valuable information for dosing optimization.

- Reversibility of opioid-agonist drug effects: Understanding the reversibility of opioid agonist effects in the brain after IN administration of naloxone is important. Since naloxone has a short duration of action compared to most opioids, multiple doses of naloxone may be required in overdose rescue situations. Research is needed to understand better factors affecting naloxone and opioid clearance from MOR-containing compartments, the kinetics of the local naloxone and opioid agonist levels, and how these affect bound naloxone and agonist concentrations and ensuing pharmacological response over time.
- Clinical efficacy on special populations: While clinical studies on opioid-addicted patients have shown promise for various applications, clinical evidence demonstrating the efficacy of IN naloxone delivery for specific populations is still limited. Further clinical or *in silico* studies may help improve IN delivery's effectiveness.

Addressing these knowledge gaps will contribute to developing safer and more effective IN naloxone drug delivery systems targeting the brain via the nasal route. Since it is challenging to study IN naloxone effects in the human brain directly, we can quantitively model the systems and study them. This can be done by quantitatively investigating the physical and physiological factors affecting naloxone delivery and therapeutic effects.

3.2. Specific aims

In this project, fentanyl was selected as the opioid-agonist to study, and the fraction of full ventilation function (i.e., the fraction of ventilation suppression) was chosen to

quantitatively represent the clinical response. The project sought to model naloxone rescue from fentanyl overdose emergencies and perform quantitative simulations of the response to naloxone administered intranasally (IN) to hypothetical patient populations showing fentanyl toxicity. The specific aims to achieve this goal are listed below.

Aim 1: Develop a PBPK model for IV and IN naloxone administration, including binding kinetics with MORs, and evaluate the equations using R.

This aim is to create a physiologically based pharmacokinetic model of naloxone using R and verify it against published clinical data. A model will be developed that accurately describes the absorption, distribution, metabolism, and excretion (ADME) of IV naloxone in the human body. Once that model was verified against published clinical data, it was extended to describe the PK of intranasally administered naloxone. Since IN administration of naloxone cannot be well-described mechanistically using general PK software, a PBPK model based on known physiological factors was developed, and the equations were numerically evaluated using the R programming language to study their effects on naloxone efficacy.

The first step was to model naloxone with a 2-compartment model, which was used to obtain some of the relevant physiological parameters. The model was then extended to three compartments to incorporate naloxone distribution into the brain and binding with MORs. This was then used to study naloxone binding kinetics at MORs in the brain for IV and IN administration. Since naloxone is a weak base and significantly bound to

plasma proteins, the model equations also accounted for the effects of pH and protein binding on the naloxone disposition.

Aim 2: Develop a PBPK model for IV fentanyl administration, including binding kinetics with MORs, and evaluate the equations using R.

This is similar to Specific Aim 1 but will be done for fentanyl and not include IN administration.

Aim 3. Combine the naloxone and fentanyl models.

The individual naloxone and fentanyl PK model equations were independent. Thus, the two models were merged into one model by combining the equations as written for the individual models except for modifying one equation: the total MOR concentration equals the sum of the free MORs plus those occupied by naloxone plus those occupied by fentanyl. This served to link the equations, so the clinical ventilation outcomes were interdependent on both naloxone and fentanyl PK.

Aim 4. Assess the models against published literature to obtain physiologically reasonable estimated ranges of PK parameters used in the simulations that follow for naloxone rescues of fentanyl overdose.

PK parameters in the model for both drugs were obtained "piecemeal" for two reasons: 1) There are more physiological parameters than data points, and 2) No studies supply data appropriate for all required parameter fitting. Specific parameters such as central and peripheral volumes, partitioning, and intercompartmental mass transport rate constants

were obtained for each drug by fitting the two-compartment models to published IV and IN data. Since the disposition of naloxone and fentanyl in the brain will have minor effects on the distribution into the central and peripheral compartments, these parameters were used to further evaluate parameters associated with the brain compartment. The PK parameters affecting disposition in the brain were estimated using published MOR expression data (plus in vitro and in vivo binding and release data as rough guides). Finally, a dose-response type of curve was constructed by comparing the concentration of MORs occupied by fentanyl with published ventilation suppression vs. time data. It would be valuable to understand the effect of drug binding affinities on the pharmacological response and ways to enhance naloxone efficacy as an opioid antagonist. This model can be extended to study the drug PKPD in special populations.

Aim 5. Perform population simulations of naloxone rescue from fentanyl overdose for various fentanyl doses and naloxone rescue regimens.

Understanding the dosing requirements and pharmacokinetics in patient populations is essential for safe and effective clinical use of naloxone. The overall model can be extended to include a patient population and study possible naloxone dosage regimens with different levels of fentanyl overdose scenarios, which is otherwise not possible to conduct on human subjects clinically.

3.3. Justification and significance

PBPK offers a tool that can be used to understand the effects of drugs administered to the body. It can also be used for dosage form development, optimization, and regulatory applications. For the specific case of naloxone rescue from opioid overdose, several points are of note.

First, PBPK modeling can help to quantitatively understand the mechanism of the drug interaction between naloxone and opioid agonists, specifically at the MORs. Understanding which factors affect the rate of delivery of naloxone to the brain, rates of binding/displacement of naloxone and the opioid agonist, and the effects vs. time profiles are central to understanding the dose-response mechanisms and dynamics.

Second, a PBPK model can be used to simulate patient populations, disease states, or different extents of opioid overdose and naloxone rescue. This is potentially significant because it is not possible to obtain clinical information related to such rescues—it is not feasible to collect clinical data from emergencies in the field where seconds and minutes are critical, nor is it ethical (or legal) to create life-threatening situations as part of a clinical study. Simulating such situations in a PBPK model may be the best way to obtain new information on emergency rescues, dosage form development, predicting rescue from opioid agonists using *in vitro* data, etc.

Third, a PBPK model may help improve understanding of the pharmacodynamics of the naloxone rescue. Predicting free and bound naloxone and displaced opioid levels vs. time

together with clinical response data (such as respiratory rate recovery) can provide information for pharmacodynamic modeling.

Fourth, a PBPK model may be helpful in the development of new dosage forms. By considering the effects of different intranasal formulation properties, such as pH and viscosity, drug distribution in the formulation, etc., a PBPK model can guide the development of new formulations. In addition, physiological factors such as mucus production and clearance (e.g., colds or allergic rhinitis), abnormalities in nasal structure, or differences due to aging, gender, or ethnicity can be incorporated, and the predicted effects can be evaluated.

CHAPTER 4. MODELING AND SIMULATION METHODS

4.1. Introduction to modeling and its general purpose

Modeling generally involves creating simplified representations or mathematical descriptions of real-world systems, phenomena, or processes. These representations are designed to capture and understand the system's essential features, behaviors, or relationships under study.

Modeling starts with a physical picture of what could occur inside the body. It should track the drug (naloxone and fentanyl) disposition after administration, including every step/process and the associated rates and extents. This research studied how naloxone interacts with the receptors in the body, how it produces its effect, how it interacts with the opioids and displaces the bound agonist in the body, the fate of the naloxone and the displaced fentanyl, and the final pharmacological response. Based on these processes, a picture was developed to describe and include all the essential aspects.

After construction, the model picture was analyzed to identify the dominant processes, including their rates and extents regarding end-results of interest. Overall, the objective was a quantitative analysis of all the processes, the fate of naloxone and fentanyl, and the ventilation suppression response. Ultimately, the model aimed to capture these processes and simulate/predict the effects of interest.

The goal of the modeling in this project was to characterize the distribution and elimination of naloxone after administration, accounting for physiological and pharmacological responses. The PBPK model captured the processes involved in the

naloxone and fentanyl pharmacokinetics and pharmacodynamics, described each step mathematically, provided information on the processes involved and what factors can affect them, made quantitative predictions by evaluating the model equations, and allowed exploration of the outcomes. The PBPK model was used to provide physiologically reasonable estimates that served as the basis for population simulations by performing simulations with a range of values for each parameter and comparing the results with literature data.

It is anticipated that the PBPK model will improve the understanding of naloxone disposition and how it affects opioid antagonist displacement from MORs. The model and its numerical implementation in R will provide a platform to explain the pharmacokinetics of naloxone disposition and opioid agonist displacement from MORs. In turn, this platform can be used as a tool to quantitatively assess and predict the impact of various factors on naloxone delivery and disposition and quantitatively characterize its interactions with opioids to understand how naloxone levels affect the opioid displacement from MORs and the time course of rescue from opioid overdose.

4.2. Steps in constructing the model

A model typically starts with a picture. Then, equations were written and programmed for numerical evaluation in an appropriate computational platform. This is done in the following steps: fit the data, pick ranges of parameters, and simulate and validate. After fitting, we simulate and compare the data, adjust the parameters, and repeat the process

until an optimum result is achieved. It is also possible to explore without fitting by employing a range of parameter values and observing the changes in the output graphs.

Typically, this relies on visual inspection of the data (simulated vs observed) or nonlinear regression analyses to find a range of values for the physiologically reasonable parameters. This means that the system of equations can be used to get reasonable blood level and peripheral data while at the same time having the flexibility to give you what appears to be reasonable enzyme and receptor activity and drug levels in the brain and other tissues. The model can predict and show approximate values for these processes in the body. The model describing IN naloxone administration is discussed below.

The model picture reflects the important physiological features: the nasal, central, peripheral, and brain compartments and how the drug goes from the nasal to the central compartment and further to the brain and peripheral compartments.

Since a model picture reflects physiology, the physical processes must be included in the system of equations, and simulations should be based on reasonable numerical values of physiological parameters such as compartment volumes and rate constants for binding, release (and displacement). When two compartments are not in equilibrium, a drug exchange can occur between them, which can be described using first-order differential equations and interactions with receptor sites. Hence, differential equations were written to represent the change of the naloxone and opioid agonist disposition in every compartment with time. The model and equations are described in the upcoming sections.

4.3. Writing the equations

This section discusses how the equations were written. This includes rate equations for exchange between compartments (diffusion of the free naloxone), receptor binding and release kinetics equations, and mass balance considerations.

4.3.1. Transport representation versus PK representation

This drug exchange is modeled using a "transport" representation, which is mathematically equivalent to the "PK" representation but potentially uses mass and physiological volumes (V_1, V_2) and chemical partitioning (K) to reduce the number of independent rate constants (as mass transport rate constants) while keeping the total number of parameters the same. Thus, compared to the PK representation, the transport representation may require obtaining fewer parameter values via fitting equations to data because physiological volumes and chemical partitioning behavior might be estimated independently of any fitting of equations to data. In addition, some of the mass transport rate constants in the transport representation might be related to physiological permeabilities, thus providing guidance regarding their orders of magnitude and independently establishing a range of values (as discussed further below).

An example of the difference is given below, using an exchange between the central and peripheral compartments in a two-compartment model.

1=central compartment, 2= peripheral compartment

Initial conditions: $M_1(0)$ = Dose (D), $M_2(0) = 0$

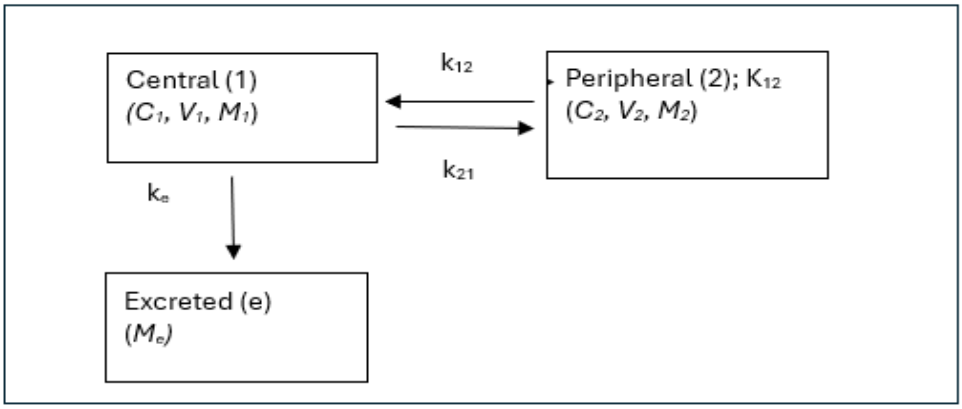

Figure 4-1. 2-compartment model in the PK representation

The differential equations in PK representation are expressed in terms of two concentrations and three rate constants as

$$\frac{dC_1}{dt} = -\left(k_{12}^* + k_e^*\right)C_1 + k_{21}^* C_2$$
$$\frac{dC_2}{dt} = k_{12}^* C_1 - k_{21}^* C_2 \qquad (4\text{-}1)$$

$$C_1 = \frac{M_1}{V_1} \qquad C_2 = \frac{M_2}{V_2} \qquad (4\text{-}2)$$

These equations express concentrations as mass per volume (uppercase *C*) rather than as molarities (lowercase *c*). (Either form of concentration can be used, as the two differ only by a molecular weight factor, which would be absorbed into the rate constants.) The three rate constants k_{12}^*, k_{21}^* and k_e^* have units of inverse time and would each be determined by fitting known equations to the experimental data (for instance, C_1 and the amount excreted in the urine) as functions of time. If mass balance is to be imposed, two additional parameters, V_1 and V_2, must be determined.

In the transport representation, the above model would be described as

$$\frac{dM_1}{dt} = -k_{12}\left(C_1 - \frac{C_2}{K_2}\right) - k_e C_1$$
$$\frac{dM_2}{dt} = k_{12}\left(C_1 - \frac{C_2}{K_2}\right) \qquad (4\text{-}3)$$

where k_{12} and k_e are in volume/time units, and the partitioning coefficient K_2 is unitless.

The transport representation requires the same number of parameters as the PK representation. In the example, if mass balance is required, five parameters are required for each representation (k_{12}^*, k_{21}^*, k_e^*, V_1, V_2 for the PK and k_{12}, K_2, k_e, V_1, V_2 for the transport representation). However, the two are subject to the same interpretation, with the transport representation being more physiochemically based.

For instance, the transport representation modeling of drug exchange between compartments is associated with diffusion modeling across a thin membrane (which can also represent a thin interfacial region).

Fick's First Law (FFL) of diffusion, describing the mass transport of a drug across a thin membrane or interface, is often written as

$$\frac{dM_{12}}{dt} = AP\left(C_1 - C_2\right) \qquad (4\text{-}4)$$

where dM_{12}/dt represents the rate of mass exchange from compartment-1 to compartment-2 (which can be in the negative direction if $C_2 > C_1$), A is the interfacial area between the two compartments, and P is the permeability coefficient of a drug in a membrane separating

the two compartments (units of length/time). This form assumes a steady state or pseudo-steady state concentration gradient across the membrane that is taken to be linear and represented as $\left(C_1 - C_2 \right) / h$, where *h* is the thickness of the membrane.

However, this is a simplified version that holds when the media in compartments -1 and -2 are similar, so the solubility of the drug in each compartment medium is the same. A more general version of FFL describes the rate of diffusion implicitly in terms of the concentration gradient inside the membrane, given as $\left(C_{m1} - C_{m2} \right) / h$, where C_{m1} and C_{m2} denote the concentrations just inside the membrane at the edge in contact with compartment-1 and -2, respectively. The general version of Fick's First Law should be written as

$$\frac{dM}{dt} = \frac{AD}{h}\left(C_{m1} - C_{m2}\right) = \frac{AD}{h}\left(\frac{C_1}{K_{m1}} - \frac{C_2}{K_{m2}} \right) = \frac{AD}{K_{m1}h}\left(C_1 - \frac{K_{m1}C_2}{K_{m2}} \right) \qquad (4\text{-}5)$$

where *D* is the drug diffusion coefficient in the membrane or interfacial region, and K_{m1} and K_{m2} are unitless coefficients defined by $C_{m1} = C_1 / K_{m1}$ and $C_{m2} = C_2 / K_{m2}$. Setting $K_2 = \frac{K_{m2}}{K_{m1}}$ and $k_{12} = \frac{AD}{K_{m1}h}$ recovers the form of Eq. (4-4)

The parameter K_2 can be interpreted as a chemical mass distribution constant between compartment-1 and -2, so no drug transport occurs between the two compartments when $C_2 = K_2 C_1$, which would occur if the two compartments were theoretically at equilibrium with respect to each other. In addition, the parameter k_{12} has the same units as the product *AP* (volume/time), thus providing a conceptual link between k_{12} and physiological

permeability coefficients. For instance, typical physiological membrane permeabilities are ~0.5-5 x 10^{-5} cm/s. Also, it is possible to estimate ranges for K_{m1} from chemical partitioning experiments (oil/water, etc.) in the laboratory. Thus, if an interfacial area is known or estimated, a physiologically based range can be established for k_{12}. Even if such a range is within just one order of magnitude, this can be a helpful limitation when performing simulations.

4.3.2 Equations for binding and release kinetics at the MORs

Equations describing binding kinetics are written in terms of molar concentrations (not mass concentrations) to reflect the interaction stoichiometry based on the number (or moles) of molecules and binding sites per volume. (Molar concentrations are denoted with lowercase *c*, and mass concentrations are denoted with uppercase *C*.) As discussed below, the equations reflect a combination of first and second-order rate processes, so the binding and release rate constants will not be in the same units as those reflecting mass transport between compartments.

The equations below illustrate naloxone binding and release kinetics with an opioid receptor. (The subscript "*N*" denotes naloxone. In later sections, binding and release for the opioid agonist fentanyl follow similar notation, but the subscript "*F*" is used to denote fentanyl.) For naloxone, the binding and release kinetics with the MORs

$$\frac{dc_{Nb,j}}{dt} = k_b c_{Nf,j} P_{f,j} - k_r c_{Nb,j} \tag{4-6}$$

where j denotes the compartment, $c_{Nf,j}$ and $c_{Nb,j}$ are the concentrations of free and bound naloxone, respectively, and $P_{f,j}$ denotes the molar concentration of the free MOR sites. It is assumed that each MOR binding site is either free (unoccupied or open) or occupied by one drug molecule. (In this example, the drug is naloxone, but in the full model, it can be naloxone and the opioid agonist.) Thus, the concentrations of occupied binding sites and bound naloxone are the same. Eq. (4-7) provides the receptor site conservation as

$$c_{Nb,j} = P_{b,j} P_{T,j} = P_{f,j} + P_{b,j} = P_{f,j} + c_{Nb,j} \tag{4-7}$$

where $P_{b,j}$ and $P_{T,j}$ denote the occupied and total binding site concentrations in the compartment, respectively. The free and bound drug masses $N_{f,j}$ and $N_{b,j}$ can be found from their concentrations, the compartment volume V_j, and the naloxone molecular weight MW_N as

$$N_{f,j} = c_{Nf,j} V_j \times MW_N \, N_{b,j} = c_{Nb,j} V_j \times MW_N \tag{4-8}$$

In the context of the PBPK model, it is necessary to include the exchange of naloxone with other compartments (for instance, between the central and brain compartments). This is accomplished by another differential equation for the rate of change of the free naloxone in the compartment due to exchange with another compartment i, as

$$\frac{dc_{Nf,j}}{dt} = \frac{1}{\left(V_j MW_N\right)} \frac{dN_{f,j}}{dt}\bigg|_{ij} - \left(k_b c_{Nf,j} P_{f,j} - k_r c_{Nb,j}\right) \tag{4-9}$$

$$\frac{dN_{f,j}}{dt} = k_{ij}\left(C_i - \frac{C_{f,j}}{K_j}\right) \quad (4\text{-}10)$$

where $\left.\frac{dN_{f,j}}{dt}\right|_{ij}$ is the mass exchange rate between compartments *i* and *j*, k_{ij} is an exchange mass transport rate constant (units of volume per time), $C_{f,j}$ and C_i are the free mass concentrations of naloxone in the compartments, and K_j is a distribution coefficient. The structure and basis for Eq. (4-10) is discussed in Section 6.3.1.

For competitive binding, the same equations are used for the naloxone and fentanyl, which assumes that they do not influence each other in any physicochemical way, so the values of the binding and release rate constants, while different for each drug, do not change when they are both present. However, they compete for open MOR binding sites, so the free site concentrations (Pf,j) are the same for both drugs (see Eq. (4-11) below). In other words, the total MOR expression (thus, the total available MOR sites) is the same for both drugs, but the total MOR sites equals the free plus the sum of the sites occupied by naloxone and the agonist.

Thus, if an opioid agonist such as fentanyl (denoted by *F* in the variable subscripts) is also included, the binding equations would be modified as

$$\frac{dc_{Nb,j}}{dt} = k_{Nb}c_{Nf,j}P_{f,j} - k_{Nr}c_{Nb,j}$$
$$\frac{dc_{Fb,j}}{dt} = k_{Fb}c_{Ff,j}P_{f,j} - k_{Fr}c_{Fb,j} \quad (4\text{-}11)$$

$$c_{Nb,j} = P_{Nb,j} c_{Fb,j} = P_{Fb,j}$$
$$P_{T,j} = P_{f,j} + P_{Nb,j} + P_{Fb,j} = P_{f,j} + c_{Nb,j} + c_{Fb,j} \quad (4\text{-}12)$$

$$N_{f,j} = c_{Nf,j} V_j \times MW_N N_{b,j} = c_{Nb,j} V_j \times MW_N$$
$$F_{f,j} = c_{Ff,j} V_j \times MW_F F_{b,j} = c_{Fb,j} V_j \times MW_F \quad (4\text{-}13)$$

where the *N* and *F* are included to denote the naloxone and fentanyl, and the binding and release rate constants are denoted as $k_{Nb,j}, k_{Nr,j}$ for naloxone and $k_{Nb,j}, k_{Nr,j}$ for the opioid. In Eq. (4-12), the total binding site is the sum of the free sites and sites occupied by naloxone and fentanyl.

4.3.3. Mass balance considerations

Two conditions of mass balance can be imposed, one global (for all compartments together) and the other local (for each compartment individually):

- The dose unabsorbed + the mass of the drug in every compartment + mass eliminated = the administered dose (Total Mass Balance)
- The rate of change of the mass in any compartment = rate in- rate out +/- rate of binding/release (Instantaneous Compartment Mass Balance)

For every compartment, we write differential equations for the drug that accounts for the exchange of the drug with other compartments to maintain the instantaneous compartment mass balance, so the sum of all equations equals zero. The total mass balance is the sum of the mass of the drug in every compartment at any time, including any unabsorbed drug and the mass has been eliminated up to that time. The sum of these

values is constant and should equal the administered dose, and the derivative of a constant is always zero.

4.3.4. Modeling the clinical response

For the simulations to be of practical interest, the PKPD output must relate to clinical outcomes or observables. In this application, respiratory depression was chosen as the quantitative clinical marker, and the degree of suppression was modeled as a function of the fraction of MORs occupied by opioid molecules. The occupation of MOR sites by naloxone has no pharmacological effect other than reducing the ability of the opioid to occupy the sites.

The occupation-response model follows the equation

$$F_{sup} = \frac{\left(1 + F_{cr}\right) F_{F,occ}}{\left(F_{F,occ} + F_{cr}\right)} \tag{4-14}$$

where F_{sup} denotes the fraction of respiratory suppression, $F_{F,occ}$ is the fraction of MOR sites occupied by the opioid agonist, and F_{cr} reflects the sensitivity or responsiveness of an individual to the occupation of MORs by fentanyl. F_{cr} is obtained for the fentanyl by fitting against clinical data and remains constant for a given individual, although it can vary among patients when simulating a population. $F_{F,occ}$ is determined as a function of time by the PKPD model simulation by dividing the bound opioid concentration by the expression of MOR sites (both in molarities). Eq. (4-14) differs from the classic dose-response sigmoidal model equation, which is typically a response vs. concentration relationship, because the occupied fraction is limited as $0 \leq F_{F,occ} \leq 1$. Thus, the bound concentration cannot exceed the concentration of binding sites, whereas the free concentration in the sigmoid model can theoretically become much greater than the binding site concentration. This choice of response model was chosen because of the competition for MOR sites between the naloxone and fentanyl, so the fraction of MOR

sites occupied by fentanyl will not be solely based on the fentanyl concentration but will also depend on the naloxone concentration at the MOR sites.

4.3.5. Include physicochemical and physiological parameters

Differential equations are written to describe the model and should include every process and feature of the mass balance. Mass balance includes passive transport, active transport, binding/release kinetics, and elimination (excretion and metabolism). These are usually described via differential equations and may be first-order, mixed first- and second-order, linear and nonlinear, depending on the processes. These are all the factors that are then put into equations to describe the overall process.

4.4. Using R as a numerical platform for solving the differential equation

4.4.1. General approach

The general approach using commonly available software, such as PK Solver, can give predictions for rates and clearance. However, when more parameters are considered, the fits are imperfect, and the underlying physiological processes are not unambiguously defined. Hence, we will evaluate the models by writing sets of differential equations and numerically solving them in R. This will allow complex mathematical modeling and simulation to help understand the naloxone disposition following intranasal dosing. The initial approach was as follows:

- Simulate a 1-compartment and 2-compartment IV model in R using the ODE solver packages (`lsoda`) to solve the differential equations.
- Import data from the literature into EXCEL sheets that can be called from R.

- Use the `optim` package in R to fit the optimum values for the PK parameters.
- Write the results into EXCEL for further analysis and plotting.
- Compare the results with PK Solver and EXCEL analyses to verify the simulation.
- Build the 2-compartment extravascular model to simulate IN naloxone delivery.

Using R allows constructing and evaluating PBPK models to more closely reflect the physiological mechanism of drug ADME and PD effects. This approach allows the evaluation of systems of equations numerically by eliminating the need to obtain exact mathematical solutions to the differential equations. This is critical because systems of differential equations can be difficult or impractical to solve analytically when the model involves more than three compartments, and systems that include nonlinear equations, such as binding and release kinetics, cannot be exactly solved analytically at all and must be solved numerically.

R provides packages for solving equations, fitting equations to data, plotting, interacting with EXCEL®, etc., using packages such as `deSolve` for solving systems of linear and nonlinear differential equations (the solver method `lsoda` is used in this project), `optim` for fitting equations to literature data, `ggplot` for plotting, `read_excel` for reading data from EXCEL®, etc. Fitting some data from the literature (`optim`) can help to narrow the range of physically acceptable parameter values.

In addition, R provides several valuable advantages. First, it can add model parameters, compartments, and enzyme/transporter/receptor effects by adding equations and then solving the updated system of differential equations. Second, R can read parameters set

up in EXCEL® and write the output data to the same spreadsheet, thus making it easy to track the individual or groups of simulations for comparisons. Finally, the R-code is reusable, making it well-suited to simulate patient populations.

A range of parameters can be obtained from the literature or graphical fits of the data (by inspection or regression fits using software, such as the `optim` package in R). Once ranges are determined, simulations can be performed and compared with published data.

4.4.2. Verification of the R Code

Several checks were performed to numerically verify the model and the correctness of the equation programming in R. These included mass balance and numerical verification.

- The mass balance was checked in two forms: global (total system) and local (each compartment):
    - Global mass balance requires that the mass (not concentrations) summed over all forms (free, bound) and compartments (including eliminated) equals the absorbed dose at all times.
    - The local mass balance was done for each compartment (including elimination and bound vs. free naloxone) and required for all times that

      $$\left[\begin{array}{l}\text{Rate of change of}\\ \text{mass in compartment}\end{array}\right] = \text{Rate in} - \text{Rate out} +/- \text{ rate of production/consumption}$$

- Numerical verification of the differential equations for each differential equation was done three times (early, mid, and late time data). The verifications were done in EXCEL.

- From the output of the ODE solver, the numerical derivative was calculated to obtain the time rates of change of naloxone and fentanyl concentrations and masses, etc., which represents the left-hand side of the exchange equations.
- The numerical value of the right-hand side of each differential equation was calculated using the output for all relevant parameters (mass or concentration vs. time).
- The left- and right-hand sides were compared and must always be equal to within numerical approximation error.

CHAPTER 5. ESTIMATING PHYSIOLOGICAL PARAMETER VALUES

The final model for naloxone plus fentanyl (Chapter 6) required 28 parameters, such as mass transport rate constants between compartments, binding constants, volumes, partitioning constants, etc. Estimating values for all 28 parameters from one set of clinical data was not possible because no single study provided clinical data from all the compartments to support such an estimation. Also, it was not possible from a numerical point of view because the number of data points in the fitting procedure must at least be equal to the number of parameters at an absolute minimum (in practice, it should be double that number or more), and no study provided 28 or more data points. Thus, the number of data points and information allowing each compartment and process rate to be evaluated was impossible to obtain directly.

However, since the goal of constructing the PBPK model in this research was for simulation and prediction of clinical results, fitting a complete data set was not required.

Instead, only physiologically reasonable estimates of "typical" parameter values and reasonable ranges about them were necessary to create hypothetical patient populations in which the typical value was taken as the population average, and the parameters were randomly varied about the average over the assumed ranges.

5.1. Approach to obtain "typical" physiological parameter values

Parts of the model were used to analyze clinical data and obtain parameter estimates in a "piecemeal" manner to obtain typical parameter values. For example, the 2-compartment IV naloxone models were fit to published plasma concentration vs. time data to estimate the volumes of the central and peripheral compartments, mass transport rate constants between the two compartments and for elimination from the central compartment and partitioning between compartments. Subsequently, the IN model was fit to published naloxone plasma vs. time clinical data to estimate the same parameters and the absorption mass transport rate constant from the nasal region (using an assumed nasal volume). After comparing common parameter values from the two sets of fitted estimates (V_{N1}, V_{N2}, k_{N12}, k_{N01}, k_{Ne}, K_{N12}), values were selected to represent the "typical" or average values in a hypothetical patient population.

Subsequently, published data on brain deposition of naloxone vs. time, given as the fraction of MORs occupied by naloxone vs. time, and published MOR expression data were fit using the full naloxone model. The previously obtained parameter estimates (VN1, V2, kN12, kN01, kNe, KN12) were assumed in those fits. The equations were fit to the data to estimate values for the mass transport rate constant between the nasal and

central compartments and the brain compartment (k_{N03} and k_{N13}), and the binding and release rate constants for naloxone and the MORs (k_{N3bM} and k_{N3rM}), were estimated.

A similar approach was employed to estimate the fentanyl parameters but omitted the nasal compartment and IN mass transport rate constant to model IN absorption. For fentanyl, an additional parameter was estimated, F_{cr}, which characterized the relation between the fentanyl-induced ventilation suppression F_{sup} and the fraction of MORs occupied by fentanyl $F_{F,occ}$, as given by Eq. (4-14). This was done by simulating $F_{F,occ}$ vs. time (obtained from bound fentanyl concentration vs. time simulations) and comparing it to the F_{sup} vs. time at corresponding times to create a plot of F_{sup} vs. $F_{F,occ}$. Eq. (4-14) was then fit to those data to obtain F_{cr}.

In addition, typical values were assumed from the literature for the fraction of each drug ionized at physiological pH (~7.34 in the plasma) and the fraction of each drug bound to plasma proteins. Naloxone and fentanyl are both weak base drugs, with their ionized forms being free soluble in water and their neutral form being soluble in lipids and membranes. These are important factors because it was assumed that only each drug's free, neutral form can cross the blood-brain barrier and other membranes.

The approach was as follows. An IV 2-compartment model was constructed with central and peripheral compartments and elimination from the central compartment. , then the 3-compartment with brain and MORs was constructed. The MOR expression was then determined from published data. Simulations of naloxone IN (without fentanyl) were performed to calculate the fraction of MORs occupied by naloxone, which were then

compared to published data on the fraction of MORs occupied by naloxone to estimate the naloxone parameters. Simulations of fentanyl IV (no naloxone) were performed to calculate the fraction of MORs occupied by fentanyl vs. time, which were then compared to published data of fractional loss of ventilation function vs. time to 1) estimate the fentanyl disposition parameters, and 2) construct a function relating the ventilation suppression to the fraction of MORs occupied by fentanyl. Finally, the naloxone and fentanyl models were combined and mathematically linked, and naloxone rescue simulations were performed.

5.2. 2-compartment model for naloxone IV and IN and fentanyl IV

Preliminary analyses of published clinical IV data using the pharmacokinetic EXCEL add-in PKSolver showed that naloxone and fentanyl followed 2-compartment models. Thus, a 2-compartment model was constructed for IV naloxone and fentanyl administration, with an extravascular route for IN administration of naloxone, as shown in Figure 5-1 and described by Eq. (5-1). The model equations represent IV administration when $k_{01} = 0$ (no transfer from the nasal region to the central compartment), $M_0(0) = 0$ and $M_1(0) = \text{Dose}$ (the entire dose is initially in the central compartment). For IN naloxone modeling, k_{01} was also estimated using the initial conditions of $M_0(0) = \text{IN Dose}$ and $M_1(0) = 0$, and V0 and F01 were assumed from the literature estimates. (F_{01} represents the IN fraction absorbed or bioavailability). These initial conditions for IV and IN modeling are given in Eq. (5-2)

Eq. (5-1) and (5-2) were fit to IV naloxone and fentanyl clinical data to obtain estimates for k_{12}, k_e, K_{12}, V_1, and V_2 for IV clinical data and to IN naloxone clinical data to estimate k_{01} subject to box constraints (maxima and minima values) on the previously obtained k_{12}, k_e, K_{12}, V_1, and V_2 values. These were imposed because analyses of IN data using PK-Solver® indicated the data were best fit by (collapsed to) a 1-compartment model, an anomaly that can occur if the time scales of compartmental distribution and extravascular absorption are similar.)

$$\begin{aligned}
\frac{dM_0}{dt} &= -F_{01}k_{01}\frac{M_0}{V_0} \\
\frac{dM_1}{dt} &= F_1 k_{01} M_0 - \left(k_{12}+k_e\right)\frac{F_{free}M_1}{V_1} + k_{12}\frac{M_2}{V_2 K_{12}} \\
\frac{dM_2}{dt} &= k_{12}\left(\frac{F_{free}M_1}{V_1} - \frac{M_2}{V_2 K_{12}}\right) \\
\frac{dM_e}{dt} &= k_e F_{free}\frac{M_1}{V_1}
\end{aligned} \tag{5-1}$$

Initial and auxiliary conditions for IV administration

$$M_1(t) = Dose \qquad M_0(0) = M_2(0) = M_e(0) = 0 \qquad F_{01} = 0,\ k_{01} = 0 \tag{5-2}$$

Initial conditions for IN administration

$$M_0(t) = Dose \qquad M_1(0) = M_2(0) = M_e(0) = 0 \qquad F_{01} > 0,\ k_{01} > 0$$

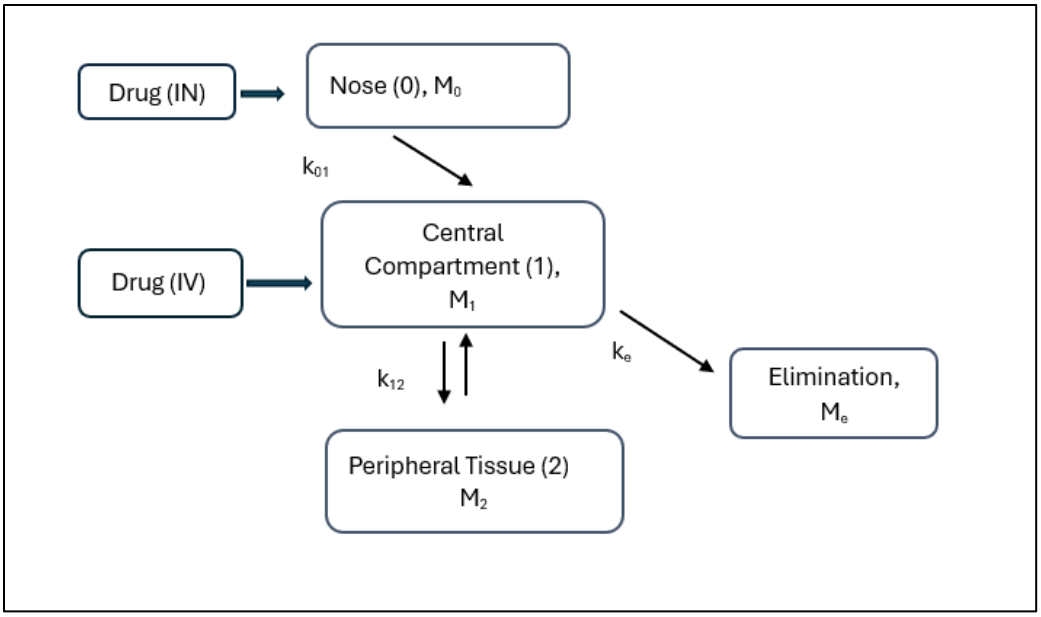

Figure 5-1. 2-compartment model for IV naloxone and fentanyl and IN naloxone.

The model equations for naloxone were fit to the IV and IN clinical data shown in Figure 5-2 and Figure 5-3. The data used for parameter estimations were obtained from the plots of 2 mg given IV and 2 mg given IN, which were digitized using WebPlot Digitizer Software version 4.7 (Ankit Rohatgi, https://automeris.io/WebPlotDigitizer.html, 2024) to obtain data as concentrations vs. time. Each plot was digitized three times, and the average of the vertical (concentration) and horizontal (time) was used as the data points in the fittings for parameter estimations, which were done in R using the `optim` function. d horizontal. The data were subjected to a preliminary analysis using PKSolver to verify that the IV data could be described using a 2-compartment model. The values obtained from the preliminary PKSolver fits were used as initial estimates in fits of Eq. (5-1) and (5-2) to the IV data done using the

`optim` functions in R. In all analyses, the free fraction of naloxone in the plasma was taken as 0.50 (i.e., 50% protein bound).

The IV data used for the parameter estimates were taken from Figure 5-2, and the IN estimates from Figure 5-3. (Although Figure 5-3 also shows IV naloxone plasma data, the consistency of those data was not as good as for the data shown in Figure 5-2.)

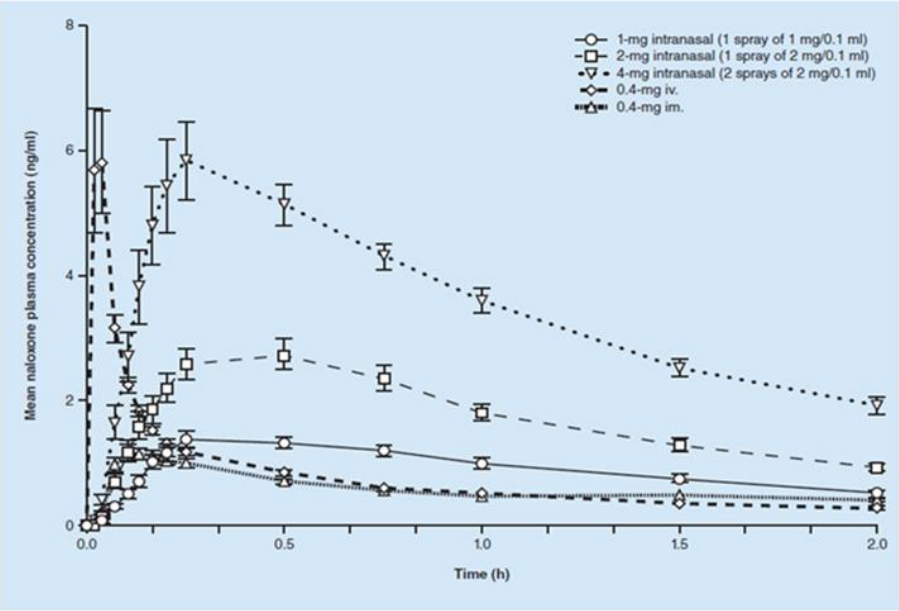

Figure 5-2. Naloxone plasma profiles following IV, IM, and IN administration. Taken from [43]

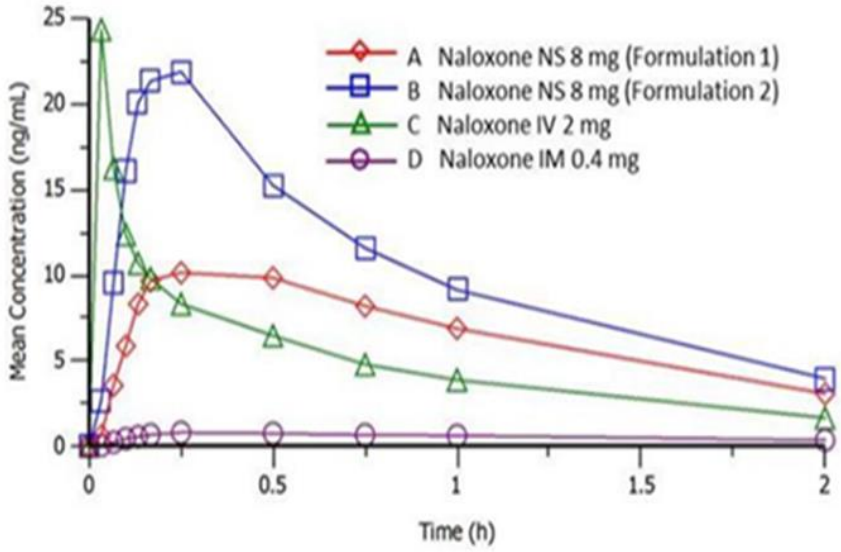

Figure 5-3. Naloxone plasma profiles following IV, IM, and IN administration. Taken from [12444]

Figure 5-4 shows the digitized IV data taken from Figure 5.2 and the result of the fit of Eq. (5-1) and (5-2) to those data, and the resulting estimated parameter values are listed in Table 5-1 for k_{N12} (the transport rate constant for mass exchange between compartment-1 and -2), k_{Ne} (the mass transport rate constant for elimination from the central compartment), K_{N12} (the mass partitioning between compartment-1 and -2), V_{N1} and V_{N2} (the volumes of compartment-1 and -2).

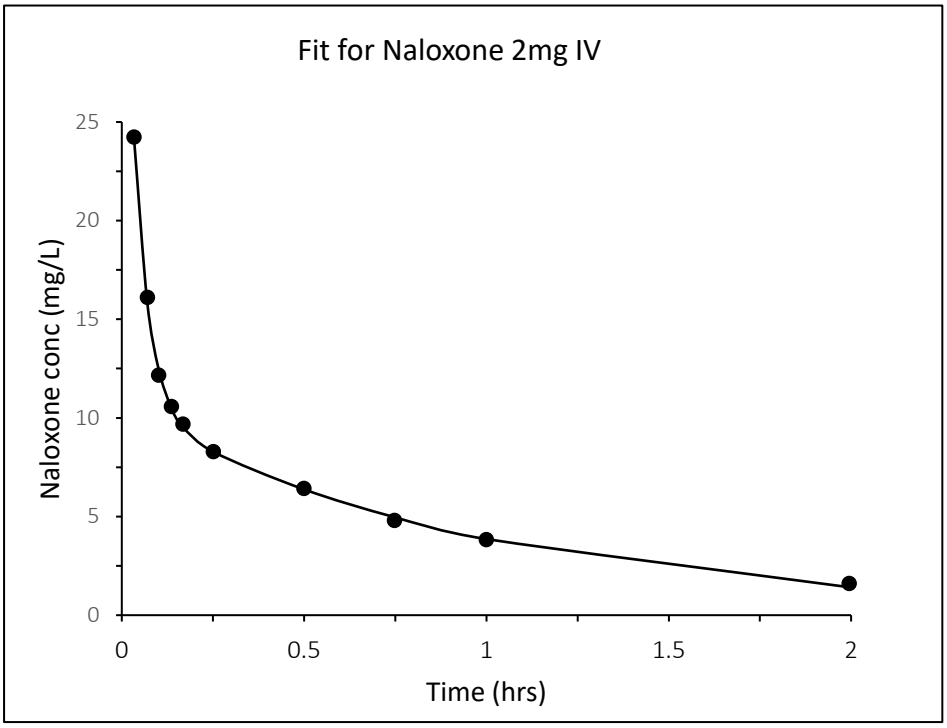

Figure 5-4. Naloxone plasma data and the fit for 2 mg IV.
The data were digitized from Figure 5.2.

Table 5-1. Naloxone IV parameter estimates from fits shown in Figure 5-4.

Parameter (units)	Value
k_{N12} (L/h)	1897.0
k_{Ne} (L/h)	371.9
K_{N12}	0.500
V_{N1} (L)	82.43
V_{N2} (L)	370.4

PKSolver did not appropriately fit the IN data for a 2-compartment model. Thus, to obtain estimates for k_{01} (characterizing the nasal absorption rate) using `optim`, box constraints were constructed around the parameter values listed in Table 5-1 for fits of Eq. (5-1) and (5-2) to the IN data. The bioavailability was taken as 25% (F_{N1} = 0.25), which was obtained by comparing the IV and IN AUCs and doses using PKSolver (analysis not shown). The box constraints were used to ensure that the fits were consistent with the IV fits and allowed the parameters from the IV estimates to vary by some, but not fractionally large, deviations in the IN fits. The effects of the constraints can be seen in Figure 5-5, where the fitted IN profile is consistent with, but shows minor deviations from, the clinical data.

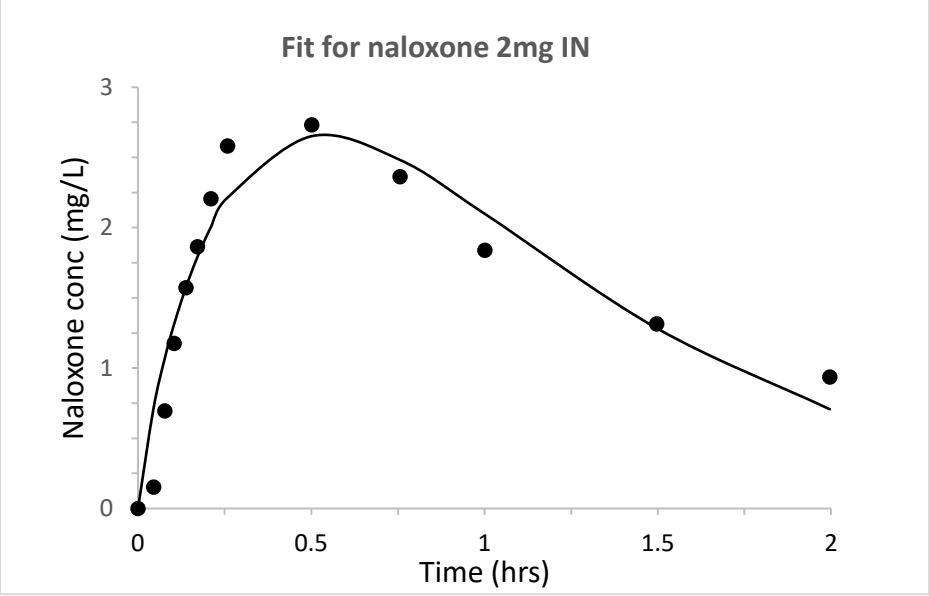

Figure 5-5. IN naloxone plasma data and the fit profile for 2 mg IN.
The data were digitized from Figure 5-3.

Table 5-2. Additional naloxone IN parameter estimates from Figure 5-5.

Parameter (units)	Value
k_{N01} (L/h)	1.029
V_{N0} (L)	0.461

A similar approach was taken for IV fentanyl. (Oral, IN and transdermal models were not constructed or evaluated for fentanyl.) Clinical plasma vs. time data after IV administration are shown in Figure 5-6, the digitized data and the fit of the IV model are shown in Figure 5-7, and the resulting parameter estimates are listed in

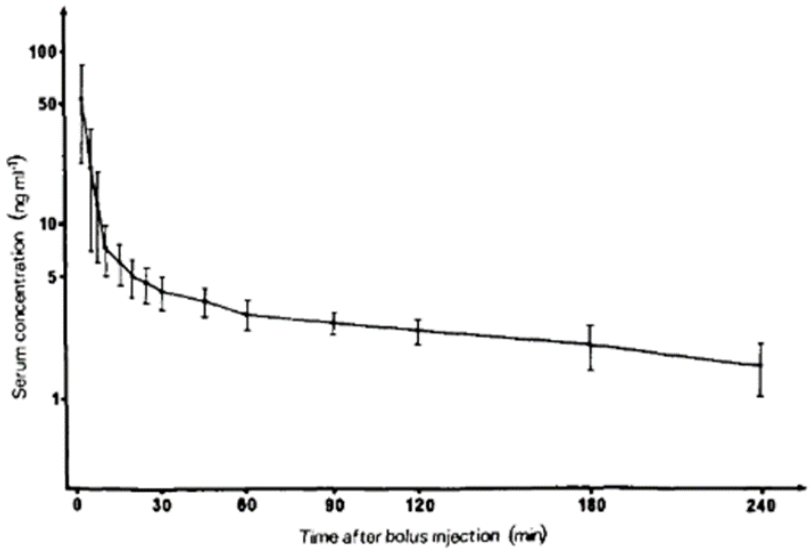

FIG. 1. Serum concentrations in five patients following a bolus injection of fentanyl 0.5 mg. Mean and standard deviation.

Figure 5-6. Fentanyl plasma profiles following 0.5 mg IV administration.
Taken from [50]

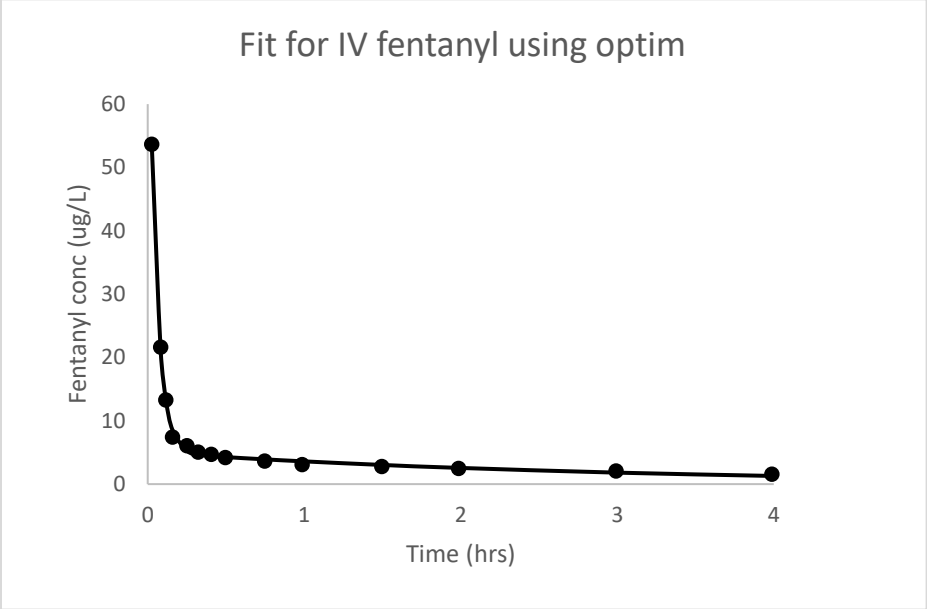

Figure 5-7. Fentanyl digitized plasma data and the fit for 0.5 mg IV.
The data were digitized from Figure 5-6.

Table 5-3. Fentanyl IV parameter estimates from fits shown in Figure 5-7.

Parameter (units)	Value
k_{F12} (L/h)	892.0
k_{Fe} (L/h)	193.8
K_{F12}	0.888
V_{F1} (L)	9.300
V_{F2} (L)	477.6

5.4 3-compartment model with binding in the brain at MORs

An IV 3-compartment model (central, peripheral brain with MORs) was constructed for naloxone and fentanyl, and that model was extended to include IN administration for

naloxone. The model is shown in Figure 5-8, and the system of equations describing the model is given in Eq. (5-3)-(5-5).

In the model equations, the binding and release kinetics (drug and MORs) are written in terms of molarities of the drug and binding site concentrations, which reflects the molecular nature of the kinetic stoichiometry. The binding of the free drug is a second-order equation that depends on the free drug and free MOR site concentrations, and the release rate is a first-order equation depending only on the bound drug concentration. This is equivalent to the occupied (bound) MOR site concentration since a 1-1 stoichiometry of the drug to the binding site was assumed.

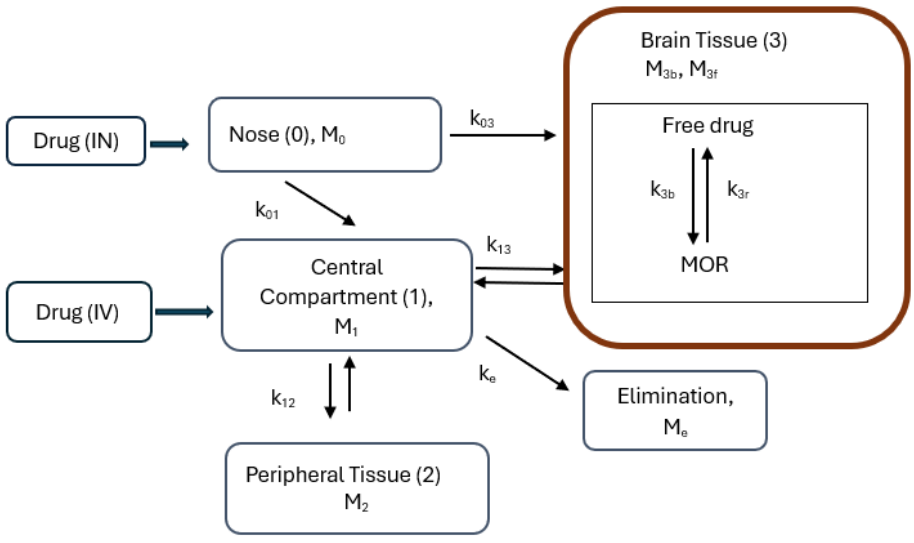

Figure 5-8. 3-compartment model with MOR binding in the brain.

The differential equations for the model:

$$\frac{dM_0}{dt} = -\left(F_{01}k_{01} + F_{03}k_{03}\right)\frac{M_0}{V_0}$$
$$\frac{dM_1}{dt} = F_{01}k_{01}\frac{M_0}{V_0} - k_{12}\left(\frac{F_{free}M_1}{V_1} - k_{12}\frac{M_2}{V_2K_{12}}\right) - k_{13}\left(\frac{F_{free}M_1}{V_1} - \frac{M_{3f}}{V_3K_{13}}\right) - F_{free}k_e\frac{M_1}{V_1}$$
$$\frac{dM_2}{dt} = k_{12}\left(\frac{F_{free}M_1}{V_1} - \frac{M_2}{V_2K_{12}}\right)$$
$$\frac{dM_{3f}}{dt} = F_{03}k_{03}\frac{M_0}{V_0} + k_{13}\left(\frac{F_{free}M_1}{V_1} - \frac{M_{3f}}{V_3K_{13}}\right) - \left(k_{3b}c_{3f}P_{3f} - k_{3r}c_{3b}\right)V_3 \times MW \qquad (5\text{-}3)$$
$$\frac{dM_{3b}}{dt} = \left(k_{3b}c_{3f}P_{3f} - k_{3r}c_{3b}\right)V_3 \times MW$$
$$\frac{dM_e}{dt} = k_eF_{free}\frac{M_1}{V_1}$$

$$c_{3f} = \frac{M_{3f}}{V_3 \times MW} \qquad c_{3b} = \frac{M_{3b}}{V_3 \times MW} \qquad P_{3T} = P_{3f} + c_{3b} \qquad (5\text{-}4)$$

Initial and auxiliary conditions for IV administration

$$M_1(t) = Dose \qquad M_0(0) = M_2(0) = M_e(0) = 0$$
$$F_{01} = 0,\ k_{01} = 0 \qquad F_{03} = 0,\ k_{03} = 0 \qquad (5\text{-}5)$$

Initial conditions for IN administration

$$M_0(t) = Dose \qquad M_1(0) = M_2(0) = M_e(0) = 0$$
$$F_{01} > 0,\ k_{01} > 0 \qquad F_{03} > 0,\ k_{03} > 0$$

P_{3T} represents the MOR expression in molarity (total moles of binding sites divided by V_3). The concentration of occupied MOR sites equals the concentration of bound drug in the brain compartment c_{3b}, and the concentration of free MOR sites is $P_{3f} = P_{3T} - c_{3b}$.

The 3-compartment model with brain and MOR receptor binding and release was fit in R (using `optim`) to published data that includes occupancy or PD effects to obtain the rest

of the parameter values. The parameter values obtained from the IV/IN naloxone data fits were kept the same in the fits for the brain parameters. This must be done because parameter estimation can only be done if there are more data points than parameters. In addition, the approach is supported because the central and peripheral compartments dominate the overall drug mass distribution in the body. Thus, by holding the parameters associated with the disposition in those compartments along with the IN absorption parameters, the fits of the full model for the remaining parameters (k_{03}, k_{13}, k_{3b} and k_{3r}) are responsive to the minimization procedure used in `optim`.

5.4.1. MOR expression in the brain

The MOR expression was calculated in compartment-3. Simulations of the bound naloxone profiles in the brain c_{3b} vs. time were compared to published data, which gave the fraction of MORs occupied by naloxone vs. time. Based on these comparisons, 1) the maximum bound naloxone concentration was required to occur at the same time as the maximum MOR occupied fraction, and 2) first estimates of the naloxone binding and release rate constants ($k3_b$ and $k3_r$) were obtained by fitting entire c_{3b} vs. time profile to best match the occupied entire fraction vs. time profile, subject the constraint that the dissociation constant $K_d = k_r / k_b$ match published values. (This was relaxed, so the individual rate constants could vary more independently when the naloxone rescue simulations were performed, so the simulated rescues were clinically reasonable with respect to their timeframes.)

The MOR expression in the brain was determined as follows. Table 5-4 [60] lists MOR expression per μg of brain tissue for various regions and also provides the average MOR expression/mg over all regions as 5.48 x 10^6 copies/mg. Assuming one binding site per MOR, the average expression was converted to 5.48 x 10^{15} sites/kg. Taking the weight of compartment-3 as 1.1-1.6 kg [61] and assuming a variation of ± 25% in the MOR sites/kg, the total MOR expression in compartment-3 was estimated as 0.4-1.1 x 10^{16} sites, or 0.007-0.018 μmoles. This was converted to molarities P_{3T} by dividing by the volume of compartment-3.

Brain copies/μg (reported average)	**5.48 x 10^6**
Temporal lobe copies/μg	2.71 x 10^6
Substantia nigra copies/μg	2.42 x 10^6
Hippocampus copies/μg	2.69 x 10^6
Cerebral cortex copies/μg	6.44 x 10^6
Putamen copies/μg	8.18 x 10^6
Caudate nucleus copies/μg	12.78 x 10^6
Nucleus accumbens copies/μg	17.20 x 10^6
Cerebellum copies/μg	19.22 x 10^6
Total MOR receptor copies in the brain	**0.4 – 1.1 x 10^{16}**
Total MOR receptor sites in the brain μmoles	**0.007 – 0.018**

Table 5-4. MOR expression in the brain.

5.4.2. Naloxone parameters associated with the brain compartment

The brain (compartment-3) fits were done by simulating the bound concentration of naloxone in the brain vs. time using the 3-compartment model with binding and release at the MOR sites. These simulations were compared to published data relating the fraction of MORs occupied by naloxone vs. time to fit for the mass transport rate constants from the nasal and central compartments to the brain compartment (k_{03} and k_{13}) and the binding and release rate constants k_{3Nb} and k_{3Nr}. Two conditions were imposed on the fits.

- The maximum bound naloxone concentration c_{3Nb} and the maximum fraction of MORs occupied by naloxone $F_{N,occ}$ were forced to be equal. This constraint affected the mass transfer rate constants k_{01} and k_{13} and the naloxone binding and release rate constants k_{3b} and k_{3r}.

- The published data indicated that the maximum fraction of MOR sites occupied by naloxone was 0.72 and occurred at ~50 minutes (0.83 h).[42] Taking $P_{3T} \sim 0.017$ μM, this corresponded to a maximum bound concentration of $c_{3Nb,\max} \sim 0.0122$ μM. From these determinations, it was possible to convert the simulated c_{3Nb} vs. time profiles to simulated profiles of $F_{N,occ}$ vs. time, which were then used to fit the published profile for the parameter estimation using `optim`.

Figure 5-9 shows the data and fits, and

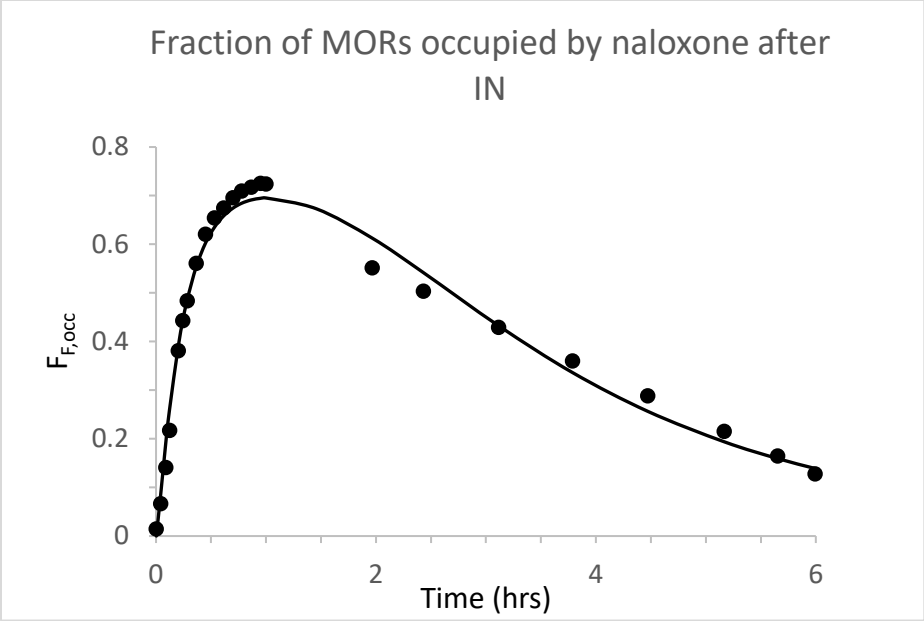

Figure 5-9. Digitized MOR fraction occupied by naloxone and the fit for 2 mg IN.

Table 5-5. Naloxone parameter estimates from fits shown in Figure 5-9.

Parameter (units)	Value
k_{N03} (L/h)	0.010
k_{N13} (L/h)	1.94
k_{Nb} (L/μmole/h)	116700
k_{Nr} (1/h)	140
K_{N13}	0.4

5.4.3. Ventilation suppression by fentanyl

Ventilation (L/h) was chosen as the quantitative function for measuring the fentanyl interaction with the MORs. Figure 5-10 shows published data for the ventilation following an IV dose of 0.3 mg/kg (300 μg/70 kg). [46]

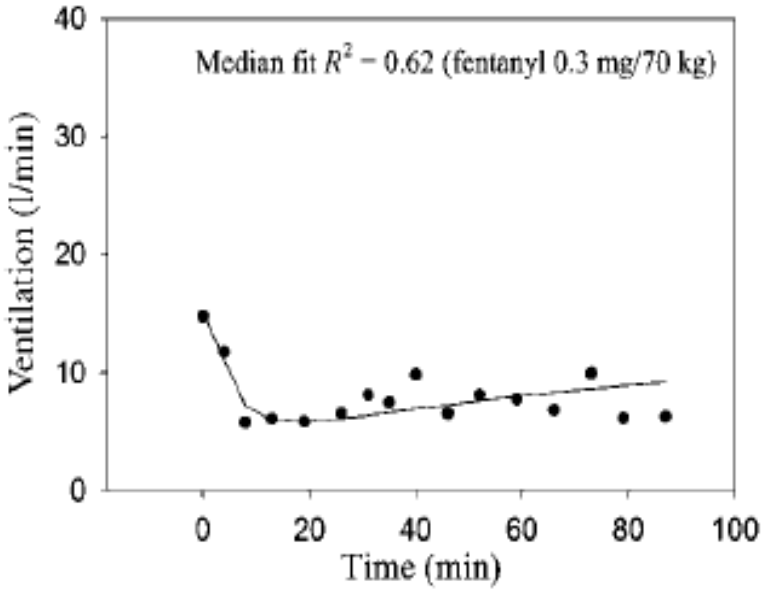

Figure 5-10. Ventilation vs. time after fentanyl 0.3mg/70kg IV.

The first 30 minutes of the ventilation vs. time data were used to construct a function relating the fraction of MORs occupied by fentanyl ($F_{F,occ}$) and the ventilation suppression fraction F_{sup}. These quantities were calculated as $F_{F,occ} = \frac{C_{3Fb}}{P_{3T}}$ and

$$F_{\text{sup}} = \frac{\left(\text{Ventilation at } t = 0\right) - \left(\text{Ventilation at time } t\right)}{\left(\text{Ventilation at } t = 0\ \right)} \tag{5-6}$$

The data in Figure 5-10 were digitized and are summarized in Table 5-6.

Table 5-6. F_{sup} vs. time calculated from the data in Figure 5-10.

Time (h)	Fraction suppressed
0.000	0.000
0.012	0.077
0.066	0.400
0.141	0.532
0.226	0.587
0.322	0.622
0.443	0.653

A ventilation response model was constructed to relate the suppression to the MOR fraction occupied by fentanyl as

$$F_{\text{sup}} = F_{F,occ} \times \frac{\left(1 + F_{cr}\right)}{\left(1 + F_{F,occ}\right)} \tag{5-7}$$

where F_{cr} is a parameter characterizing the response relation and $0 \le F_{sup}$ and $F_{F,occ} \le 1$.

The form of Eq. (5-7) was chosen to reflect the fraction of MORs occupied by fentanyl instead of the commonly used sigmoidal relationship, which would be based on the

fentanyl concentration at the MORs. This was done because the relation between the fentanyl concentration at the MORs and the ensuing bound concentration changes with the presence and concentration of naloxone. The competition between naloxone and fentanyl will be simulated in the full model that combines the two drugs.

A Fsup vs. time profile was constructed using Eq. (5-6), and $F_{F,occ}$ vs. time profiles were obtained from model simulations. Taking values of F_{sup} and $F_{F,occ}$ at the same times and using Eq. (5-7), it is possible to compare clinical and simulated F_{sup} vs. time profiles, which allows fitting the equations to the clinical data to estimate the brain-related parameters and F_{cr} using `optim`. The digitized data and results of the fits are displayed in Figure 5-11, and Table 5-7 lists the resulting parameter estimates.

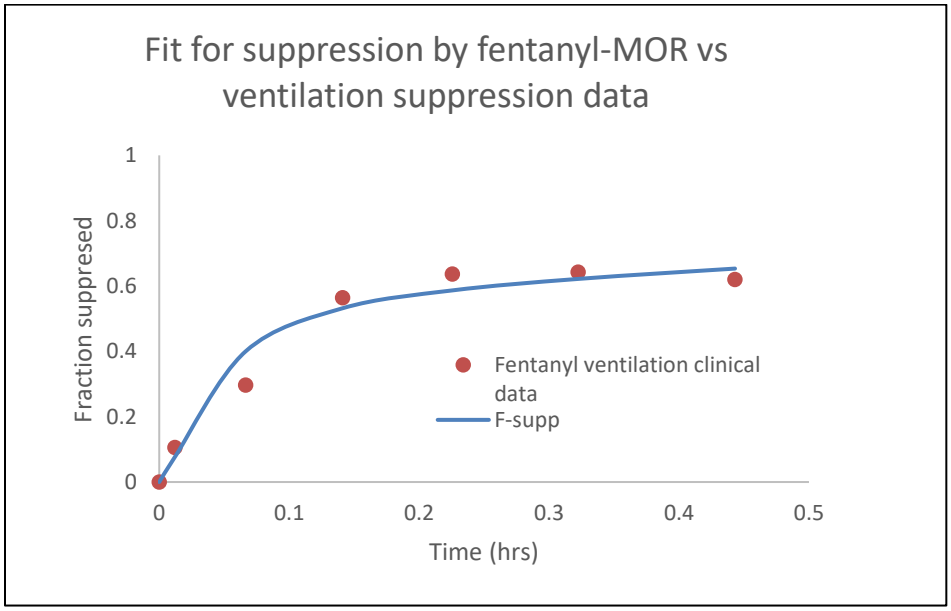

Figure 5-11. Digitized data and fits for ventilation suppression vs. the MOR occupancy by fentanyl.

Table 5-7. Parameter estimates from fits shown in Figure 5-11.

Parameter (units)	Value
F_{cr} (unitless)	0.716
k_{F13} (L/h)	11.0
k_{Fb} (L/μmole/h)	7335
k_{Fr} (1/h)	10.27
K_{F13}	2.40

CHAPTER 6. THE NALOXONE RESCUE MODEL

After estimating individual parameter values for the fentanyl and naloxone models, a full IN naloxone rescue model was constructed by combining the differential equations and the initial conditions. The fentanyl and naloxone equations are independent except for one coupling equation that reflects the competitive MOR binding, and the naloxone displacement of bound fentanyl depends on binding and release rate constants and the drug concentrations (free and bound) in the brain.

6.1. Combining the individual models to construct the naloxone rescue model

The final rescue model is shown in Figure 6-1 below.

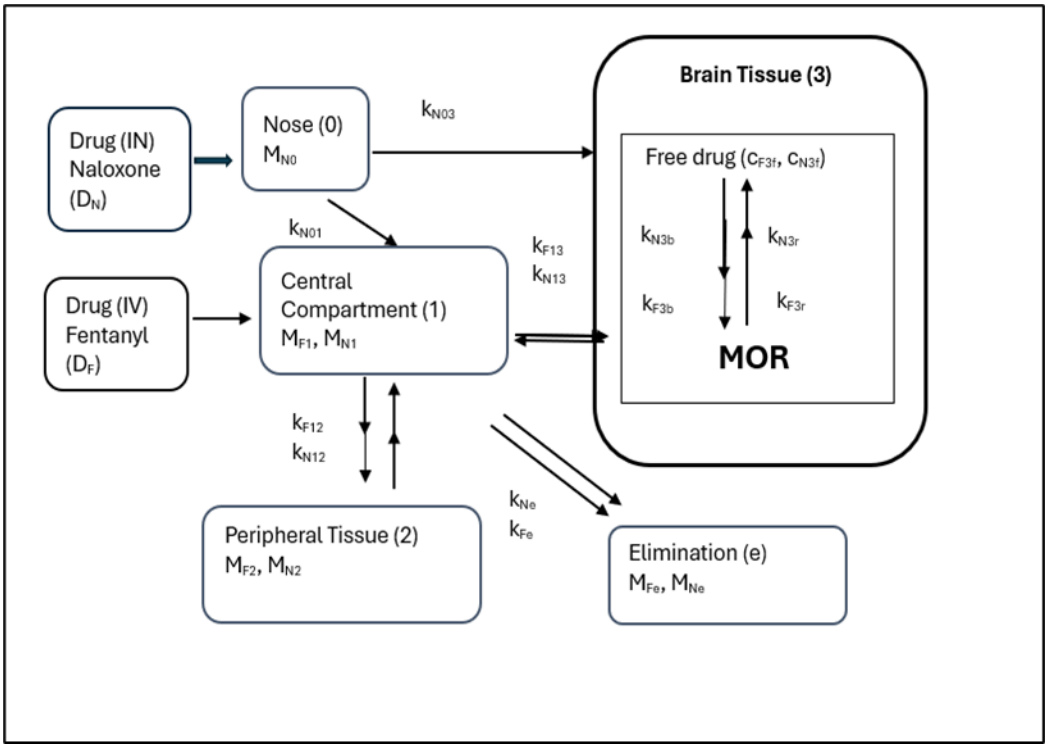

Figure 6-1. IN naloxone and IV fentanyl model with MOR binding and release

In Figure 6-1, $M_{N0,}$ M_{N1}, $M_{N2,}$ M_{F1} and $M_{F2,}$ denote the naloxone and fentanyl mass in the nasal, central and peripheral compartments; k_{N02}, k_{N03}, $k_{N12,}$ and k_{N13} denote the nasal-central, nasal-brain, central-peripheral and central-brain compartments mass transfer rate constants; k_{Ne} denotes the elimination mass transfer rate constant for naloxone; $k_{F12,}$ and k_{F13} denote the central-peripheral and central-brain compartments mass transfer rate constants; k_{Fe} denotes the elimination mass transfer rate constant for fentanyl. k_{N3fM}, k_{N3rM}, k_{F3fM} and k_{F3rM} denote the drug-MOR binding and release rate constants in the brain compartment for naloxone and fentanyl, respectively.

The mathematical description of the 3-compartment IN naloxone model is given in Eq. (6-1)-(6-6). In Eq. (6-2) for fentanyl and Eq. (6-3) for naloxone, the mass rate-of-change equations are written in terms of compartmental concentrations, which are then related to the compartmental masses and volumes in Eq. (6-4).

The naloxone and fentanyl equations are independent except for competing for MOR binding sites, where the bound concentrations of fentanyl and naloxone are coupled as

$$\begin{bmatrix}\text{Total MOR site}\\ \text{molarity } P_{3T}\end{bmatrix}=\begin{bmatrix}\text{Free MOR site}\\ \text{molarity } P_{3f}\end{bmatrix}+\begin{bmatrix}\text{Bound fentanyl}\\ \text{molarity in}\\ \text{compartment-3 } c_{3Fb}\end{bmatrix}+\begin{bmatrix}\text{Bound naloxone}\\ \text{molarity in}\\ \text{compartment-3 } c_{3Nb}\end{bmatrix}$$

The system of equations for the naloxone rescue model is as follows:

Initial conditions

$$M_{F1}(0) = D_F \quad M_{F2}(0) = M_{F3f}(0) = M_{F3b}(0) = M_{Fe}(0) = 0$$
$$M_{N0}(0) = M_{N1}(0) = M_{N2}(0) = M_{N3f}(0) = M_{N3b}(0) = M_{Ne}(0) = 0 \tag{6-1}$$

Differential equation:

$$\frac{dM_{F1}}{dt} = -k_{F12}\left(fr_{F1}C_{F1} - \frac{C_{F2}}{K_{F12}} \right) - k_{F13}\left(fr_{F1}C_{F1} - \frac{C_{F3f}}{K_{F13}} \right) - k_{Fe}\, fr_{F1}C_{F1}$$
$$\frac{dM_{F2}}{dt} = k_{F12}\left(fr_{F1}C_{F1} - \frac{C_{F2}}{K_{F12}} \right)$$
$$\frac{dM_{F3f}}{dt} = k_{F13}\left(fr_{F1}C_{F1} - \frac{C_{F3f}}{K_{F13}} \right) - k_{F3b}\frac{C_{F3f}}{MW_F}P_{3f} + k_{F3r}\frac{C_{F3b}}{MWF} \tag{6-2}$$
$$\frac{dM_{F3b}}{dt} = k_{F3b}\frac{C_{F3f}}{MW_F}P_{3f} - k_{F3r}\frac{C_{F3b}}{MWF}$$
$$\frac{dM_{Fe}}{dt} = k_{Fe}\, fr_{F1}C_{F1}\frac{dM_{N0}}{dt} = -\left(F_{N1}k_{N01} + F_{N3}k_{N03}\right)C_{N0}$$

$$\frac{dM_{N0}}{dt} = -\left(F_{N1}k_{N01} + F_{N3}k_{N03}\right)C_{N0} + \sum_{n=1}^{4} D_N \times \text{UIF}(t_n) \qquad \text{for } t_n < t$$
$$\frac{dM_{N1}}{dt} = F_{N1}k_{N01}C_{N0} - k_{N12}\left(fr_{N1}C_{N1} - \frac{C_{N2}}{K_{N12}} \right) - k_{N13}\left(fr_{N1}C_{N1} - \frac{C_{N3f}}{K_{N13}} \right)$$
$$-k_{Ne}\, fr_{N1}C_{N1}$$
$$\frac{dM_{N2}}{dt} = k_{N12}\left(fr_{N1}C_{N1} - \frac{C_{N2}}{K_{N12}} \right) \tag{6-3}$$
$$\frac{dM_{N3f}}{dt} = F_{N3}k_{N03}C_{N0} + k_{N13}\left(fr_{N1}C_{N1} - \frac{C_{N3f}}{K_{N13}} \right) - k_{N3b}\frac{C_{N3f}}{MW_N}P_{3f} + k_{N3r}\frac{C_{N3b}}{MW_N}$$
$$\frac{dM_{N3b}}{dt} = k_{N3b}\frac{C_{N3f}}{MW_N}P_{3f} - k_{N3r}\frac{C_{N3b}}{MW_N}$$
$$\frac{dM_{Ne}}{dt} = k_{Ne}\, fr_{N1}C_{N1}$$

Auxiliary equations

$$C_{N0}=\frac{M_{N0}}{V_0},\quad C_{N1}=\frac{M_{N1}}{V_1},\quad C_{N2}=\frac{M_{N2}}{V_2},\quad C_{N3f}=\frac{M_{N3f}}{V_3},\quad C_{N3b}=\frac{M_{N3b}}{V_3}$$
$$c_{N3f}=\frac{C_{N3f}}{MW_N}\qquad c_{N3bM}=\frac{C_{N3b}}{MW_N}$$
$$C_{N0}=\frac{M_{N0}}{V_0},\quad C_{N1}=\frac{M_{N1}}{V_1},\quad C_{N2}=\frac{M_{N2}}{V_2},\quad C_{N3f}=\frac{M_{N3f}}{V_3},\quad C_{N3b}=\frac{M_{N3b}}{V_3} \tag{6-4}$$
$$c_{N3f}=\frac{C_{N3f}}{MW_N}\qquad c_{N3bM}=\frac{C_{N3b}}{MW_N}$$

Mass balance

$$M_{F1}+M_{F2}+M_{F3f}+M_{F3b}+M_{Fe}=D_F$$
$$M_{N0}+M_{N1}+M_{N2}+M_{N3f}+M_{N3b}+M_{Ne}=\sum_{n=1}^{N}D_F\times\ \mathrm{UIF}(t_n)\ \text{ for } t_n<t \tag{6-5}$$
$$P_{3f}=P_{3T}-\left(c_{F3b}+c_{N3b}\right)$$

Unit impulse function (for naloxone IN administration)

$$UIF\left(t_n\right)=2\sqrt{\frac{a}{\pi}}e^{-a\left(t-t_n\right)^2}\quad a=500,\ \ n=1,2,3,4 \tag{6-6}$$

$t_n =$ time of the n^{th} naloxone nasal spray

The equations accommodated up to four naloxone sprays via the UIF but could simulate fewer sprays by setting spray times t_n to exceed the simulated timeframe. For instance, setting t_1 = 0.0833 hours and t_2-t_4 = 100 hours, a simulation over 8 hours would account for a single IN dose at 5 minutes.

The *UIF* was used to represent short bursts in the rate of naloxone delivery, such as would occur with a spray of naloxone solution. Figure 6-2 shows the total naloxone administered vs. time for a three-spray rescue with 4mg naloxone. Three properties make the *UIF* appropriate for representing the naloxone dosing. 1)The *UIF* effectively equals except for times close to t_n and becomes more narrow and sharply peaked as the value of a in Eq. (6-6) increases. Figure 6-3 shows *UIF*s for $a = 500\ h^{-2}$ used in the simulations) and $a = 100\ h^{-2}$ (not used because the peaks were not sharp enough to represent the nearly instant delivery of a spray). 2) The *UIF* is a continuous function, so it is well-suited to evaluation by the ODE solver in R. 3) The integral over a time interval from before to after each t_n equals 1, so $\int_{t_n-\Delta t}^{t_n+\Delta t} D_F \times UIF(t_n)\,dt$ equals the dose delivered by that pulse.

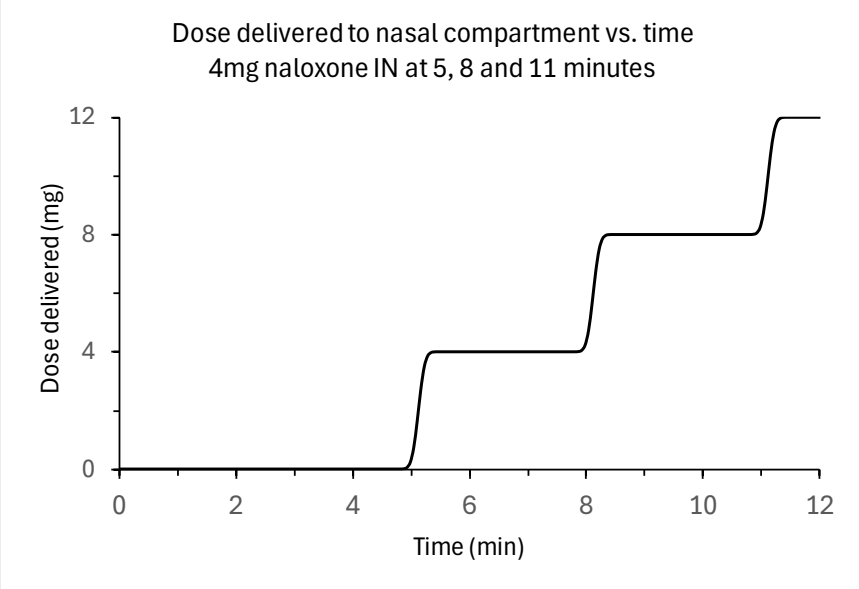

Figure 6-2. Hypothetical naloxone administered at 5, 8 and 11 minutes using the UIF function.

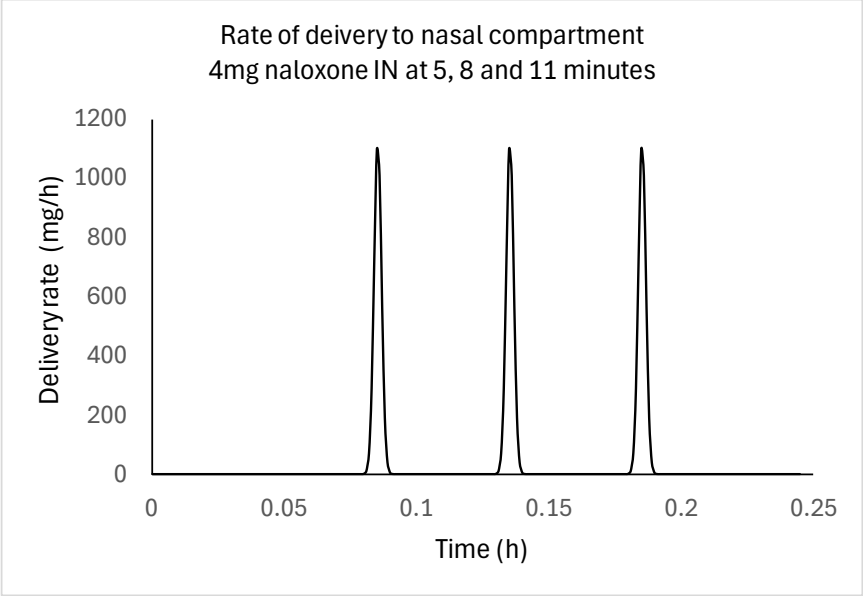

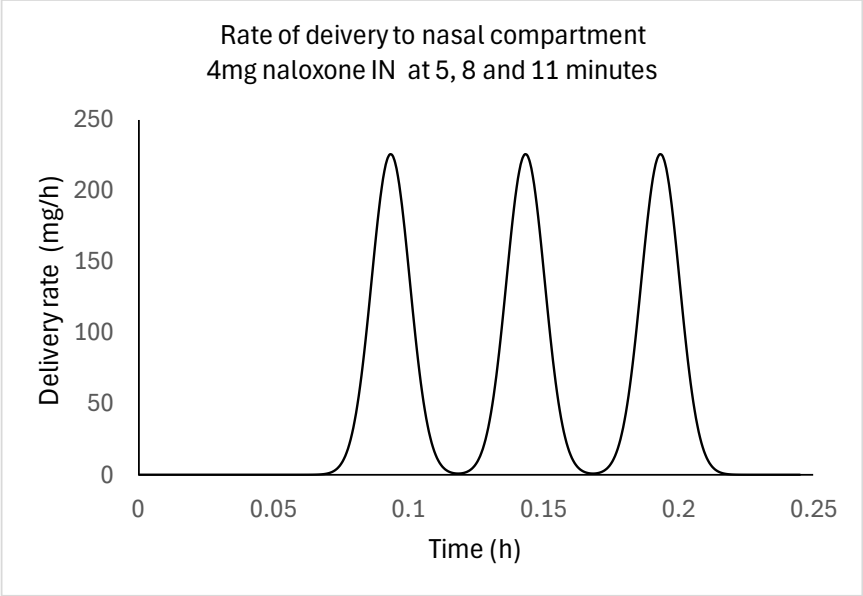

Figure 6-3. UIF function for three naloxone doses.
Top: $a = 500\ h^{-2}$. Bottom: $a = 100\ h^{-2}$

6.2. Verification of the rescue model

The R-code was numerically checked as described in Section 4.4.2 for the individual rate equations and the mass balances for fentanyl and naloxone. An extra numerical check was also implemented by performing simulations to mimic the individual model simulations. The initial conditions

- Fentanyl 500 μg IV with no naloxone dosing. The initial conditions were set according to Eq. (6-1) and t_1- t_4 = 100 hours (no naloxone doses were given in the simulation of 0-8 hours).

- Naloxone 2 mg IN single dose at t = 0. The initial conditions were set according to Eq. (6-1) except $\underline{D_F}$ = 0, t_1 = 0 and t_2-t_4 = 100 hours.

The total mass was checked for each drug and found to be constant with the individual dose administered D_F and D_N. Also, the fentanyl and naloxone simulations generated the same output as when individual models for each drug were run in R. This is shown in Figure 6-4 and Figure 6-5.

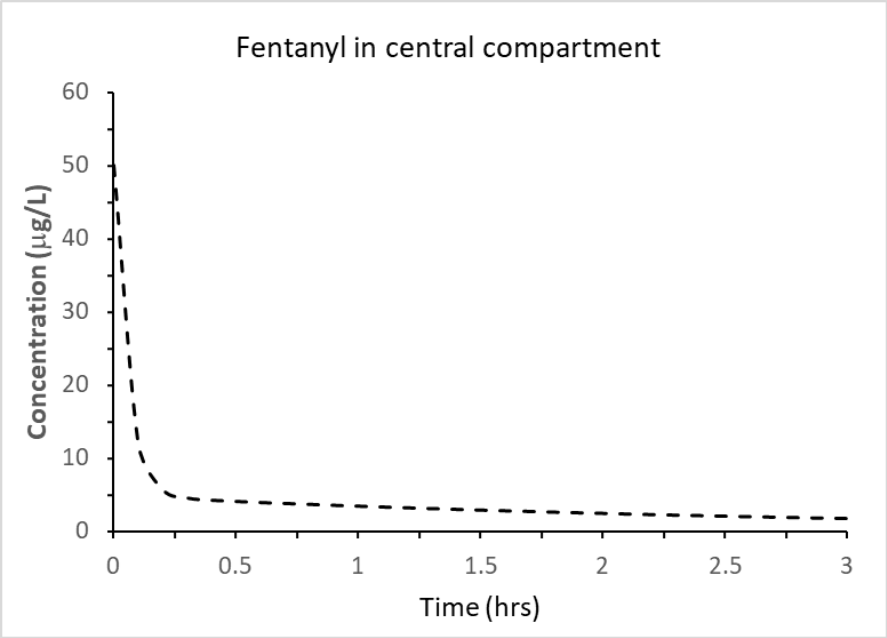

Figure 6-4. Concentration-time plot for IV 500µg fentanyl and no naloxone.

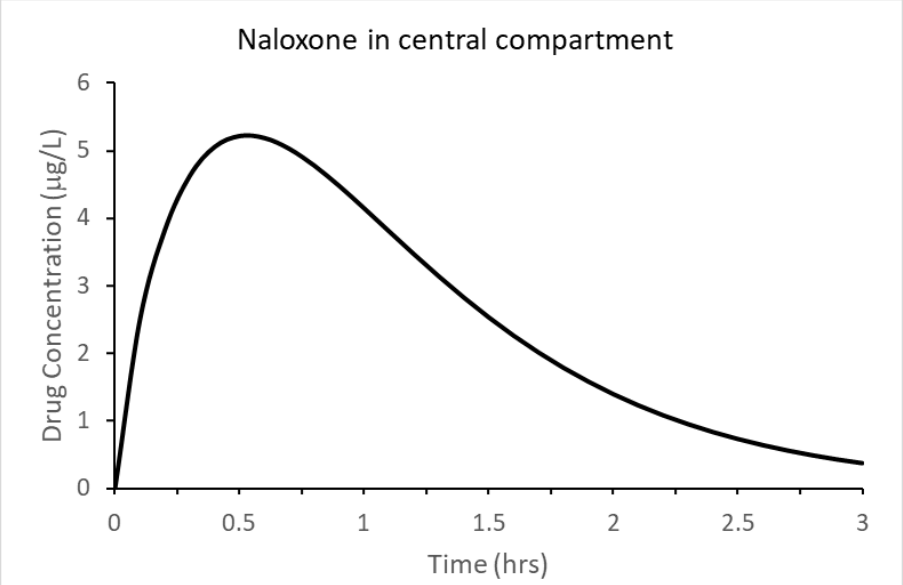

Figure 6-5. Concentration-time plot for 2000 µg naloxone IN and no fentanyl.

6.3. Simulations using the naloxone rescue model

To simulate fentanyl overdose scenario and naloxone rescue simulations, the initial conditions for each drug given by (6-1) were as follows. High fentanyl concentrations to approach 60-90% ventilation suppression were generated by inputting fentanyl 500ug and 1000ug IV as overdoses. The first naloxone dose was given at 5 minutes (t_1 = 0.0833 h) after the fentanyl IV dose, which mimics the overdose scenario (including initial fentanyl disposition) and rescues the naloxone situation.

The simulations demonstrated that naloxone could displace bound fentanyl and reduce ventilation suppression. The rescue was a function of the fentanyl IV dose, the naloxone administered per dose, and the number of naloxone doses given. Plots for fentanyl and naloxone concentrations in the brain and changes in ventilation response illustrate the impact of varied naloxone dosing on the rescue effect.

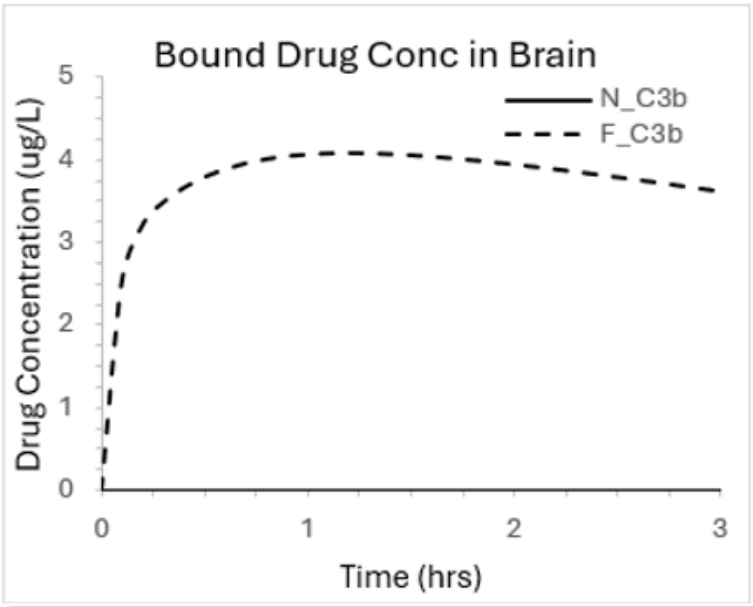

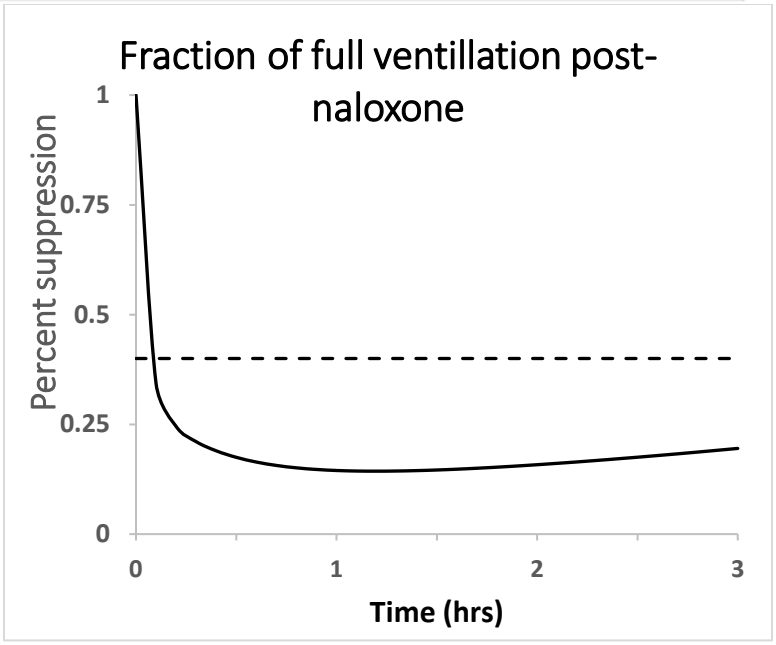

Figure 6-6. Fentanyl 500 μg IV and no naloxone IN dose at 5 minutes.

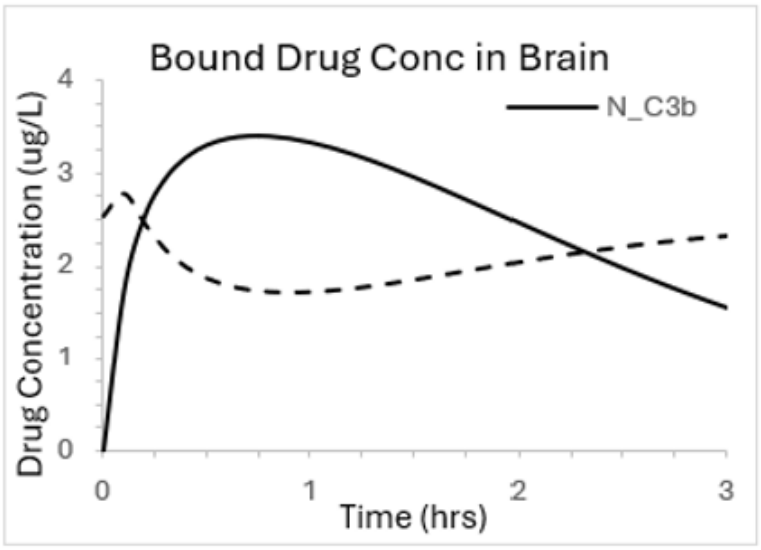

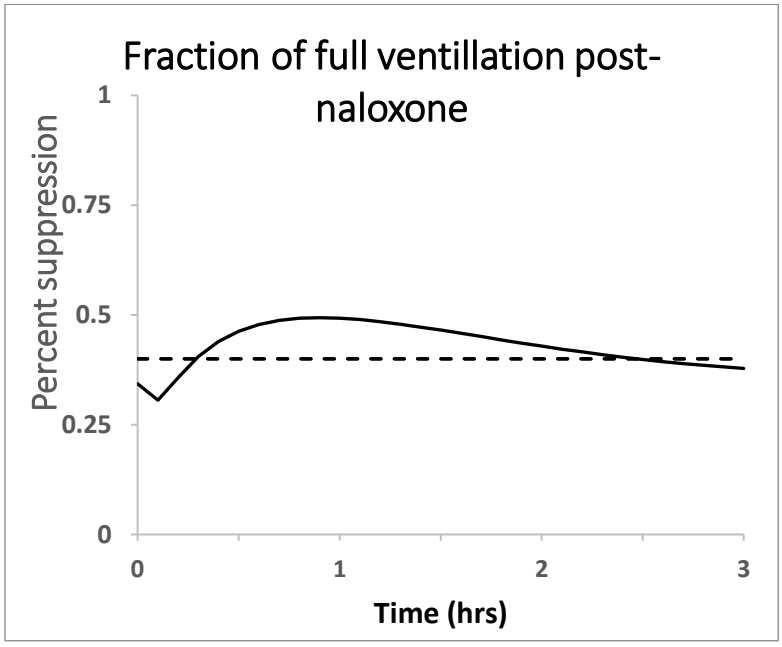

Figure 6-7. Fentanyl IV 500 μg followed by 4 mg naloxone IN at 5 minutes.

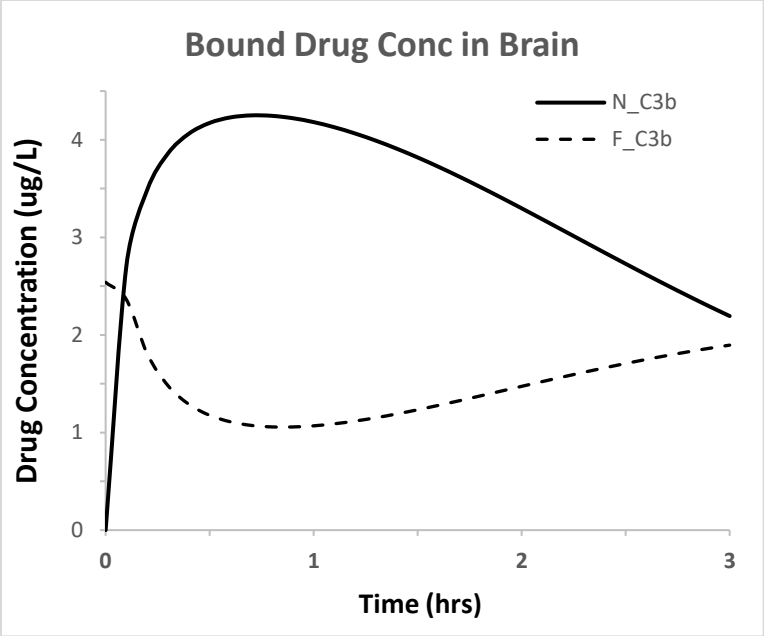

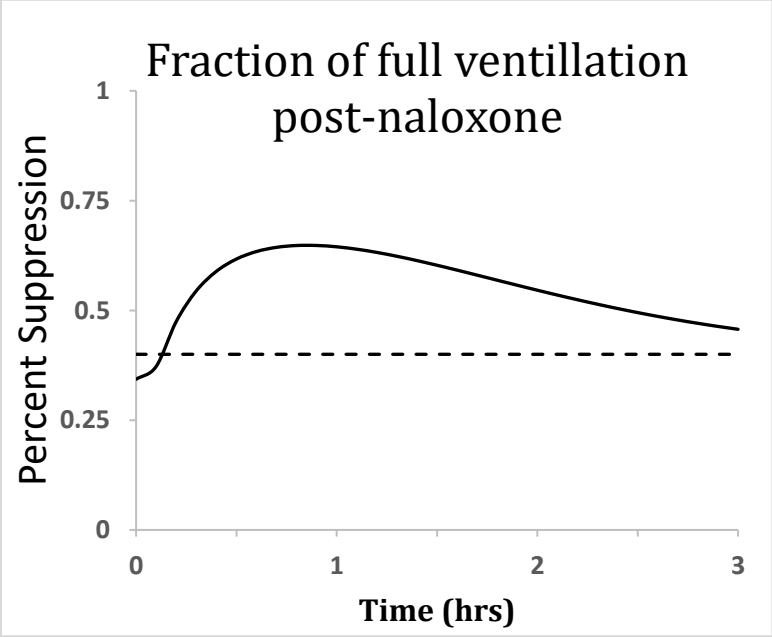

Figure 6-8. Fentanyl 500 μg IV followed by naloxone 8mg IN at 5 minutes.

CHAPTER 7. PATIENT POPULATION SIMULATIONS

The combined fentanyl overdose and naloxone rescue model was modified to simulate results for a hypothetical patient population and predict the population pharmacokinetics of fentanyl and naloxone. It describes the variability in drug exposure and response among different individuals. Understanding the variability, clinicians can tailor treatments to optimize naloxone efficacy, optimize dosage regimen, ensure more effective treatments and minimize adverse effects.

7.1. Generating a hypothetical patient population

The hypothetical patient population was generated using the physiologically relevant parameter values obtained from the individual drug models. The hypothetical range (minimum to maximum) assigned to each parameter value was based on assumed physiologically reasonable estimates. In the population, each patient has a unique combination of parameter values.

To simulate the patient variations in the population, physiologically "reasonable" ranges (minimum-maximum) of parameter values were assumed for each physiological parameter. A set of 1000 patients (1000 sets of parameter values) was then created by creating random variations around each average. This was done in R using the function `rlnormTrunc`, which produces a truncated log-normal distribution around the average. In generating the parameter distributions, the standard deviation for each parameter was taken as 0.5×(maximum – minimum), and the truncation required all values generated to fall between the minimum and maximum.

The parameters used (base, standard deviation, minimum and maximum) are listed in Table 7-1 and written into an EXCEL file as 1000 rows x 28 columns. (Table 7-1 lists 29 parameters, but the volume of the brain compartment was taken as equal for naloxone and fentanyl.) In each population simulation, the parameter values were imported into R as a matrix and read one row (patient) at a time to simulate that individual patient. For each patient, the values of the 23 variables of interest (mass, concentration, etc. vs. time) were stored. After the entire population was simulated, the average and standard deviation were calculated for each variable and at each time.

The target base parameter values and ranges are listed in Table 7-1. After generating the patient population, the averages and standard deviations for the generated population were calculated. As shown in Table 7-2, they were consistent with but varied slightly from, the target values used to generate the population.

Table 7-1. Target parameters for the hypothetical patient population.

Parameter	**Name in R**	**Base value**	**Min**	**Max**
Fentanyl free fraction in the blood, fr_{F1}	fr_F1	0.15	0.1	0.2
Naloxone free fraction in the blood, fr_{N1}	fr_N1	0.5	0.4	0.6
Fentanyl mass transfer rate constant (compartment-1 and -2), k_{F12}	k_F12	892	700	1100
Fentanyl mass transfer rate constant (compartment-1 and -3), k_{F12}	k_F13	11.02	9	14
Fentanyl distribution constant (compartment-1 and -2), K_{F12}	K_F12	0.89	0.5	1.5

Fentanyl distribution constant (compartment-1 and -3), K_{F13}	K_F13	2.4	2	3.5
Fentanyl elimination mass transfer rate constant, k_{Fe}	k_Fe	195	120	350
Fentanyl binding rate constant at MORs, k_{F3f}	k_F3b	7335	5000	11000
Fentanyl release rate constant at MORs, k_{F3r}	k_F3r	10.27	7	25
Fentanyl central compartment volume, V_{1F}	V_1F	10	4.5	20
Fentanyl peripheral compartment volume, V_{2F}	V_2F	480	250	800
Fentanyl brain compartment volume, V_{3F}	V_3F	1.3	1	1.6
Fraction absorbed (nasal to central compartment) for naloxone, F_{N1}	F_N1	0.4	0.2	0.5
Fraction absorbed (nasal to brain compartment) for naloxone, F_{N3}	F_N3	0.4	0.2	0.5
Naloxone mass transfer rate constant (nasal to compartment-1), k_{N01}	k_N01	1.03	0.4	2.5
Naloxone mass transfer rate constant (nasal to brain), k_{N03}	k_N03	0.01	0.005	0.02
Naloxone mass transfer rate constant (compartment-1 and -2), k_{N12}	k_N12	1900	1000	3500
Naloxone mass transfer rate constant (compartment-1 and -2), k_{N13}	k_N13	3.07	2	5
Naloxone distribution constant (compartment-1 and -2), K_{N12}	K_N12	0.25	0.15	0.5
Naloxone distribution constant (compartment-1 and -3), K_{N13}	K_N13	0.54	0.25	1
Naloxone elimination mass transfer rate constant, k_{Ne}	k_Ne	400	200	600
Naloxone binding rate constant at MORs, k_{N3b}	k_N3b	116700	70000	200000
Naloxone release rate constant at MORs, k_{N3r}	k_N3r	140	70	350
Naloxone nasal compartment volume, V_{0N}	V_0N	0.47	0.25	1
Naloxone central compartment volume, V_{1N}	V_1N	85	40	150

Naloxone peripheral compartment volume, V_{2N}	V_2N	370	200	750
Naloxone brain compartment volume, V_{3N}	V_3	1.3	1.0	1.6
Total MOR receptor, P_{3t}	P_3t	0.017	0.007	0.02
Fentanyl critical value, F_{cr}	F_cr	0.71	0.6	0.8

Table 7-2. Average parameters for the population generated from Table 7-1.

Parameter	**Name in R**	**Base value**	**Standard Dev**
Fentanyl free fraction in the blood, fr_{F1}	fr_F1	0.144	0.029
Naloxone free fraction in the blood, fr_{N1}	fr_N1	0.494	0.058
Fentanyl mass transfer rate constant (compartment-1 and -2), k_{F12}	k_F12	886.6	113.5
Fentanyl mass transfer rate constant (compartment-1 and -3), k_{F12}	k_F13	11.30	1.46
Fentanyl distribution constant (compartment-1 and -2), K_{F12}	K_F12	0.905	0.269
Fentanyl distribution constant (compartment-1 and -3), K_{F13}	K_F13	2.633	0.402
Fentanyl elimination mass transfer rate constant, k_{Fe}	k_Fe	217.4	65.8
Fentanyl binding rate constant at MORs, k_{F3f}	k_F3b	7673	1738
Fentanyl release rate constant at MORs, k_{F3r}	k_F3r	13.90	4.97
Fentanyl central compartment volume, V_{1F}	V_1F	10.22	4.40
Fentanyl peripheral compartment volume, V_{2F}	V_2F	473.8	154.7
Fentanyl brain compartment volume, V_{3F}	V_3F	1.281	0.170
Fraction absorbed (nasal to central compartment) for naloxone, F_{N1}	F_N1	0.336	0.089

Fraction absorbed (nasal to brain compartment) for naloxone, F_{N3}	F_N3	0.327	0.085
Naloxone mass transfer rate constant (nasal to compartment-1), k_{N01}	k_N01	1.030	0.051
Naloxone mass transfer rate constant (nasal to brain), k_{N03}	k_N03	0.011	0.001
Naloxone mass transfer rate constant (compartment-1 and -2), k_{N12}	k_N12	2022	714
Naloxone mass transfer rate constant (compartment-1 and -2), k_{N13}	k_N13	3.190	0.759
Naloxone distribution constant (compartment-1 and -2), K_{N12}	K_N12	0.286	0.099
Naloxone distribution constant (compartment-1 and -3), K_{N13}	K_N13	0.544	0.203
Naloxone elimination mass transfer rate constant, k_{Ne}	k_Ne	364.0	112.5
Naloxone binding rate constant at MORs, k_{N3b}	k_N3b	122699	36474
Naloxone release rate constant at MORs, k_{N3r}	k_N3r	172.7	77.8
Naloxone nasal compartment volume, V_{0N}	V_0N	0.541	0.204
Naloxone central compartment volume, V_{1N}	V_1N	83.72	31.21
Naloxone peripheral compartment volume, V_{2N}	V_2N	421.5	157.8
Naloxone brain compartment volume, V_{3N}	V_3	1.281	0.170
Total MOR receptor, P_{3t}	P_3t	0.012	0.004
Fentanyl critical value, F_{cr}	F_cr	0.695	0.058

Simulations of the patient population naloxone rescue involved the following steps.

1. The combined model was run in R with the 1000 patient parameters.
2. R read each line of the parameter values as a single patient, and the model was run to solve the ODEs.

3. The output data (e.g., mass and concentration of both drugs in different compartments vs. time) were stored internally in R.
4. Once the code was run on all the 1000 patients, data stored internally in R were evaluated internally, and the average of all the outputs, their standard deviation, and the maximum and minimum values were output in the form of a matrix in R.
5. This output data was exported to Excel for further graphical analysis and to create population study plots.
6. All the outputs were plotted as three lines—the average and two lines for the average plus and minus one standard deviation at each time point for the plotted variable.
7. The ventilation suppression was also calculated and plotted, representing the primary clinical outcome in patient response for different overdose and rescue situations.
8. Simulations were repeated with different fentanyl overdoses and naloxone doses, and the responses were compared.
9. For comparison purposes, the rescue level was assigned to 40% of base ventilation,
    - If the ventilation function did not reach 40%, no rescue was possible with naloxone administration.
    - If the ventilation function reached 40% or above, the time to rescue t_{rescue} was taken as the time between the first naloxone dose and the time at which 40% function was achieved.
10. The time to return to 40% ventilation is also an important factor since a more extended time means the patient cannot be resuscitated due to apnea or cardiac failure.

Figures 7-1 to 7-20 show various simulations for the hypothetical populations, with the solid line representing the average output variable vs. time (mass, concentration, ventilation fraction, etc.) and the dashed lines representing the data ± one standard deviation about the mean at each time.

7.2. Initial simulation of fentanyl 500 μg IV and naloxone 4 mg after 5 minutes

An initial patient population simulation was done for fentanyl 500μg IV fentanyl and naloxone 4 mg IN administered after 5 minutes (0.0833 h). The outputs included plots for the masses and concentrations (mass/volume) of both drugs vs. time in central (M_{F1}, M_{N1}; C_{F1}, C_{N1}) and peripheral (M_{F2}, M_{N2}; C_{F2}, C_{N2}) compartments, the masses and molar concentrations in the brain for the free drug (M_{F3f}, M_{N3f}; c_{F3f}, c_{N3f}) and the bound drug (M_{F3b}, M_{N3b}; c_{F3b}, c_{N3b}) in the brain compartment, as well as the corresponding concentrations of both drugs (C_{F1}, C_{N1}), peripheral (C_{F2}, C_{N2}) and free (C_{F3f}, C_{N3f}), and bound drug (C_{F3b}, C_{N3b}) in the brain compartment, molar concentration of free (c_{F3f}, c_{N3f}), and bound drug (c_{F3b}, c_{N3b})in brain and the ventilation fraction with time.

Figure 7-1 to Figure 7-4 show the fentanyl dispositions vs. time in different compartments. The simulations display rapid distribution from the central compartment to the peripheral and brain compartments. Also, the fentanyl quickly binds to the MORs, reaching its maximum bound concentration in the brain in ~ 9 minutes.

Figure 7-5 - Figure 7-8 display the naloxone dispositions vs. time in the same compartments shown for fentanyl. The simulations indicate that naloxone IN is absorbed rapidly into the central compartment and is distributed quickly to the peripheral and brain compartments. After entering the brain compartment, the simulations show the naloxone displaces the fentanyl, with the effects beginning to show as soon as 2 minutes after the IN administration, even though the bound naloxone does not reach its maximum concentration until l~ 30 minutes after IN administration.

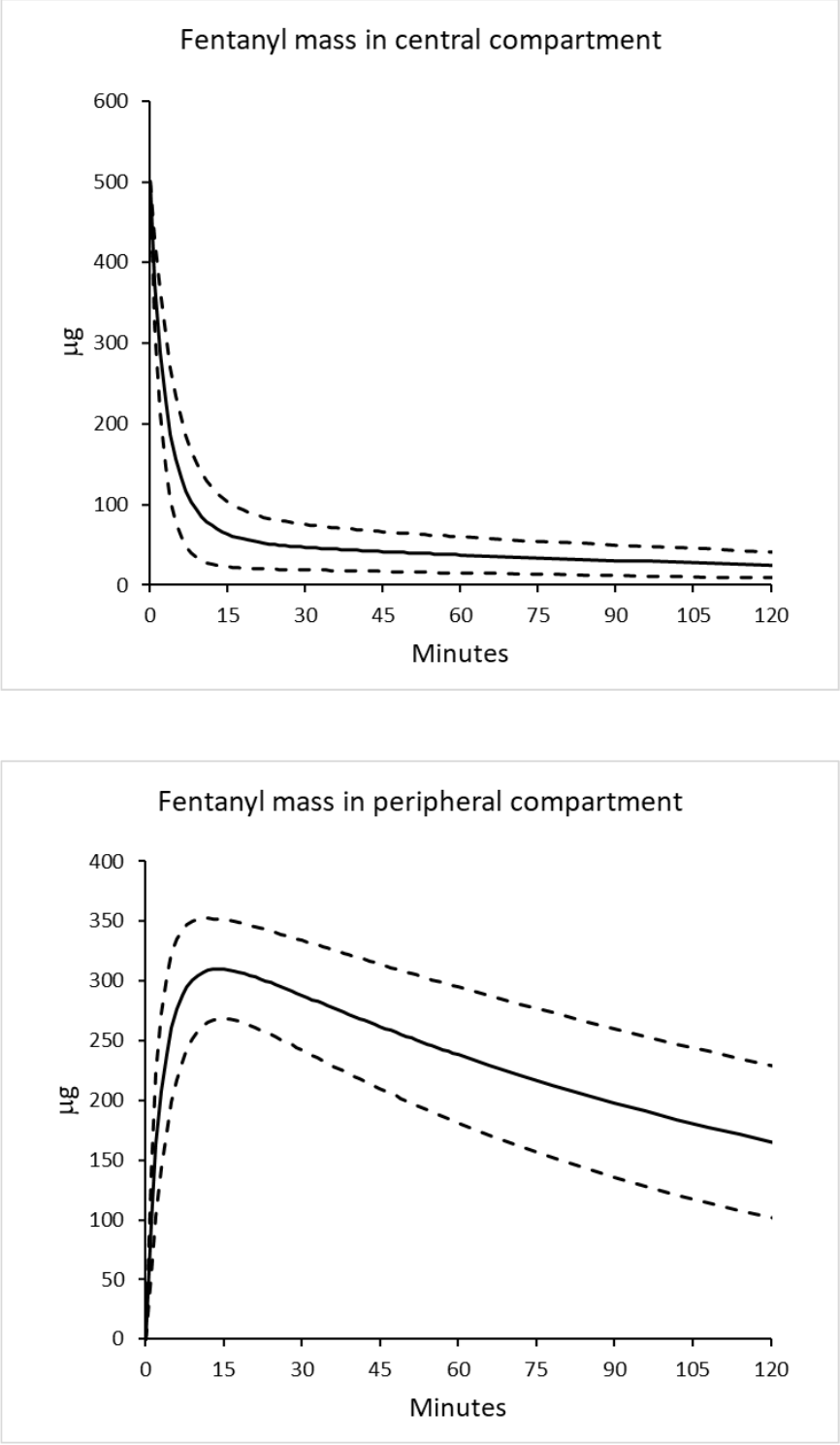

Figure 7-1. Fentanyl mass in the central and peripheral compartments.

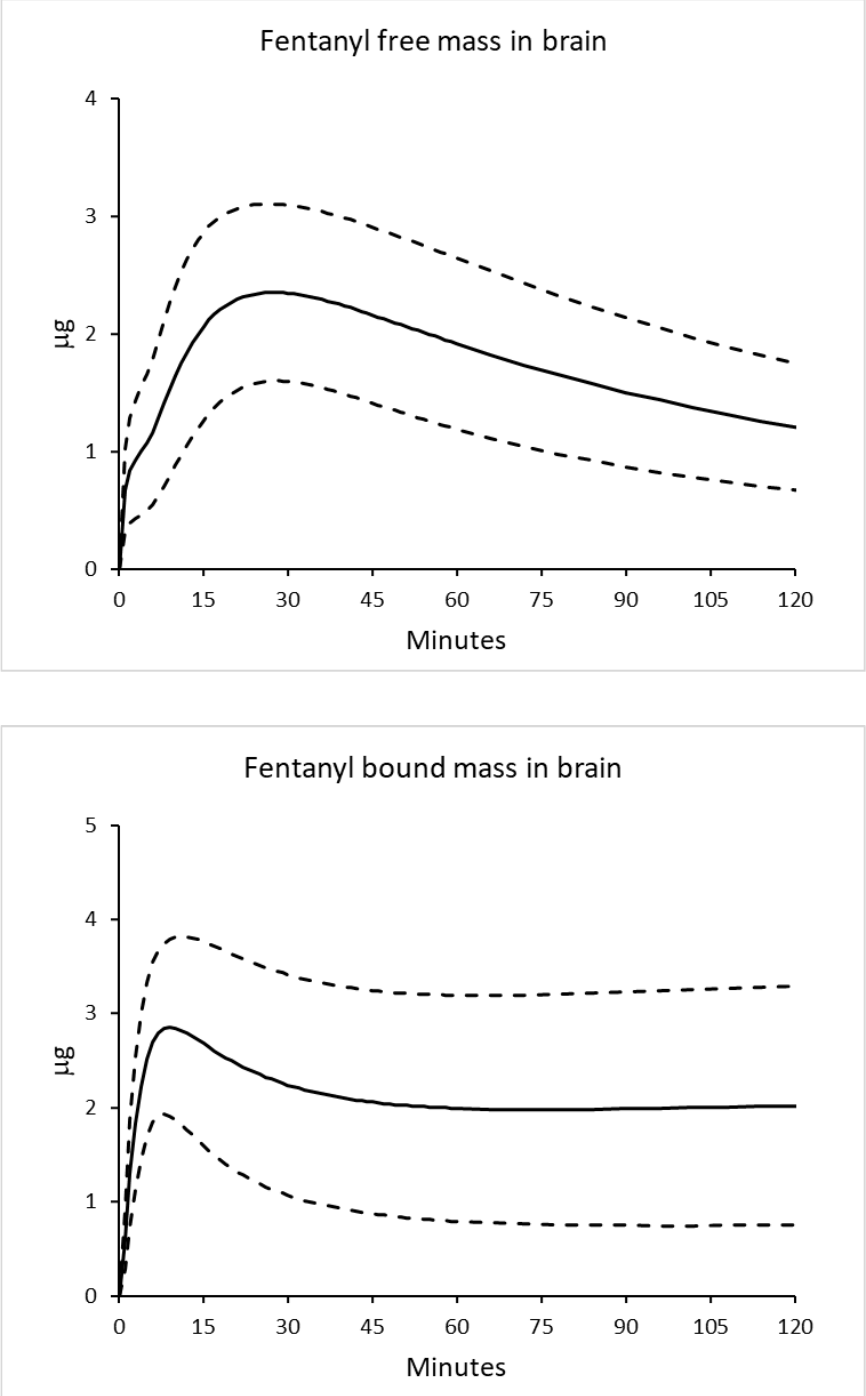

Figure 7-2. Fentanyl free and bound mass in the brain.

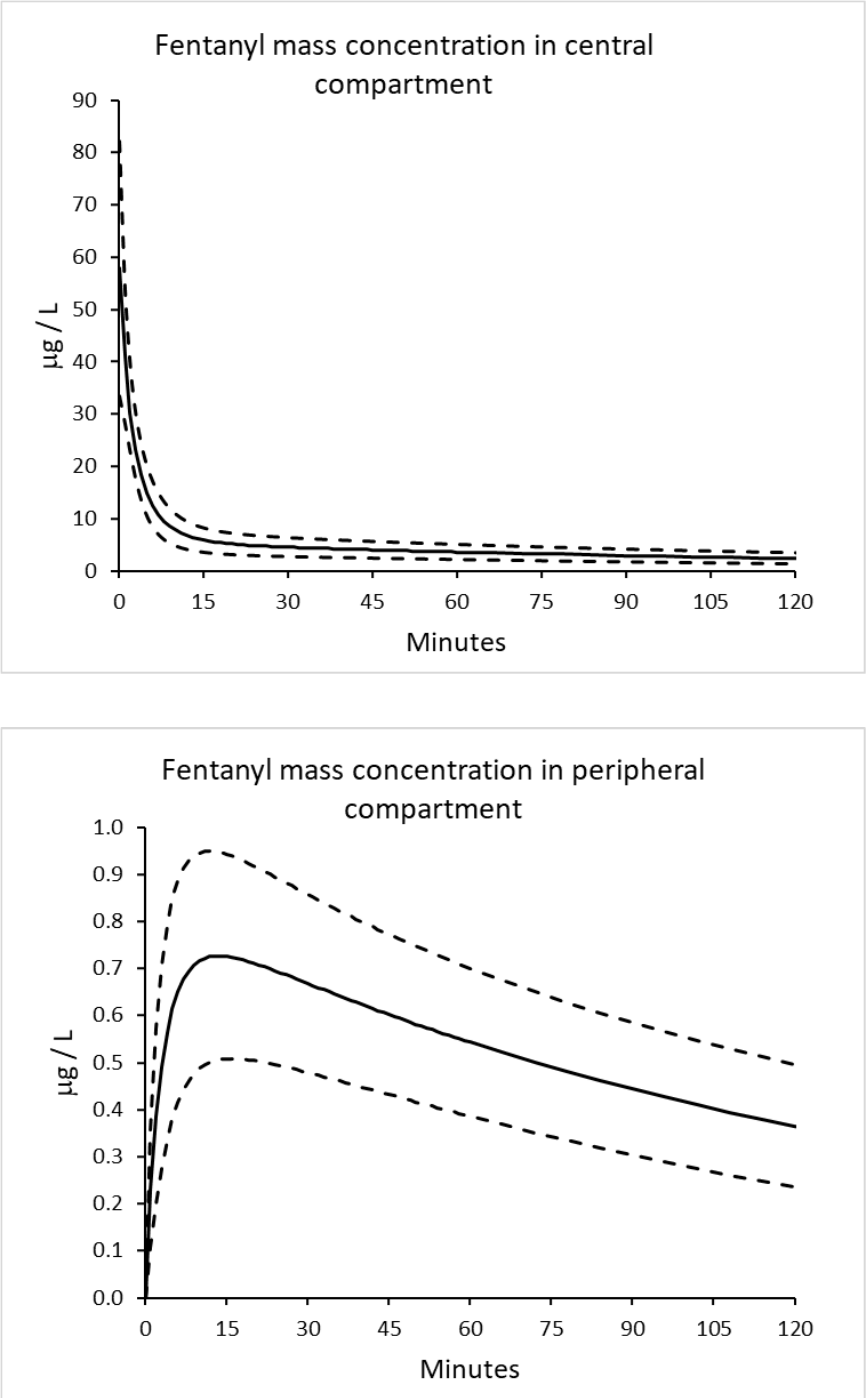

Figure 7-3. Fentanyl mass concentrations in the central and peripheral compartments.

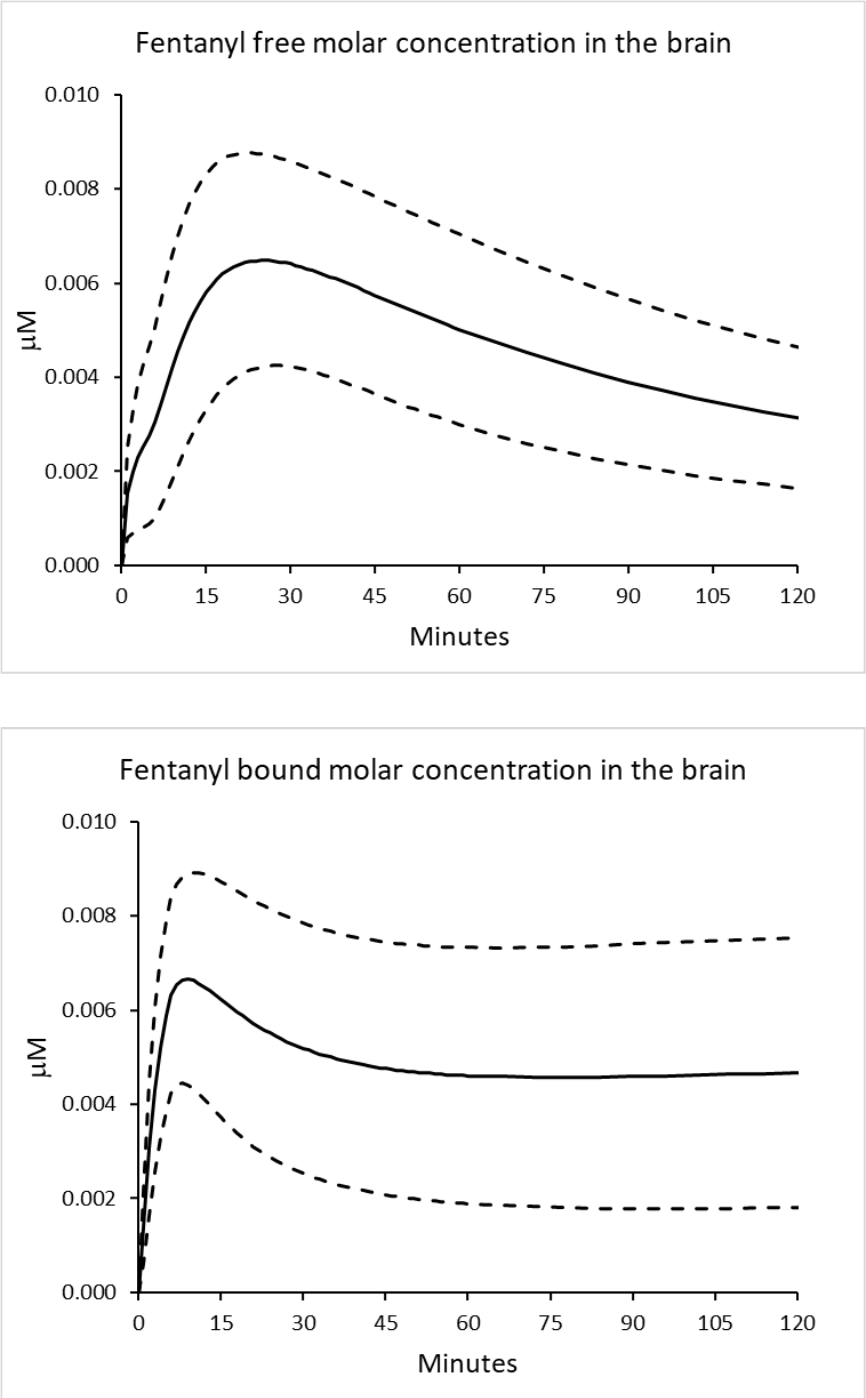

Figure 7-4. Fentanyl free and bound molar concentrations in the brain.

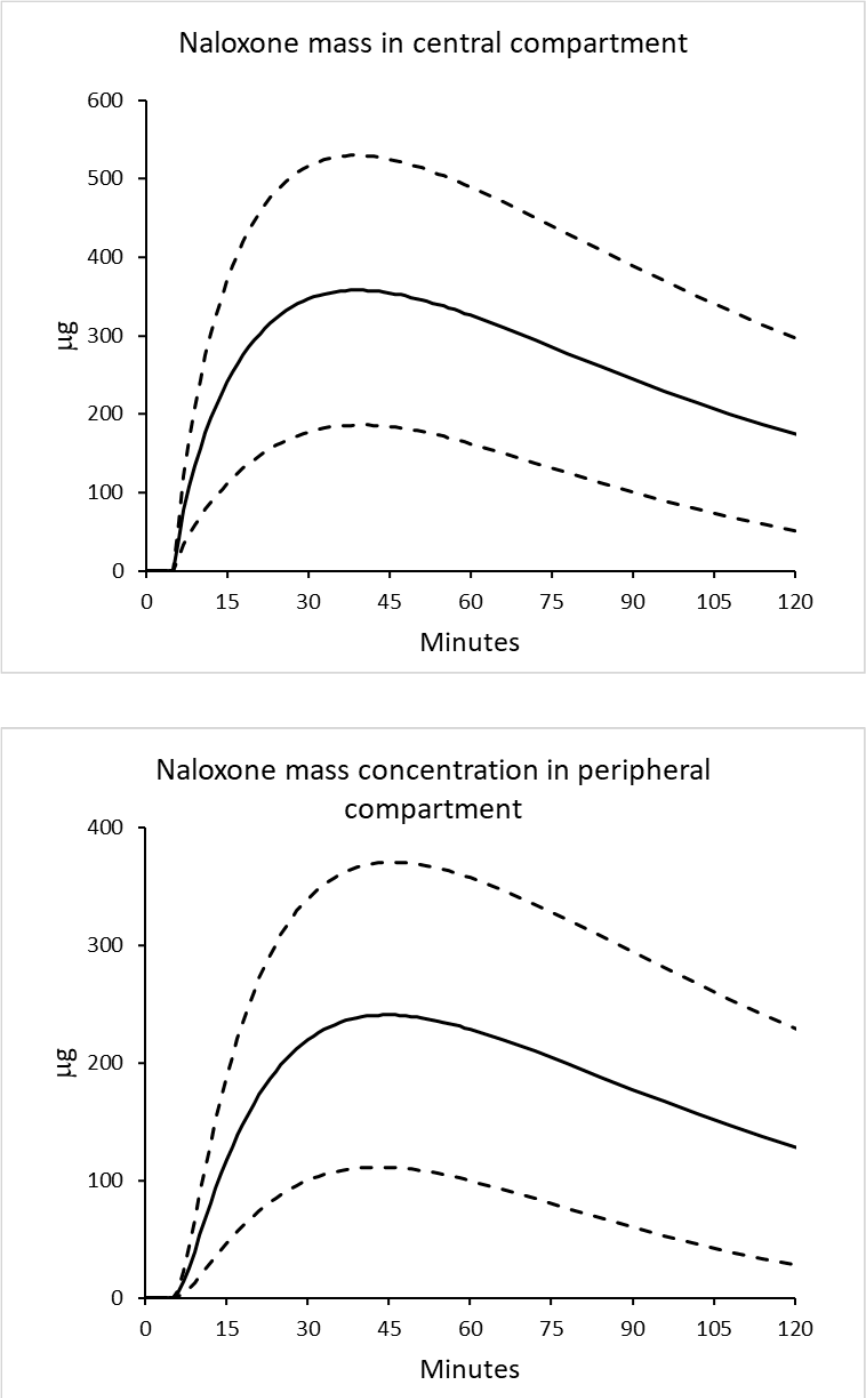

Figure 7-5. Naloxone mass in the central and peripheral compartments.

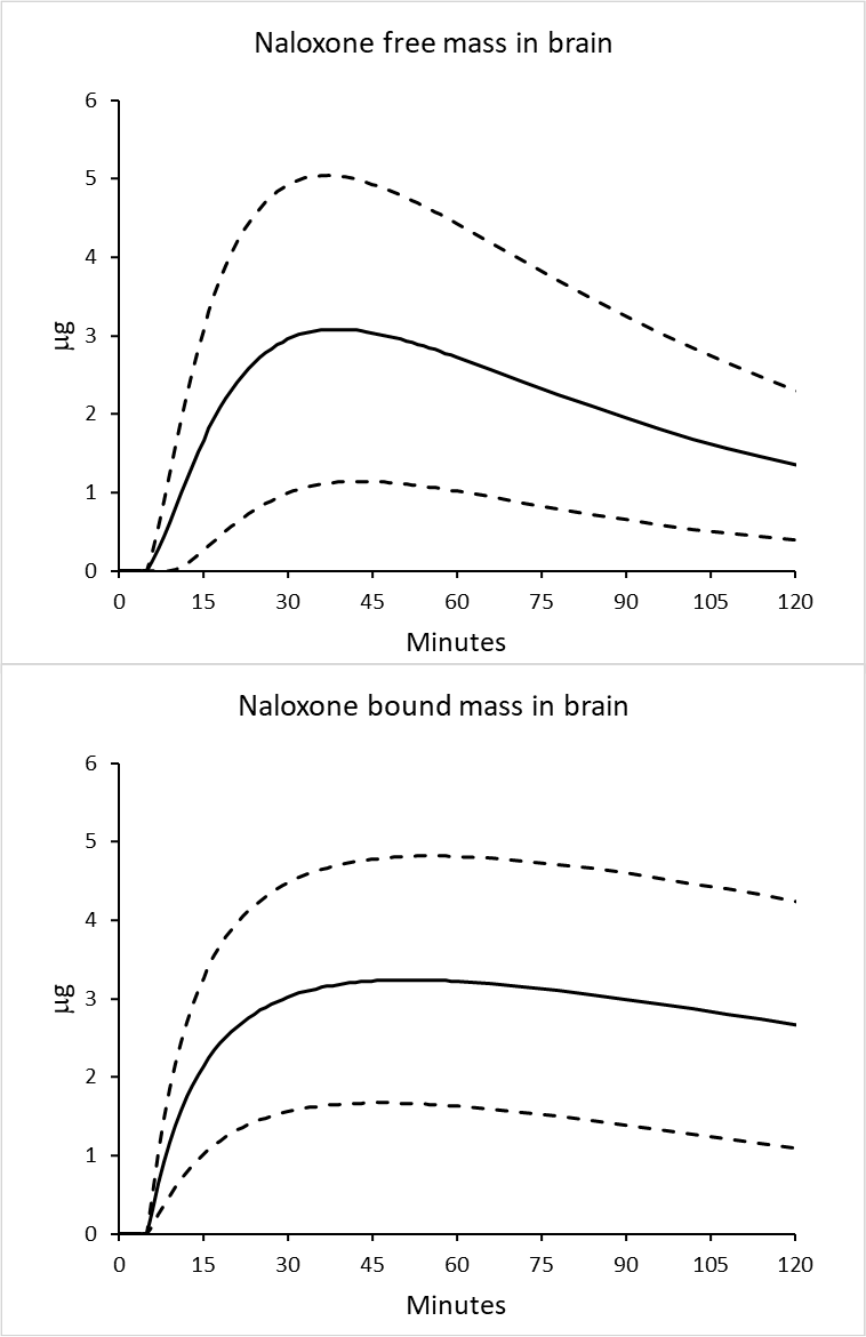

Figure 7-6. Naloxone free and bound mass in the brain.

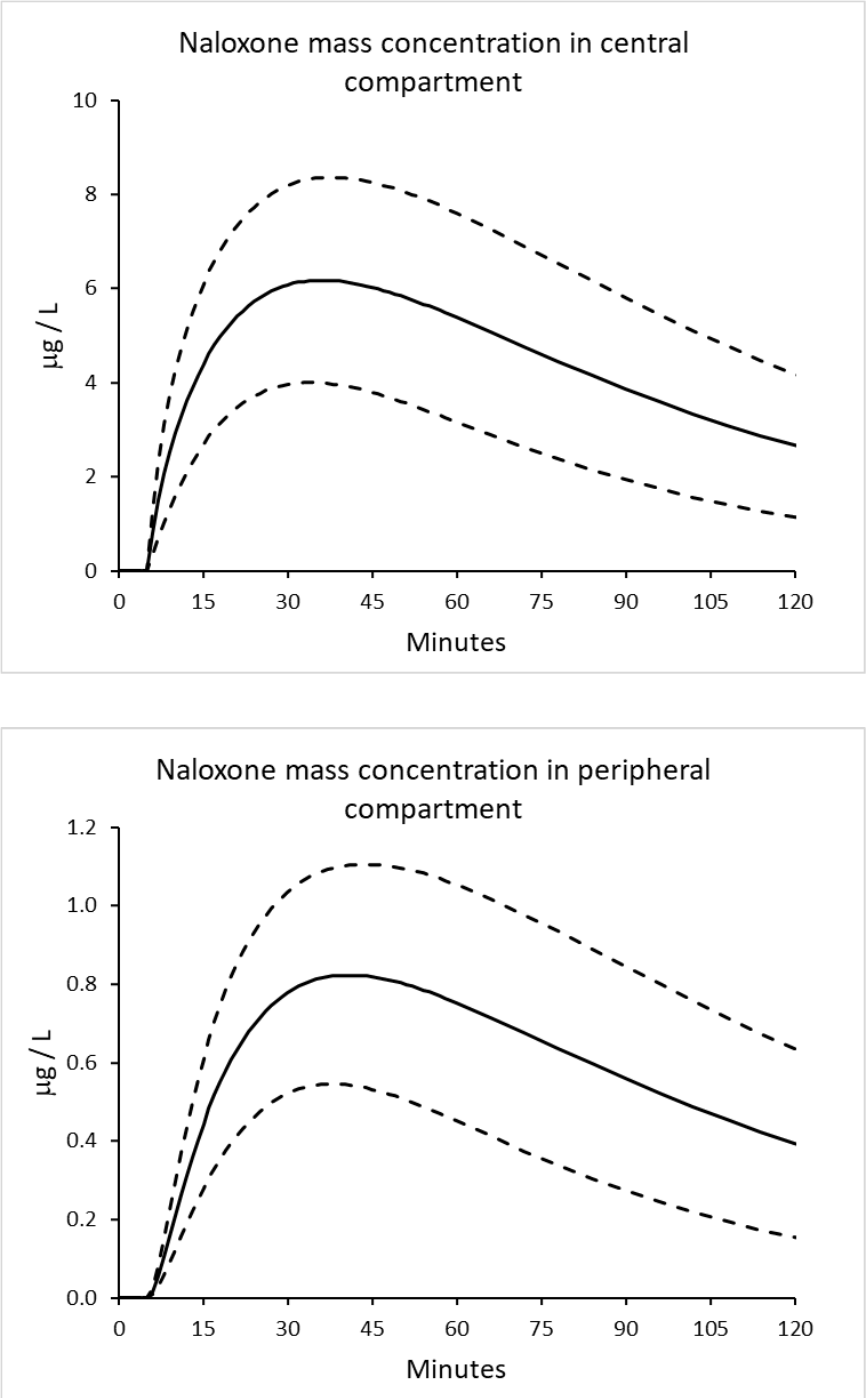

Figure 7-7. Naloxone mass concentration in the central and peripheral compartments.

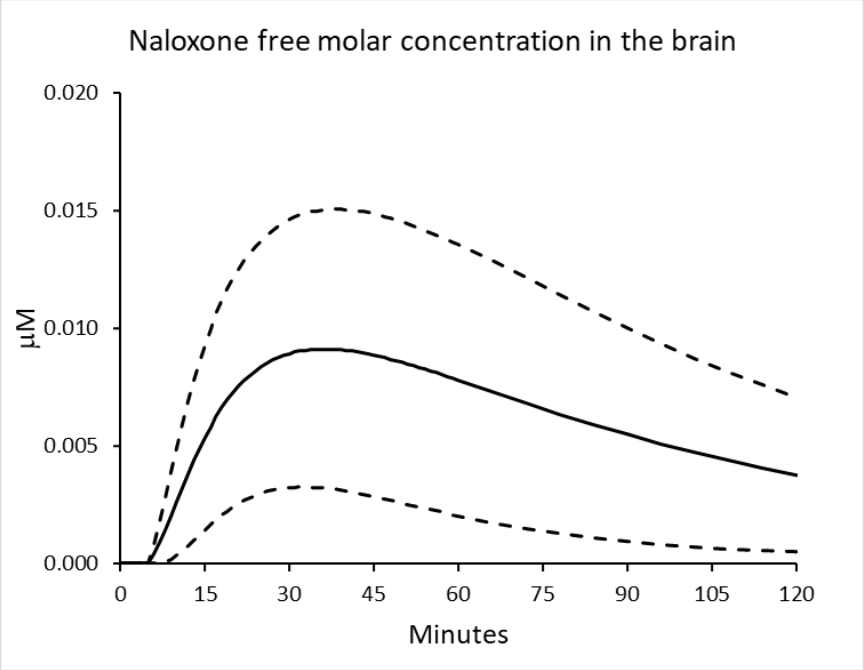

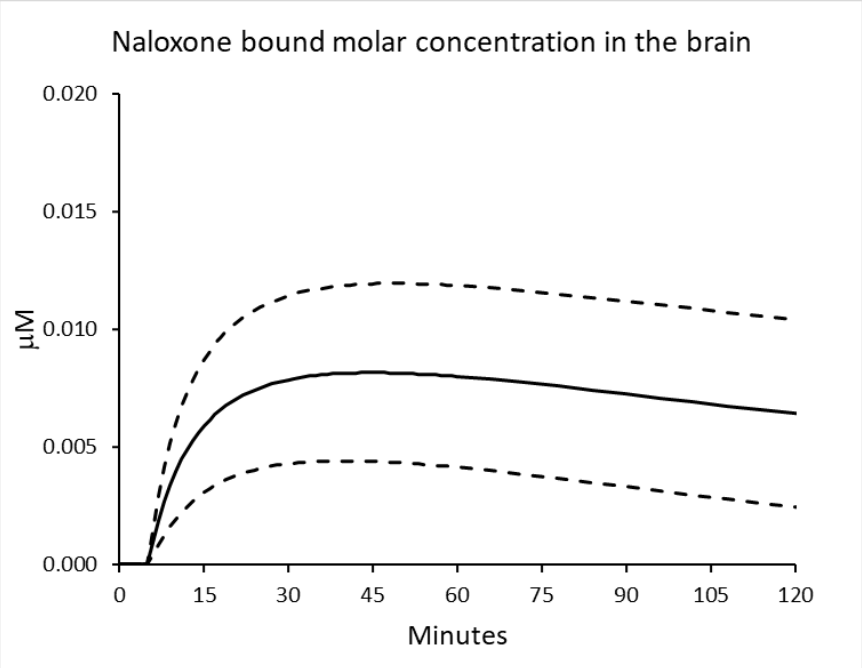

Figure 7-8. Naloxone free and bound mass in the brain.

Percent of full ventilation when IN naloxone is given at 5 minutes. Figure 7-9 shows the percent of full ventilation function vs. the elapsed time after the IN naloxone dose. The plots show the same data on two timescales, 0-60 and 0-480 minutes. In all ventilation recovery plots that follow, the first (or only) naloxone dose is given 5 minutes after the IV fentanyl overdose. The plots show that a single 4 mg of IN naloxone dose can displace fentanyl and increase the ventilation function. The decline in ventilation is not very deep, falling to an average minimum of 31% and rising back to 50% in about 1 hour. Thus, rescue in patients with 500µg fentanyl is possible with 1 dose of 4000µg IN naloxone.

Figure 7-11 is the prototype plot to show the clinical response after naloxone rescue dosing. A horizontal dotted line at 40% is included because 40% ventilation is (arbitrarily) chosen as the percent function at which a successful rescue has occurred. For successful rescues, the time interval between the first naloxone dose and when the ventilation reaches 40% is defined as the rescue time (t_{rescue}).

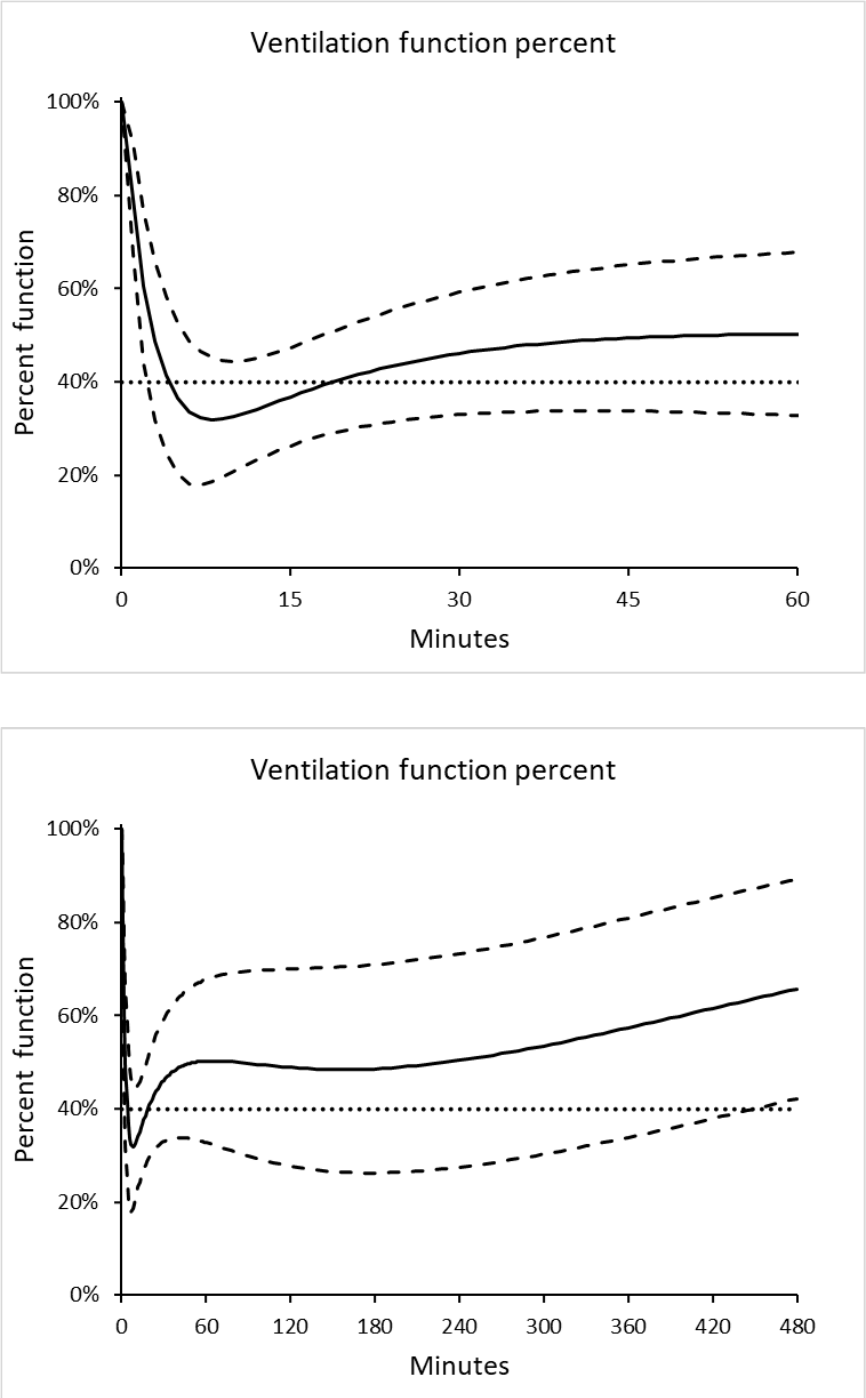

Figure 7-9. Percent of full ventilation when IN naloxone is given at 5 minutes.

7.3. Rescue simulations for other fentanyl doses and naloxone rescue regimens

For comparison of different clinical overdose scenarios, only the ventilation function was considered. Other plots were quite similar, and few differences were observed depending on the mass of the drug. The main rescue effect was due to naloxone binding to the MOR, which lessens the extent of fentanyl binding to the MORs in the brain compartment. The ventilation response in the patients more effectively represents these effects.

Various rescue simulations and their interpretations are given below. Two general observations were made from the scenarios that follow.

- The initial drop in the ventilation function that occurs over the first five minutes of the simulations is a critical parameter. This represents the loss of ventilation before the naloxone dosing and establishes the starting point for the rescue. For lower doses of fentanyl, $F_{vent,min}$ is not at a life-threatening level. However, it becomes lower with higher fentanyl doses and reaches potentially low levels for fentanyl IV doses of 1000μg or more.

- The initial drop in ventilation function is very rapid at all fentanyl doses, and almost all of the initial drop in ventilation function occurs in the first 5 minutes. Thus, for a given fentanyl dose, the drop in ventilation to $F_{vent,min}$ is essentially independent of the naloxone rescue regimen.

- The rescue time t_{rescue} was used for sensitivity analyses but may not be the most appropriate factor for assessing the likelihood of an overdose fatality. From a clinical perspective in the field, avoiding a fatality is perhaps better assessed by the ventilation fraction several minutes after the first naloxone dose. If it is too low at 10-12 minutes (5-7 minutes after the rescue regimen is started), the overdose is likely fatal.

7.3.1. Simulations for IV fentanyl 500µg and 1000µg IV, no naloxone.

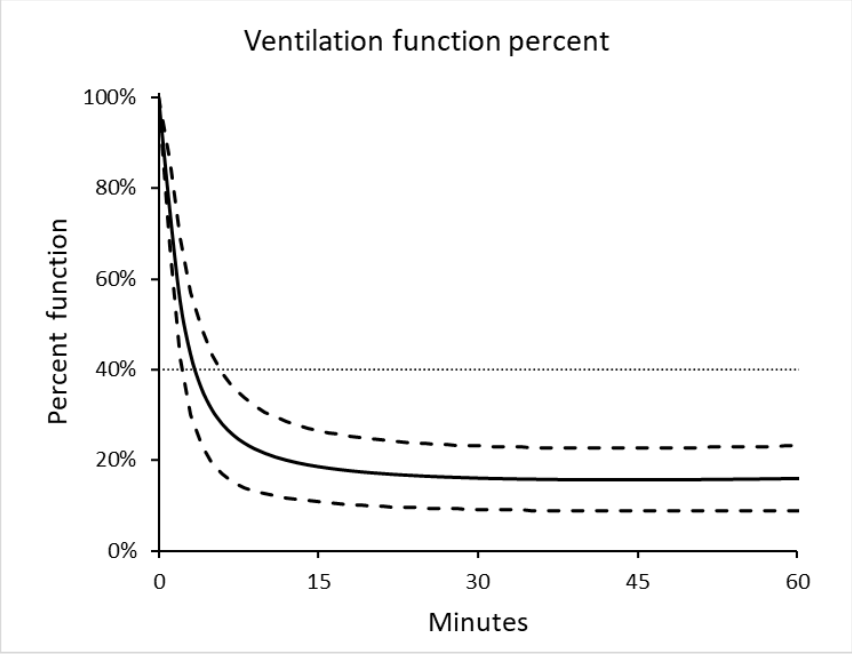

Figure 7-10. Ventilation after 500 IV fentanyl and no naloxone rescue.

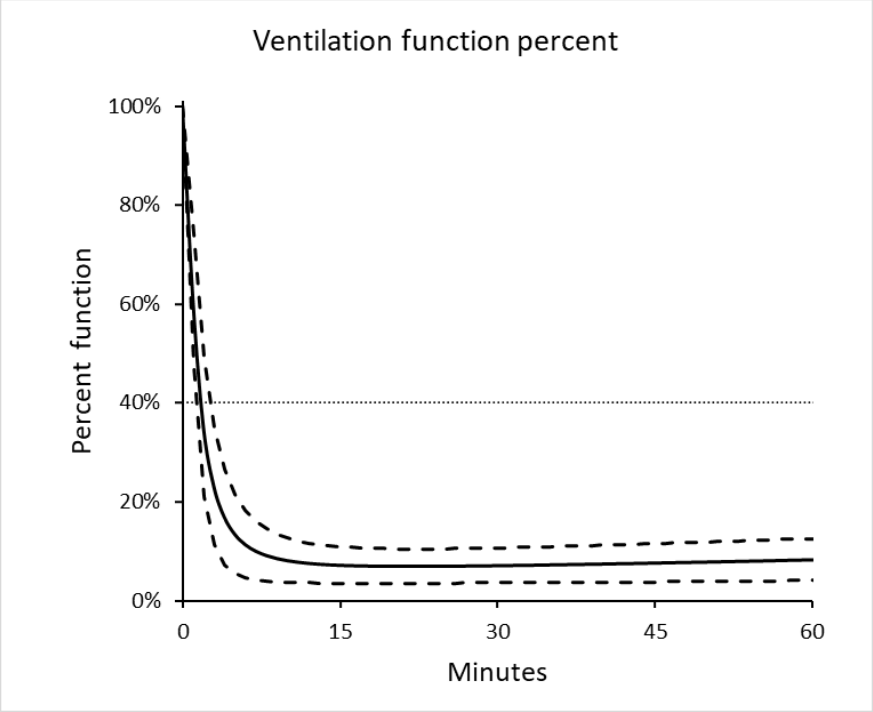

Figure 7-11. Ventilation after 1000µg IV fentanyl and no naloxone rescue.

Without naloxone administration, a 500µg fentanyl overdose can be fatal for some fraction of the patient population, with a rapid fall in ventilation that averages below 20% for more than an hour. In a clinical situation, this might be a fatal condition for some patients, so quick naloxone administration is imperative to rescue some patients from a 500µg fentanyl overdose.

A 1000µg fentanyl overdose is likely to be fatal, with the ventilation falling to below 10% for at least an hour. Not shown are simulations for 2000 µg and 4000 µg IV fentanyl, in which the ventilation falls to below 5% and is fatal without naloxone intervention.

7.3.2. Simulation for 300µg IV fentanyl overdose and one dose of 4 mg IN naloxone given after 5 minutes.

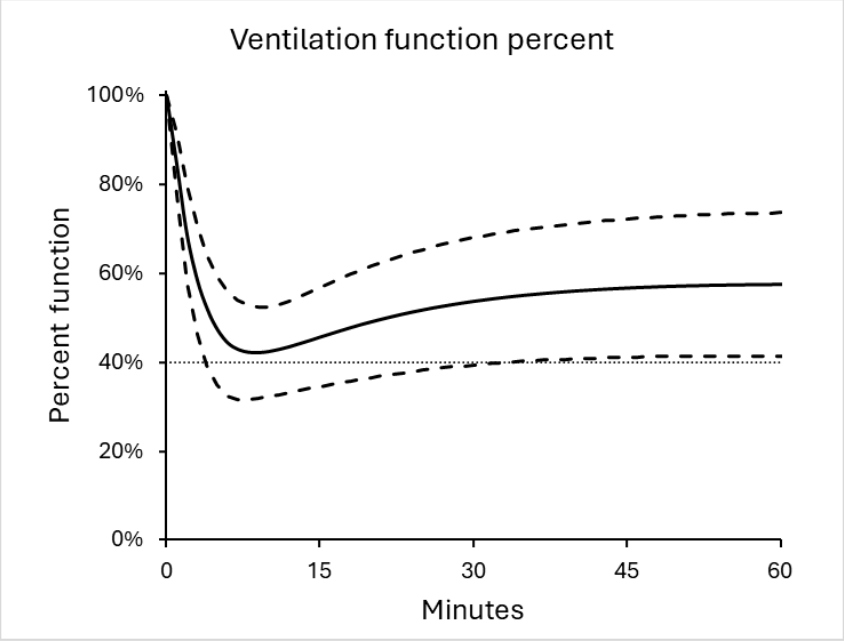

Figure 7-12. Ventilation after 300µg IV fentanyl and single naloxone 4mg IN dose after 5 minutes.

The ventilation only declines to ~42%, and a single 4 mg of IN naloxone dose can increase the ventilation function to ~50% in 25 minutes. So, rescue in patients with 300µg fentanyl overdose is possible with only 1 dose of 4 mg IN naloxone.

7.3.3. Simulations for 500µg IV fentanyl overdose and multiple IN doses of naloxone 4 mg

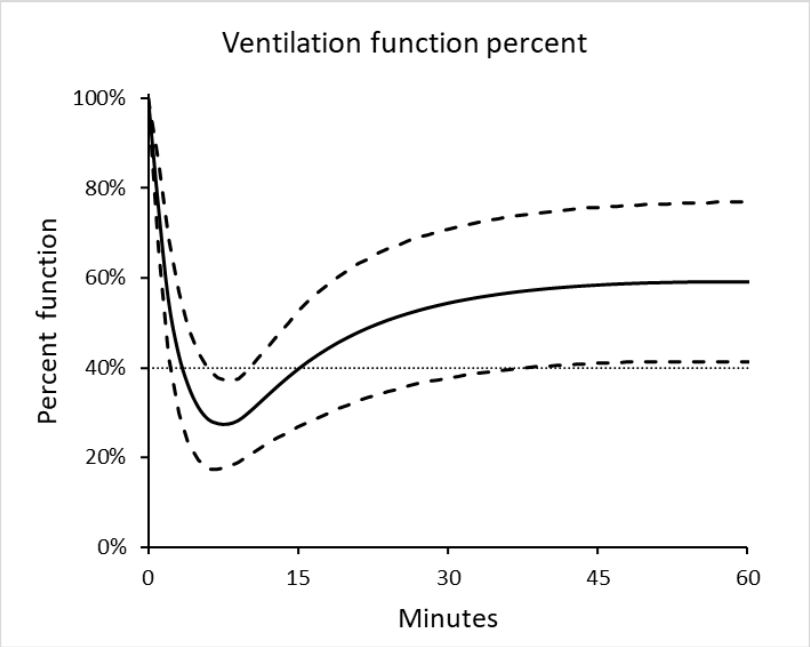

Figure 7-13. Ventilation after 500µg IV fentanyl and naloxone 4mg at 5 and 8 minutes.

Clinical implication: The fall in ventilation is not much, about 27% on average, and two 4000µg of IN naloxone doses can increase the ventilation function; it rises back after 3 minutes of naloxone addition and reaches 40% in about 15 minutes. Two doses bring the rescue faster than a single dose of naloxone. So, rescue in patients with 500µg fentanyl overdose is quickly possible with two doses of 4 mg IN naloxone.

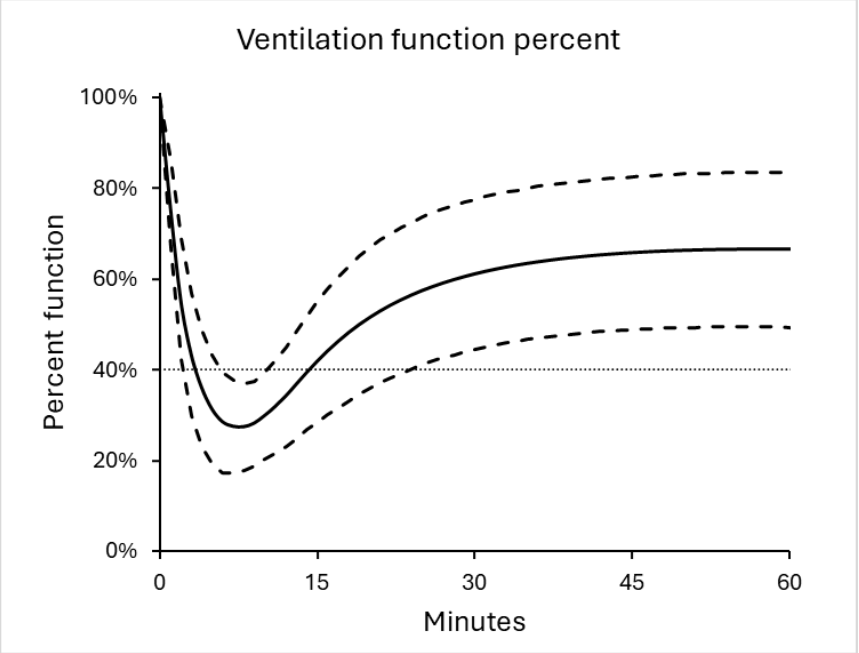

Figure 7-14. Ventilation after 500 µg IV fentanyl and naloxone 4mg at 5, 8 and 11 minutes.

The fall in ventilation is not much, about 27% on average, and as shown earlier, two 4 mg of IN naloxone doses can increase the ventilation function, so giving an additional dose is unnecessary. Instead, three doses can cause withdrawal symptoms due to high doses of naloxone and rapid fentanyl displacement. Thus, two doses are likely sufficient to rescue a 500µg fentanyl overdose for most patients simulated.

7.3.4. Simulations for 1000µg IV fentanyl and multiple 4 mg IN doses.

Simulations are shown for naloxone 4 mg rescue doses given at 5, 5 and 8, and 5,8 and 11 minutes.

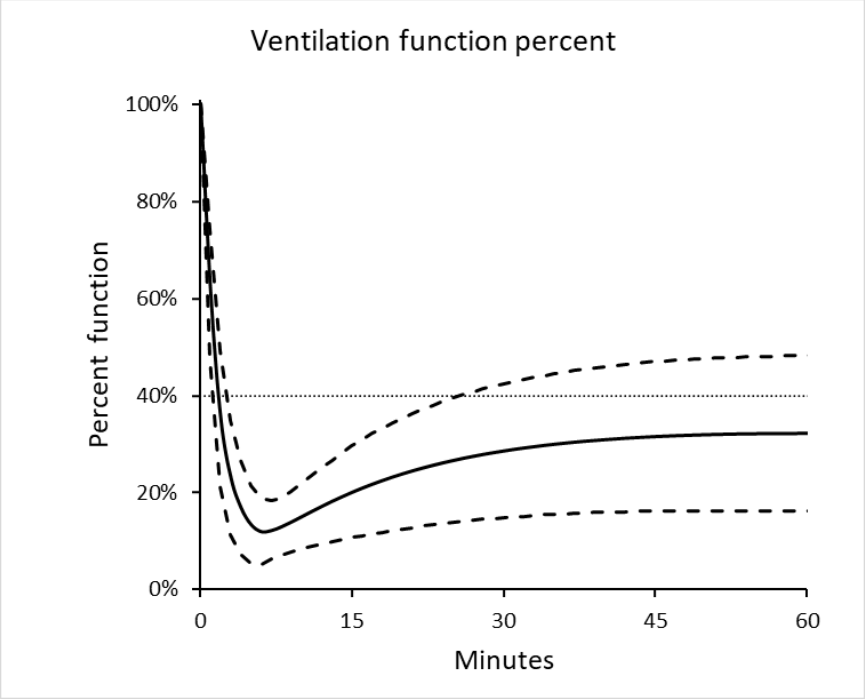

Figure 7-15. Ventilation after 1000 µg IV fentanyl and naloxone 4mg at 5 minutes.

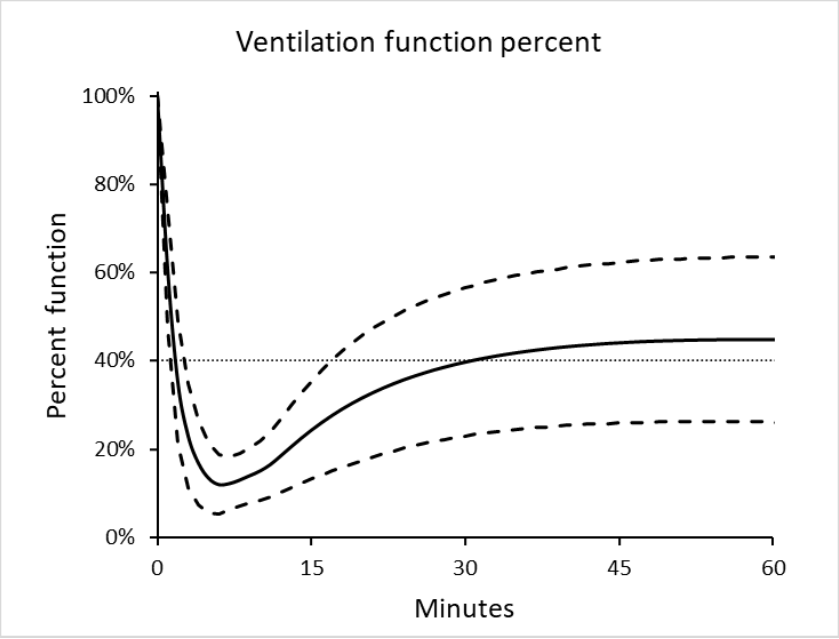

Figure 7-16. Ventilation after 1000 µg IV fentanyl and naloxone 4mg at 5 and 8 minutes.

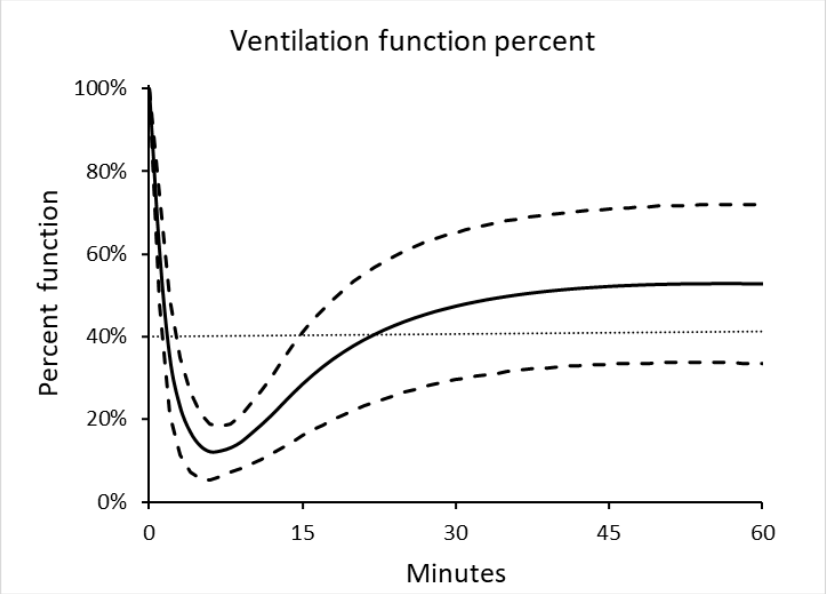

Figure 7-17. Ventilation after 1000 µg IV fentanyl and naloxone 4mg at 5, 8 and 11 minutes.

For all three simulations, there is a severe and rapid decline in the ventilation to ~ 12% on average, and a single 4 mg of IN naloxone dose cannot increase the ventilation function to 40%. The situation would be fatal, and a higher dose of naloxone would be needed to rescue the patient. Administering two rescue doses of 4 mg of IN naloxone increases the ventilation function somewhat but would not fully rescue the ventilation function rapidly enough to avoid likely supportive measures. Administering three rescue doses improved the rescue but still required too much time for the rescue to avoid supportive measures.

7.3.5. Simulations for 2000µg and 4000 µg IV fentanyl and naloxone 4mg at 5, 8 and 11 minutes

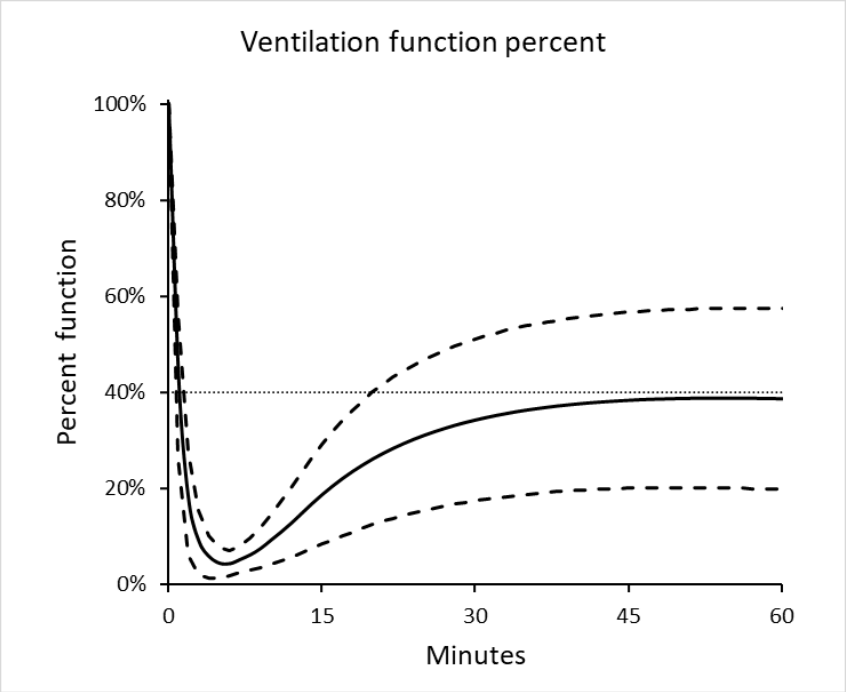

Figure 7-18. Ventilation after 2000 µg IV fentanyl and naloxone 4mg at 5, 8 and 11 minutes.

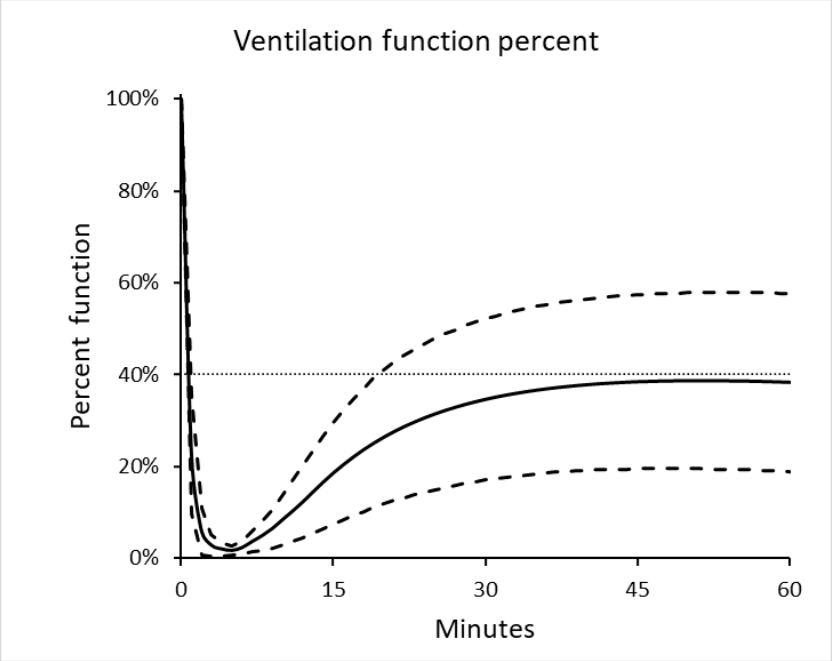

Figure 7-19. Ventilation after 4000 µg IV fentanyl and naloxone 4mg at 5, 8 and 11 minutes.

Clinical implication: The fall in ventilation is severe, to below ~ 5% on average before the first dose of naloxone is given, and the three doses of 4 mg of IN naloxone dose cannot increase the average ventilation function to 40%, although s substantial fraction of the patient population is rescued to above 40%. However, the rescue times are likely too long to avoid patient deaths, with the ventilation fractions 6 minutes after the naloxone dose recovering to only ~9% on average and ~17% for the patients who respond best.

For the 2000µg fentanyl dose, the initial drop in ventilation is to ~2% over the 5 minutes before the naloxone dose is administered. The three doses of 4 mg of IN naloxone do not raise the ventilation function sufficiently by 12-15 minutes to avoid fatality, and the 40% rescue is never reached on average. The initial rapid decrease to such a low ventilation

function is itself fatal. The fentanyl is already a lethal dose, and no amount of naloxone, no matter how quickly administered, is likely to rescue the patient.

7.3.6. Simulations for 1000µg IV fentanyl and naloxone 8 mg at 5 and 8 minutes

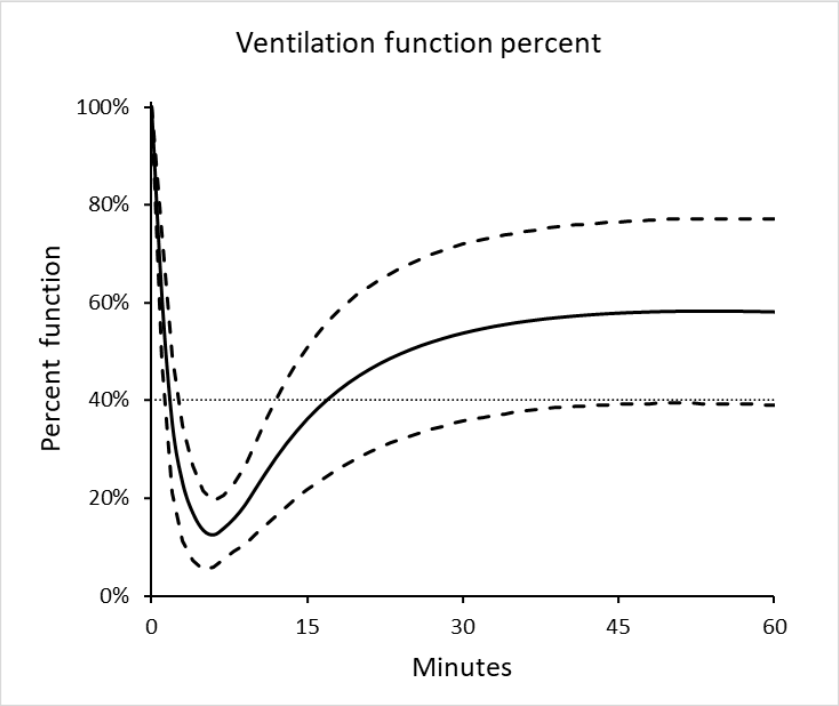

Figure 7-20. Ventilation after 1000 µg IV fentanyl and naloxone 8mg at 5 and 8 minutes.

The fall in ventilation is much greater, to ~12%, and two doses of 8 mg of IN naloxone can rapidly increase the ventilation function; it rises back to 40% in about 16 minutes. However, this might result in effects and be more detrimental to the patient since fentanyl concentration falls and rises rapidly. So, rescue in patients with 1000µg fentanyl

overdose would be better with three doses of 4 mg IN naloxone instead of a higher dose at once.

7.4. Parameter sensitivity analyses on the population simulations

It is useful to assess the sensitivity of the analyses with respect to changes in the parameter values, which can identify which parameters are most important to characterize accurately. Theoretically, the sensitivity can be assessed for each output variable (mass, concentration) for each time, compartment and drug as a function of each parameter. However, this is impractical and not needed. Instead, the sensitivities were assessed for two outcomes: the minimum fraction of full ventilation function ($F_{vent,\min}$) during an overdose and rescue simulation and the time from the first naloxone dose to when the ventilation reaches 40% of its full function (the rescue time t_{rescue}).

The sensitivity analysis was done over the entire population (i.e., for 1000 sets of the 28 28 parameters). The same population of 1000 patients (base population) described above was used, and each of the 28 parameters was varied one at a time by increasing the respective parameter value by 5% from its base value. This resulted in constructing 28 other populations (sets of 1000 parameter values), with only one parameter in each of the 28 populations differing from the base set of values.

Thus, there were 29 populations (including the base), so 29 full patient population simulations were run. The simulations were done for 500 mg fentanyl IV with a single

dose of naloxone 4 mg IN given 5 minutes after the fentanyl, and the average $F_{vent,\min}$ and t_{rescue} were calculated for each of the 29 population simulations.

The sensitivities were defined as the ratio of the fractional change in the outcome to the fractional change in the parameter (always 0.05, or 5%) or

$$\begin{aligned}\Delta F_{vent,\min} / \Delta P &= \frac{\left(Varied\, F_{vent,\min} - base\, F_{vent,\min}\right)}{\left(base\, F_{vent,\min}\right)} / 0.05 \\ \Delta t_{rescue} / \Delta P &= \frac{\left(Varied\, t_{rescue} - base\ t_{rescue}\right)}{\left(base\ t_{rescue}\right)} / 0.05\end{aligned} \tag{7-1}$$

The sensitivities are shown in Table 7-3 and 7-4, along with 1) the base value of the outcome (from the base population simulation), 2) the calculated values of the respective outcome when the base parameter value was increased by the 5% used to calculate the sensitivity, and 3) the calculated outcome and percent difference from the base calculation if the respective parameter value is raised by 1.0 standard deviation.

The results indicate that $F_{vent,min}$ was sensitive to several parameters, as highlighted in bold in Table 7-3, and relatively insensitive to variations in the others. On the other hand, the recovery as characterized by t_{rescue} was much more sensitive to more parameters, highlighted in bold in

Table 7-4.

Generally, these parameters reflect the availability of both drugs to the brain compartment and characterize the competition between fentanyl and naloxone for binding sites at the MORs.

Table 7-3. Parameter sensitivities for the minimum fraction of full ventilation.

			With + 1.0 SD change	
Parameter P	$F_{Vent,min}$	$\Delta F_{Vent,min} / \Delta P$	% change	Calc value
Base parms	0.274039			
fr_F1	0.269212	-0.08911	0.26921	-1.7614%
fr_N1	0.274082	0.00133	0.27408	0.0156%
k_F12	0.279478	0.15504	0.27948	1.9849%
k_F13	**0.262448**	**-0.32698**	**0.26245**	**-4.2296%**
K_F12	0.274833	0.00973	0.27483	0.2899%
K_F13	0.272976	-0.02543	0.27298	-0.3880%
k_Fe	0.275818	0.02145	0.27582	0.6491%
k_F3f	0.269216	-0.07769	0.26922	-1.7600%
k_F3r	0.278485	0.04536	0.27849	1.6225%
V_1F	0.279116	0.04305	0.27912	1.8526%
V_2F	0.274833	0.00888	0.27483	0.2899%
F_N1	0.275686	0.02278	0.27569	0.6011%
F_N3	0.274039	0.00000	0.27404	0.0000%
k_N01	0.274020	-0.00144	0.27402	-0.0071%
k_N03	0.275634	0.01497	0.27563	0.5819%
k_N12	0.274033	-0.00006	0.27403	-0.0021%
k_N13	0.274037	-0.00003	0.27404	-0.0007%
K_N12	0.274038	-0.00001	0.27404	-0.0005%
K_N13	0.274091	0.00050	0.27409	0.0188%
k_Ne	0.274037	-0.00002	0.27404	-0.0006%
k_N3f	0.274643	0.00741	0.27464	0.2202%
k_N3r	0.273527	-0.00415	0.27353	-0.1870%
V_0N	0.272525	-0.01467	0.27252	-0.5526%
V_1N	0.273998	-0.00041	0.27400	-0.0151%

V_2N	0.274038	-0.00001	0.27404	-0.0005%
V_3	**0.284542**	**0.28835**	**0.28454**	**3.8328%**
P_3t	**0.261329**	**-0.15905**	**0.26133**	**-4.6381%**
F_cr	**0.281288**	**0.31715**	**0.28129**	**2.6451%**

Table 7-4. Parameter sensitivities for the rescue times.

			With + 1.0 SD change	
Parameter *P*	t_{Rescue} (minutes)	$\Delta t_{Rescue} / \Delta P$	% change	Calc value
Base parms	19.9			
fr_F1	20.2	0.05488	20.2	1.08%
fr_N1	19.8	-0.04838	19.8	-0.57%
k_F12	19.3	-0.20712	19.4	-2.65%
k_F13	**21.1**	**0.36903**	**20.9**	**4.77%**
K_F12	19.4	-0.07624	19.5	-2.27%
K_F13	**20.8**	**0.23415**	**20.7**	**3.57%**
k_Fe	19.4	-0.06839	19.5	-2.07%
k_F3f	**21.6**	**0.30049**	**21.3**	**6.81%**
k_F3r	**18.4**	**-0.17551**	**18.7**	**-6.28%**
V_1F	19.7	-0.02592	19.7	-1.12%
V_2F	19.4	-0.06957	19.5	-2.27%
F_N1	**18.5**	**-0.22779**	**18.8**	**-6.01%**
F_N3	19.9	0.00000	19.9	0.00%
k_N01	20.2	0.18634	20.1	0.92%
k_N03	**18.7**	**-0.13073**	**18.9**	**-5.08%**
k_N12	20.0	0.00247	20.0	0.09%
k_N13	20.2	0.04181	20.1	1.00%
K_N12	20.0	0.00658	20.0	0.23%
K_N13	19.5	-0.05086	19.6	-1.90%
k_Ne	20.0	0.00640	20.0	0.20%
k_N3f	**18.9**	**-0.13559**	**19.1**	**-4.03%**
k_N3r	**21.1**	**0.10053**	**20.9**	**4.53%**
V_0N	**21.1**	**0.12191**	**20.9**	**4.59%**
V_1N	20.1	0.01618	20.1	0.60%

V_2N	20.0	0.00610	20.0	0.23%
V_3	19.8	-0.05421	19.8	-0.72%
P_3t	**24.1**	**0.57620**	**23.3**	**16.80%**
F_cr	20.0	0.00257	20.0	0.02%

CHAPTER 8. DISCUSSION AND SUMMARY

The project aimed to study the pharmacokinetics of naloxone and the opioid drug fentanyl, develop a model based on physiological characteristics and pharmacological response, and model naloxone rescue from overdose situations. This involved modeling naloxone and fentanyl individually, then putting the drug models together to model and simulate naloxone rescue from a fentanyl overdose.

Both naloxone and fentanyl produce their pharmacological effect by binding with the μ-opioid receptors (MORs) in the brain. When natural or synthetic opioids bind to these receptors, they can alleviate pain and cause euphoria, induce more adverse effects such as ventilation suppression. The models in this project focused on the interactions of naloxone and fentanyl with the MORs, which are involved with the adverse pharmacological effects of fentanyl and the naloxone rescue.

The PBPK model captured the processes involved in drug pharmacokinetics and pharmacodynamics and described each step mathematically to understand the process involved and the factors affecting the process. These processes included 1) IV fentanyl disposition according to a 3-compartment model (central, peripheral and brain compartments) with binding and release kinetics at the MOR binding sites; 2) IV and IN naloxone disposition according to a 3-compartment model (central, peripheral and brain

compartments) with binding and release kinetics at the MOR binding sites; 3) the kinetics of naloxone and fentanyl competitive binding for MOR sites; 4) a clinical response function—the ventilation suppression as a function of the fraction of MORs occupied by fentanyl.

Physiologically relevant parameters were estimated from component clinical studies and used to generate a hypothetical patient population in which the parameters were randomly varied. The population simulations made quantitative predictions by evaluating the systems of equations using the R programming language, and the outcomes were explored.

Several points were key elements of this work. The central and peripheral compartments dominate the mass distribution of both fentanyl and naloxone. This allowed obtaining some of the physiological parameters from estimates of IV clinical data for fentanyl and IV and IN clinical data for naloxone. These estimated parameter values were then used to fit clinical data involving MOR occupation fractions vs. time for naloxone and ventilation response vs. time for fentanyl. Fitting the models to these data allowed estimating parameter values for the drug dispositions in the brain, including the binding and release kinetics with the MORs and constructing a relationship between the fentanyl occupation of MOR sites and the clinical ventilation suppression. Based on these parameters, simulations of naloxone rescue from fentanyl overdose for a variety of Points about naloxone.

The simulations led to several observations. First, published *in vitro* binding and release rate constants for fentanyl and naloxone with MORs likely underestimate their values *in vivo.* In particular, the release rate constant for fentanyl from MORs is likely too small by a factor of 5-10 or more. Simulations using published *in vitro* release rate constants could not reproduce realistic rescue situations because the ventilation rescue was predicted to take too much time. The model indicates that the fentanyl must be released from MOR sites and replaced by naloxone to prevent fentanyl from re-occupying the sites. If the fentanyl release is too slow, this process will take too long.

A related observation is that the naloxone binding rate constant must be significantly larger than that of fentanyl, so MOR sites that release fentanyl are preferentially filled by naloxone. Also, for naloxone to dominate fentanyl in competitive binding to MORs, there must be a sufficient free concentration of naloxone relative to the free concentration of fentanyl in the brain. Thus, naloxone must enter the brain quickly to build up such levels. Also, this explains why too little naloxone or too much fentanyl renders a successful rescue unlikely.

In conclusion, this study successfully modeled the disposition of fentanyl and naloxone and their interactions with MORs, characterized quantitative relationships between the fentanyl interactions with the MORs and the fentanyl-induced ventilation suppression, and quantitatively predicted the ventilation rescue by naloxone administration. These results provide new insight into clinical dosage regimens that can be used to rescue patients from fentanyl overdose. Further studies can be done on expanding the model

with combined opioids and how to prevent withdrawal effects or to study special target patient populations.

REFERENCES

1. World Health Organization (2023). Opioid overdose. https://www.who.int/news-room/fact-sheets/detail/opioid-overdose. (Accessed 10/11/2023)
2. CDC . https://www.cdc.gov/nchs/hus/topics/drug-overdose-deaths.htm. Accessed December 11, 2023
3. https://en.wikipedia.org/wiki/Fentanyl (Accessed 4/6/2024)
4. Lynn, R.R., Galinkin, J. L. (2018). Naloxone dosage for opioid reversal: current evidence and clinical implications. In Therapeutic Advances in Drug Safety (Vol. 9, Issue 1, pp. 63–88). SAGE Publications Ltd. https://doi.org/10.1177/2042098617744161
5. Wikipedia. Naloxone. https://en.wikipedia.org/wiki/Naloxone#Pharmacology (Accessed on 10/11/2023)
6. van Lemmen, M., Florian, J., Li, Z., van Velzen, M., van Dorp, E., Niesters, M., Sarton, E., Olofsen, E., van der Schrier, R., Strauss, D. G., & Dahan, A. (2023). Opioid Overdose: Limitations in Naloxone Reversal of Respiratory Depression and Prevention of Cardiac Arrest. In Anesthesiology (Vol. 139, Issue 3, pp. 342–353). Lippincott Williams and Wilkins. https://doi.org/10.1097/ALN.0000000000004622
7. Drugs.com (2023). Naloxone. https://www.drugs.com/naloxone.html (accessed:9/24/2023)
8. Vahedi, H. S. M., Hajebi, H., Vahidi, E., Nejati, A., & Saeedi, M. (2019). Comparison between intravenous morphine versus fentanyl in acute pain relief in drug abusers with acute limb traumatic injury. *World Journal of Emergency Medicine*, *10*(1), 27–32. https://doi.org/10.5847/wjem.j.1920-8642.2019.01.004
9. https://drugs.ncats.io/drug/36B82AMQ7N (Accessed on 10/10/2023)
10. Merlin, M. A., Saybolt, M., Kapitanyan, R., Alter, S. M., Jeges, J., Liu, J., Calabrese, S., Rynn, K. O., Perritt, R., Pryor, P. W. (2010). Intranasal naloxone delivery is an alternative to intravenous naloxone for opioid overdoses. American Journal of Emergency Medicine, 28(3), 296–303. https://doi.org/10.1016/j.ajem.2008.12.009

11. PubChem: National Library of Medicine (US), National Center for Biotechnology Information; 2004-. PubChem Compound Summary for CID 5284596, Naloxone; https://pubchem.ncbi.nlm.nih.gov/compound/Naloxone (accessed 2023 Oct. 12).
12. https://sciencenotes.org/henderson-hasselbalch-equation-and-examples/
13. https://www.accessdata.fda.gov/drugsatfda_docs/label/2022/215457s000lbl.pdf; FDA Access Data.
14. https://www.accessdata.fda.gov/drugsatfda_docs/label/2015/208411lbl.pdf.
15. https://www.drugs.com/fentanyl.html (Accessed on 3/29/2024)
16. Comer, S. D., & Cahill, C. M. (2019). Fentanyl: Receptor pharmacology, abuse potential, and implications for treatment. In *Neuroscience and Biobehavioral Reviews* (Vol. 106, pp. 49–57). Elsevier Ltd. https://doi.org/10.1016/j.neubiorev.2018.12.005
17. Eshleman, A. J., Nagarajan, S., Wolfrum, K. M., Reed, J. F., Nilsen, A., Torralva, R., & Janowsky, A. (2020). Affinity, potency, efficacy, selectivity, and molecular modeling of substituted fentanyls at opioid receptors. *Biochemical Pharmacology, 182*. https://doi.org/10.1016/j.bcp.2020.114293
18. https://go.drugbank.com/drugs/DB00813 (Accessed on 3/29/2024)
19. Fentanyl injection product information DATA SHEET. (n.d.). by Juno Pharmaceuticals NZ Limited.
20. Illum, L. (2003). Nasal drug delivery - Possibilities, problems and solutions. J. Controlled Rel., 87(1–3), 187–198. https://doi.org/10.1016/S0168-3659 (02) 00363-2
21. Fortuna, A., Schindowski, K., Sonvico, F. (2022). Editorial: Intranasal Drug Delivery: Challenges and Opportunities. In Frontiers in Pharmacology (Vol. 13). Frontiers Media S.A. https://doi.org/10.3389/fphar.2022.868986.

22. Pardeshi, C. V., Belgamwar, V. S. (2013). Direct nose to brain drug delivery via integrated nerve pathways bypassing the blood-brain barrier: An excellent platform for brain targeting. In Expert Opinion on Drug Delivery (Vol. 10, Issue 7, pp. 957–972). https://doi.org/10.1517/17425247.2013.790887
23. Ulusoy S, Bayar Muluk N, Karpischenko S, Passali GC, Negm H, Passali D, Milkov M, Kopacheva-Barsova G, Konstantinidis I, Dilber M, Cingi C. (2022) Mechanisms and solutions for nasal drug delivery - a narrative review. Eur Rev Med Pharmacol Sci. 2022 Dec;26(2 Suppl):72-81. doi: 10.26355/eurrev_202212_30487. PMID: 36524914.
24. Fisher, A. N., Brown, K., Davis, S. S., Parr, G. D., & Smith, D. A. (1987). The effect of molecular size on the nasal absorption of water-soluble compounds in the albino rat. *Journal of Pharmacy and Pharmacology*, *39*(5), 357–362. https://doi.org/10.1111/j.2042-7158.1987.tb03398.x
25. Sabale A, Kulkarni A, Sabale A. Nasal In Situ Gel: Novel Approach for Nasal Drug Delivery. JDDT [Internet]. 15Apr.2020 [cited 26Dec.2023];10(2-s):183-97. Available from: https://jddtonline.info/index.php/jddt/article/view/4029
26. Selvaraj, K., Gowthamarajan, K., Karri, V. V. S. R. (2018). Nose to brain transport pathways an overview: potential of nanostructured lipid carriers in nose to brain targeting. In Artificial Cells, Nanomedicine and Biotechnology (Vol. 46, Issue 8, pp. 2088–2095). Taylor and Francis Ltd. https://doi.org/10.1080/21691401.2017.1420073
27. Pardridge, W. M. (2011). Drug transport in brain via the cerebrospinal fluid. In Fluids and Barriers of the CNS (Vol. 8, Issue 1). https://doi.org/10.1186/2045-8118-8-7
28. Upadhyay, S., Parikh, A., Joshi, P., Chotai, N. P., Upadhyay, U. M. (2011). Intranasal drug delivery system— A glimpse to become maestro. J. Applied Pharmaceutical Science 01 (03), 34-44.

29. Marcello, E., Chiono, V. (2023). Biomaterials-Enhanced Intranasal Delivery of Drugs as a Direct Route for Brain Targeting. In International Journal of Molecular Sciences (Vol. 24, Issue 4). MDPI. https://doi.org/10.3390/ijms24043390
30. Baldo, B. A. (2022). Current research in pathophysiology of opioid-induced respiratory depression, neonatal opioid withdrawal syndrome, and neonatal antidepressant exposure syndrome. *Current Research in Toxicology*, *3*. https://doi.org/10.1016/j.crtox.2022.100078
31. X. Zhuang and C. Lu, "PBPK modeling and simulation in drug research and development," Acta Pharm. Sin. B, vol. 6, no. 5, pp. 430–440, 2016.
32. P. L. Bonate, (2011). "The Art of Modeling," Chapter 1 in *Pharmacokinetic-Pharmacodynamic Modeling and Simulation, 2nd Ed*., Springer, New York.
33. Elzey, M. J., Fudin, J., Edwards, E. S. (2017). Take-home naloxone treatment for opioid emergencies: a comparison of routes of administration and associated delivery systems. In Expert Opinion on Drug Delivery (Vol. 14, Issue 9, pp. 1045–1058). Taylor and Francis Ltd. https://doi.org/10.1080/17425247.2017.1230097
34. Dowling J, Isbister GK, Kirkpatrick CM, Naidoo D, Graudins A. (2008) Population pharmacokinetics of intravenous, intramuscular, and intranasal naloxone in human volunteers. Ther Drug Monit 2008 Aug;30(4):490-6. doi: 10.1097/FTD.0b013e3181816214. PMID: 18641540.
35. Mundin, G., McDonald, R., Smith, K., Harris, S., Strang, J. (2017). Pharmacokinetics of concentrated naloxone nasal spray over first 30 minutes post-dosing: analysis of suitability for opioid overdose reversal. Addiction, 112(9), 1647–1652. https://doi.org/10.1111/add.13849
36. Barton ED, Colwell CB, Wolfe T, Fosnocht D, Gravitz C, Bryan T, Dunn W, Benson J, Bailey J. (2005) Efficacy of intranasal naloxone as a needleless alternative for treatment of opioid overdose in the prehospital setting. J Emerg Med. 2005 Oct;29(3):265-71. doi: 10.1016/j.jemermed.2005.03.007. PMID: 16183444.

37. Kelly AM, Kerr D, Dietze P, Patrick I, Walker T, Koutsogiannis Z. (2005). Randomised trial of intranasal versus intramuscular naloxone in prehospital treatment for suspected opioid overdose. Med J Aust. 2005 Jan 3;182(1):24-7. doi: 10.5694/j.1326-5377.2005.tb06550.x. PMID: 15651944.
38. Kerr D, Kelly AM, Dietze P, Jolley D, Barger B. (2009) Randomized controlled trial comparing the effectiveness and safety of intranasal and intramuscular naloxone for the treatment of suspected heroin overdose. Addiction. 2009 Dec;104(12):2067-74. doi: 10.1111/j.1360-0443.2009.02724.x. PMID: 19922572..
39. Krieter, P. A., Chiang, C. N., Gyaw, S., McCann, D. J. (2019). Comparison of the Pharmacokinetic Properties of Naloxone Following the Use of FDA-Approved Intranasal and Intramuscular Devices Versus a Common Improvised Nasal Naloxone Device. Journal of Clinical Pharmacology, 59(8), 1078–1084. https://doi.org/10.1002/jcph.1401
40. Merlin, M. A., Saybolt, M., Kapitanyan, R., Alter, S. M., Jeges, J., Liu, J., Calabrese, S., Rynn, K. O., Perritt, R., Pryor, P. W. (2010). Intranasal naloxone delivery is an alternative to intravenous naloxone for opioid overdoses. American Journal of Emergency Medicine, 28(3), 296–303. https://doi.org/10.1016/j.ajem.2008.12.009
41. https://www.baxter.ca/sites/g/files/ebysai1431/files/2021-07/Naloxone_EN.pdf
42. Johansson, J., Hirvonen, J., Lovró, Z., Ekblad, L., Kaasinen, V., Rajasilta, O., Helin, S., Tuisku, J., Sirén, S., Pennanen, M., Agrawal, A., Crystal, R., Vainio, P. J., Alho, H., Scheinin, M. (2019). Intranasal naloxone rapidly occupies brain mu-opioid receptors in human subjects. Neuropsychopharmacology, 44(9), 1667–1673. https://doi.org/10.1038/s41386-019-0368-x
43. Ryan, S. A., Dunne, R. B. (2018). Pharmacokinetic properties of intranasal and injectable formulations of naloxone for community use: a systematic review. In Pain management (Vol. 8, Issue 3, pp. 231–245). https://doi.org/10.2217/pmt-2017-0060

44. https://www.azbio.org/insys-therapeutics-announces-results-of-pk-study-assessing-proprietary-intranasal-naloxone-formulations-versus-intramuscular-and-intravenous-naloxone-for-opioid-overdose
45. Yassen, A., Olofsen, E., van Dorp, E., Sarton, E., Teppema, L., Danhof, M., Dahan, A. (2007). Mechanism-Based Pharmacokinetic-Pharmacodynamic Modelling of the Reversal of Buprenorphine-Induced Respiratory Depression by Naloxone A Study in Healthy Volunteers. Clin Pharmacokinet (Vol. 46, Issue 11).
46. Yassen, A., Olofsen, E., Romberg, R., Sarton, E., Teppema, L., Danhof, M., & Dahan, A. (2007). Mechanism-based PK/PD modeling of the respiratory depressant effect of buprenorphine and fentanyl in healthy volunteers. *Clinical Pharmacology and Therapeutics*, *81*(1), 50–58. https://doi.org/10.1038/sj.clpt.6100025
47. Encinas, E., Calvo, R., Lukas, J. C., Vozmediano, V., Rodriguez, M., & Suarez, E. (2013). A predictive pharmacokinetic/pharmacodynamic model of fentanyl for analgesia/sedation in neonates based on a semi-physiologic approach. *Pediatric Drugs*, *15*(3), 247–257. https://doi.org/10.1007/s40272-013-0029-1
48. Lötsch, J., Walter, C., Parnham, M. J., Oertel, B. G., & Geisslinger, G. (2013). Pharmacokinetics of non-intravenous formulations of fentanyl. In *Clinical Pharmacokinetics* (Vol. 52, Issue 1, pp. 23–36). https://doi.org/10.1007/s40262-012-0016-7
49. Singleton, M. A., Rosen, J. I., & Fisher, D. M. (1988). Pharmacokinetics of fentanyl in the elderly. In *Br. J. Anaesth* (Vol. 60). http://bja.oxfordjournals.org/
50. Hengstmann, J. H., Stoeckel, H., & Schuttler, J. (1980). INFUSION MODEL FOR FENTANYL BASED ON PHARMACOKINETIC ANALYSIS. In *Br.J. Anaesth* (Vol. 52). http://bja.oxfordjournals.org/
51. Reilly, C.S., Wood, A.J., and Wood, M. (1985). Variability of fentanyl pharmacokinetics in man: Computer predicted plasma concentrations for three intravenous dosage regimens. *Anaesthesia*, *40*(9), 837–843. https://doi.org/10.1111/j.1365-2044.1985.tb11043.x

52. Christrup, L. L., Foster, D., Popper, L. D., Troen, T., & Upton, R. (2008). Pharmacokinetics, efficacy, and tolerability of fentanyl following intranasal versus intravenous administration in adults undergoing third-molar extraction: A randomized, double-blind, double-dummy, two-way, crossover study. *Clinical Therapeutics*, *30*(3), 469–481. https://doi.org/10.1016/j.clinthera.2008.03.001
53. Schug, S. A., & Ting, S. (2017). Fentanyl Formulations in the Management of Pain: An Update. In *Drugs* (Vol. 77, Issue 7, pp. 747–763). Springer International Publishing. https://doi.org/10.1007/s40265-017-0727-z
54. Sabzghabaee, A. M., Eizadi-Mood, N., Yaraghi, A., & Zandifar, S. (2014). Naloxone therapy in opioid overdose patients: Intranasal or intravenous? A randomized clinical trial. *Archives of Medical Science*, *10*(2), 309–314. https://doi.org/10.5114/aoms.2014.42584
55. Amponsah, S.K., Adams, I. (2023). Drug Absorption via the Nasal Route: Opportunities and Challenges. In: Pathak, Y.V., Yadav, H.K.S. (eds) Nasal Drug Delivery. Springer, Cham. https://doi.org/10.1007/978-3-031-23112-4_3
56. Kaufman RD, Gabathuler ML, Bellville JW. (1981) Potency, duration of action and pA2 in man of intravenous naloxone measured by reversal of morphine-depressed respiration. J Pharmacol Exp Ther 1981; 219: 156–162.
57. Nallani, S. C., Smith, L. T., Uppoor, R. S., Mehta, M. U. (2021). Reversal of high potency synthetic opioid overdose: literature review. FDA Science Forum 2021 Poster, https://www.fda.gov/science-research/fda-science-forum/reversal-high-potency-synthetic-opioid-overdose-literature-review
58. Olofsen, E., van Dorp, E., Teppema, L., Aarts, L., Smith, T.W., Dahan, A., Sarton, E.; Naloxone Reversal of Morphine- and Morphine-6-Glucuronide-induced Respiratory Depression in Healthy Volunteers: A Mechanism-based Pharmacokinetic–Pharmacodynamic Modeling Study. Anesthesiology 2010; 112:1417–1427 https://doi.org/10.1097/ALN.0b013e3181d5e29d

59. Cassel, J. A., Daubert, J. D., & DeHaven, R. N. (2005). [3H]Alvimopan binding to the μ opioid receptor: Comparative binding kinetics of opioid antagonists. *European J. of Pharmacology*, *520*(1–3), 29–36. https://doi.org/10.1016/j.ejphar.2005.08.008
60. Peng, J., Sarkar, S., & Chang, S. L. (2012). Opioid receptor expression in human brain and peripheral tissues using absolute quantitative real-time RT-PCR. Drug and Alcohol Dependence, 124(3), 223–228. https://doi.org/10.1016/j.drugalcdep.2012.01.013
61. https://en.wikipedia.org/wiki/Human_brain

APPENDIX 1. Notation and Glossary of Terms

The general notation used is as follows.

Symbols and subscripts conventions

Subscripts 1,2,… denote the compartment
Subscripts *f* and *b* denote free and bound forms of a drug
N, F, etc. denote the drug (N = naloxone, F = Fentanyl)
C (uppercase) denotes concentration in mass per volume (for instance, $C_1 = N_1/V_1$)
c (lowercase) denotes molar concentrations (mM, μM, nM). It can be used as a subscript or as a variable with a subscript denoting the drug and compartment.
P denotes receptor binding site concentration

Glossary of terms

0,1,2,3; f, r	Denote compartment number (0=nasal, 1=central, 2=peripheral, 3=brain) f=free and b=bound forms
C_0	Naloxone concentration in compartment-0 (mass/vol) =N0/V0
C_1	Naloxone concentration in compartment-1 (mass/vol) =N1/V1
C_2	Naloxone concentration in compartment-2 (mass/vol) = N2/V2
C_{3f}	Naloxone free concentration in compartment-3 (mass/vol) = N3f/V3
C_{3b}	Naloxone bound concentration in compartment-3 (mass/vol) = N3b/V3
C_0	Naloxone concentration in compartment-1 (molarity) = C0/MWN
c_1	Naloxone concentration in compartment-1 (molarity) = C1/MWN
c_2	Naloxone concentration in compartment-2 (molarity) = C3/MWN
c_{3f}	Naloxone free concentration in compartment-3 (molarity) = C3f/MWN
c_{3b}	Naloxone bound concentration in compartment-3 (molarity) = C3b/MWN = P3bc
D	Naloxone dose (mg)
k_{03}	Mass transfer absorption rate constant compartment-0 to compartment-3
k_{12}	Mass transfer exchange rate constant between compartments 1 and 2
k_{13}	Mass transfer exchange rate constant between compartments 1 and 3
k_{3b}	Binding rate constant of naloxone with MOR ($conc^{-1}$ $time^{-1}$)
k_{3r}	Release rate constant of naloxone with MOR ($time^{-1}$)
ke	Elimination rate constant of naloxone from the central compartment
K_{03}	Mass distribution constant between compartments 0 and 3, defined by theoretical equilibrium condition $K_{03}C_0$= (no exchange)
K_{12}	Mass distribution constant between compartments 1 and 2, defined by theoretical equilibrium condition $K_{12}C_1=C_2$ (no exchange)
K_{13}	Mass distribution constant between compartments 1 and 3, defined by theoretical equilibrium condition $K_{13}C_1=C_3$ (no exchange)
MW_N	Molecular weight of naloxone (g/mole)
MW_F	Molecular weight of fentanyl (g/mole)
M_{N0}	Mass of naloxone in compartment-0

M_{N1}	Mass of naloxone in compartment-1
M_{N2}	Mass of naloxone in compartment-2
M_{N3}	Mass of free naloxone in compartment-3
M_{N3b}	Mass of bound naloxone in compartment-3
M_{N3bc}	Naloxone bound concentration in compartment-3 (molarity)—same as c3n
M_{Ne}	Mass of excreted naloxone
P_{3b}	Number of occupied MOR sites (moles)
P_{3f}	Number of free (empty) MOR sites (moles)
P_{3t}	Total MOR binding sites (moles) = P3b + P3f
P_{3bc}	Concentration of occupied MOR sites (molarity)
P_{3fc}	Concentration of free (empty) MOR sites (molarity)
P_{3tc}	Total MOR binding site concentration = P3bc + P3fc
V_0	Volume of compartment-0
V_1	Volume of compartment-1
V_2	Volume of compartment-2
V_3	Volume of compartment-3
fr_{F1}	Fentanyl free fraction in the blood
fr_{N1}	Naloxone free fraction in the blood
k_{F12}	Fentanyl mass transfer rate constant (compartment-1 and -2)
k_{F12}	Fentanyl mass transfer rate constant (compartment-1 and -3)
K_{F12}	Fentanyl distribution constant (compartment-1 and -2)
K_{F13}	Fentanyl distribution constant (compartment-1 and -3)
k_{Fe}	Fentanyl elimination mass transfer rate constant
k_{F3b}	Fentanyl binding rate constant at MORs
k_{F3r}	Fentanyl release rate constant at MORs,
V_{1F}	Fentanyl central compartment volume
V_{2F}	Fentanyl peripheral compartment volume
V_{3F}	Fentanyl brain compartment volume
F_{N1}	Fraction absorbed (nasal to central compartment) for naloxone
F_{N3}	Fraction absorbed (nasal to brain compartment) for naloxone
k_{N01}	Naloxone mass transfer rate constant (nasal to compartment-1)
k_{N03}	Naloxone mass transfer rate constant (nasal to brain)
k_{N12}	Naloxone mass transfer rate constant (compartment-1 and -2)
k_{N13}	Naloxone mass transfer rate constant (compartment-1 and -2)
K_{N12}	Naloxone distribution constant (compartment-1 and -2)
K_{N13}	Naloxone distribution constant (compartment-1 and -3)
k_{Ne}	Naloxone elimination mass transfer rate constant
k_{N3b}	Naloxone binding rate constant at MORs

k_{N3r}	Naloxone release rate constant at MORs
V_{0N}	Naloxone nasal compartment volume
V_{1N}	Naloxone central compartment volume
V_{2N}	Naloxone peripheral compartment volume
V_{3N}	Naloxone brain compartment volume
F_{cr}	Fentanyl critical value

APPENDIX 2. R-code for fentanyl and naloxone model

Fentanyl and Naloxone

2024-02-22

```
install.packages("tidyverse")
```

```
## Installing package into '/cloud/lib/x86_64-pc-linux-gnu-library/4.3'
## (as 'lib' is unspecified)
```

```
install.packages("deSolve")
```

```
## Installing package into '/cloud/lib/x86_64-pc-linux-gnu-library/4.3'
## (as 'lib' is unspecified)
```

```
install.packages("openxlsx")
```

```
## Installing package into '/cloud/lib/x86_64-pc-linux-gnu-library/4.3'
## (as 'lib' is unspecified)
```

```
install.packages("EnvStats")
```

```
## Installing package into '/cloud/lib/x86_64-pc-linux-gnu-library/4.3'
## (as 'lib' is unspecified)
```

```
install.packages("readxl")
```

```
## Installing package into '/cloud/lib/x86_64-pc-linux-gnu-library/4.3'
## (as 'lib' is unspecified)
```

```
library(readxl)
library(deSolve)
library(openxlsx)
library(dplyr)
```

```
##
## Attaching package: 'dplyr'
```

```
## The following objects are masked from 'package:stats':
##
##     filter, lag
```

```
## The following objects are masked from 'package:base':
##
##     intersect, setdiff, setequal, union
```

```
library(EnvStats)
```

```
##
## Attaching package: 'EnvStats'

## The following objects are masked from 'package:stats':
##
##     predict, predict.lm

wb <- read_xlsx(path="Parameter ranges 100 output.xlsx")
datapr <- read_excel("Parameter ranges 100 output.xlsx", sheet = 1, ran
ge = "A1:AB2")
parm_val<- as.matrix(datapr)
print(parm_val)

##          fr_F1   fr_N1    k_F12    k_F13     K_F12    K_F13     k_Fe
   k_F3b
## [1,] 0.1228866 0.50902 1015.045 11.71936 0.8520223 2.332139 382.5261
 6197.306
##        k_F3r    V_1F     V_2F      F_N1      F_N3    k_N01       k_N
03
## [1,] 8.699147 9.35216 287.7599 0.3277552 0.4954297 1.146603 0.006757
631
##         k_N12    k_N13     K_N12     K_N13     k_Ne   k_N3b   k_N3r
     V_0N
## [1,] 1229.532 1.826812 0.4915135 0.4000497 314.6411 72932.38 140.617
9 0.3338698
##          V_1N     V_2N      V_3      P_3t      F_cr
## [1,] 83.13529 231.1986 1.192162 0.01603567 0.7705217

ChangeofMass <- function(t,x,parms){
  M_F1 <- x[1]
  M_F2 <- x[2]
  M_F3b <- x[3]
  M_F3r <-x[4]
  M_Fe <- x[5]
  C_F1 <- xTaken froi]
  C_F2 <- x[7]
  C_F3f <- x[8]
  C_F3b <-x[9]
   M_N0 <- x[10]
  M_N1 <- x[11]
  M_N2 <- x[12]
  M_N3b <- x[13]
  M_N3r <-x[14]
  M_Ne <- x[15]
  C_N0 <- x[16]
  C_N1 <- x[17]
  C_N2 <- x[18]
  C_N3f <- x[19]
```

```
 C_N3b <-x[20]
 D_F <- parms["D_F"]
 D_N <- parms["D_N"]
 MW_F <- parms["MW_F"]
 MW_N <- parms["MW_N"]
 fr_F1 <- parms ["fr_F1"]
 fr_N1 <- parms ["fr_N1"]
 k_F12 <- parms["k_F12"]
 k_F13 <- parms["k_F13"]
 K_F12 <- parms["K_F12"]
 K_F13 <- parms["K_F13"]
 k_Fe <- parms["k_Fe"]
 k_F3b <- parms["k_F3b"]
 k_F3r <- parms["k_F3r"]
 V_1F <- parms["V_1F"]
 V_2F <- parms["V_2F"]
 F_N1 <- parms["F_N1"]
 F_N3 <- parms["F_N3"]
 k_N01 <- parms["k_N01"]
 k_N03 <- parms["k_N03"]
 k_N12 <- parms["k_N12"]
 k_N13 <- parms["k_N13"]
 K_N12 <- parms["K_N12"]
 K_N13 <- parms["K_N13"]
 k_Ne <- parms["k_Ne"]
 k_N3b <- parms["k_N3b"]
 k_N3r <- parms["k_N3r"]
 V_0N <- parms["V_0N"]
 V_1N <- parms["V_1N"]
 V_2N <- parms["V_2N"]
 V_3 <- parms["V_3"]
 P_3t<- parms["P_3t"]
  F_cr <- parms["F_cr"]



  c_F3b = M_F3b/(V_3*MW_F)
  c_N3b = M_N3b/(V_3*MW_N)
  P_3b = c_N3b + c_F3b # unit is umol/L
  P_3f= P_3t-P_3b


 dM_F1dt=  -k_F12*((fr_F1*M_F1/V_1F)-(M_F2/(K_F12*V_2F)))-k_F13*((fr_F1
*M_F1/V_1F)-(M_F3f/(K_F13*V_3)))-k_Fe*(fr_F1*M_F1/V_1F)

 dM_F2dt= k_F12*((fr_F1*M_F1/V_1F)-(M_F2/(K_F12*V_2F)))
```

```
 dM_F3fdt= k_F13*((fr_F1*M_F1/V_1F) - (M_F3f/(K_F13*V_3))) - (k_F3b*(M_
F3f/(V_3*MW_F))*(P_3f) - k_F3r*(M_F3b/(V_3*MW_F)))*(V_3*MW_F)

dM_F3bMdt= (k_F3b*(M_F3f/(V_3*MW_F))*(P_3f) - k_F3r*(M_F3b/(V_3*MW_F)))
*(V_3*MW_F)

dM_Fedt= k_Fe*(fr_F1*M_F1/V_1F)

dC_F1dt=dM_F1dt/V_1F
dC_F2dt=dM_F2dt/V_2F
dC_F3fdt=dM_F3fdt/V_3
dC_F3bdt=dM_F3bdt/V_3

 a=1000
 ti_1= 0.0833
   ti_2=0.1
   ti_3=105
   ti_4=110
 dM_N0dt= -k_N01*(M_N0/V_0N)-k_N03*(M_N0/V_0N) + (F_N1*D_N * a / sqrt(p
i)) * ( exp(-a^2*(t-ti_1- 1/a)^2)  + exp(-a^2*(t-ti_2-1/a)^2)+ exp(-a^2
*(t-ti_3-1/a)^2) + exp(-a^2*(t-ti_4+1/a)^2) )

 dM_N1dt= k_N01*(M_N0/V_0N)-k_N12*((fr_N1*M_N1/V_1N)-(M_N2/(K_N12*V_2N)
))-k_N13*((fr_N1*M_N1/V_1N)-(M_N3f/(K_N13*V_3)))-k_Ne*(fr_N1*M_N1/V_1N)

 dM_N2dt= k_N12*((fr_N1*M_N1/V_1N)-(M_N2/(K_N12*V_2N)))

 dM_N3fdt= k_N03*(M_N0/V_0N) + k_N13*((fr_N1*M_N1/V_1N) - (M_N3f/(K_N13
*V_3))) - (k_N3b*(M_N3f/(V_3*MW_N))*(P_3f) - k_N3r *(M_N3b/(V_3*MW_N)))
*(V_3*MW_N)

dM_N3bMdt= (k_N3b*(M_N3f/(V_3*MW_N))*(P_3f) - k_N3r*(M_N3b/(V_3*MW_N)))
*(V_3*MW_N)

dM_Nedt= k_Ne*(fr_N1*M_N1/V_1N)

dC_N0dt=dM_N0dt/V_0N
dC_N1dt=dM_N1dt/V_1N
dC_N2dt=dM_N2dt/V_2N
dC_N3fdt=dM_N3fdt/V_3
dC_N3bdt=dM_N3bdt/V_3

# Mass balance
M_Ft = M_F1 + M_F2 + M_F3f + M_F3b + M_Fe
```

```
M_Nt = M_N0 + M_N1 + M_N2 + M_N3f + M_N3b + M_Ne

dxdt <- c(dM_F1dt, dM_F2dt, dM_F3fdt, dM_F3bdt,dM_Fedt, dC_F1dt, dC_F2d
t, dC_F3fdt, dC_F3bdt, dM_N0dt, dM_N1dt, dM_N2dt, dM_N3fdt, dM_N3bdt,dM
_Nedt, dC_N0dt, dC_N1dt, dC_N2dt, dC_N3fdt, dC_N3bdt )

list(dxdt)
}


parms= c( D_F=500, D_N=4000, MW_F=336.47 , MW_N=327.37, parm_val[1,1],
parm_val[1,2], parm_val[1,3], parm_val[1,4], parm_val[1,5], parm_val[1,
6], parm_val[1,7], parm_val[1,8], parm_val[1,9], parm_val[1,10], parm_v
al[1,11], parm_val[1,12], parm_val[1,13], parm_val[1,14],parm_val[1,15]
, parm_val[1,16], parm_val[1,17], parm_val[1,18], parm_val[1,19], parm_
val[1,20], parm_val[1,21], parm_val[1,22], parm_val[1,23], parm_val[1,2
4], parm_val[1,25], parm_val[1,26], parm_val[1,27], parm_val[1,28])

times= c(seq(from=0, to=1, by=1/60),seq(1,3,by=5/60))

parmdf<-data.frame( rbind(parms))

xstart= c(M_F1=parmdf$'D_F', M_F2=0, M_F3f=0, M_F3b=0, M_Fe=0, C_F1=par
mdf$'D_F'/parmdf$'V_1F', C_F2=0, C_F3f=0, C_F3b=0, M_N0=0 , M_N1=00, M_
N2=0, M_N3f=0, M_N3b=0, M_Ne=0, C_N0=0, C_N1=0, C_N2=0, C_N3f=0, C_N3b=
0)


out <- data.frame(ode(xstart,times,ChangeofMass,parms,method="lsoda"))

colnames(out) = c("Time_hrs", "M_F1", "M_F2", "M_F3f", "M_F3b", "M_Fe",
 "C_F1", "C_F2", "C_F3f", "C_F3b", "M_N0" , "M_N1", "M_N2", "M_N3f", "M
_N3b", "M_Ne", "C_N0", "C_N1", "C_N2", "C_N3f", "C_N3b")

head(out)

##     Time_hrs     M_F1      M_F2     M_F3f    M_F3b      M_Fe     C_F
1
## 1 0.00000000 500.0000   0.00000 0.0000000 0.0000000   0.00000 53.463
58
## 2 0.01666667 370.3072  92.48064 0.5434302 0.5382664  36.13045 39.595
90
## 3 0.03333333 279.5836 155.42255 0.6185743 1.2486387  63.12666 29.895
08
## 4 0.05000000 216.0122 197.80531 0.6378049 1.8163646  83.72829 23.097
58
```

```
## 5 0.06666667 171.3674 225.88524 0.6531288 2.2494615  99.84472 18.323
84
## 6 0.08333333 139.9180 244.02180 0.6715832 2.5816186 112.80699 14.961
04
##        C_F2     C_F3f    C_F3b          M_N0          M_N1
M_N2
## 1 0.0000000 0.0000000 0.0000000  0.000000e+00  0.000000e+00  0.00000
0e+00
## 2 0.3213813 0.4558357 0.4515043  0.000000e+00  0.000000e+00  0.00000
0e+00
## 3 0.5401120 0.5188675 1.0473732  0.000000e+00  0.000000e+00  0.00000
0e+00
## 4 0.6873971 0.5349984 1.5235885  0.000000e+00  0.000000e+00  0.00000
0e+00
## 5 0.7849783 0.5478523 1.8868754 2.816893e-121 1.205115e-123 3.753311
e-182
## 6 0.8480050 0.5633321 2.1654928  1.123611e+02  1.250063e-01  2.68868
8e-04
##           M_N3f        M_N3b          M_Ne          C_N0          C_
N1
## 1  0.000000e+00  0.000000e+00  0.000000e+00  0.000000e+00  0.000000e
+00
## 2  0.000000e+00  0.000000e+00  0.000000e+00  0.000000e+00  0.000000e
+00
## 3  0.000000e+00  0.000000e+00  0.000000e+00  0.000000e+00  0.000000e
+00
## 4  0.000000e+00  0.000000e+00  0.000000e+00  0.000000e+00  0.000000e
+00
## 5 7.102480e-126 4.753567e-183 9.697750e-183 8.437099e-121 1.449583e-
125
## 6  6.171077e-04  1.213336e-04  6.899778e-05  3.365416e+02  1.503649e
-03
##            C_N2         C_N3f        C_N3b
## 1  0.000000e+00  0.000000e+00  0.000000e+00
## 2  0.000000e+00  0.000000e+00  0.000000e+00
## 3  0.000000e+00  0.000000e+00  0.000000e+00
## 4  0.000000e+00  0.000000e+00  0.000000e+00
## 5 1.623414e-184 5.957646e-126 3.987349e-183
## 6  1.162934e-06  5.176373e-04  1.017761e-04
```

```
all_outputs=data.frame(out)
write.xlsx(all_outputs, 'Conc-Time profile for IV Fentanyl and Naloxone
 3C ODE in R model2.xlsx')

c_F3bM = out$'C_F3b'/ parmdf$'MW_F'
c_N3bM = out$'C_N3b'/ parmdf$'MW_N'
P_3bM = c_N3bM + c_F3bM
```

```
  #fraction of free receptor
  c_F3bM_Frac= c_F3bM/parmdf$'P_3tM'
  c_N3bM_Frac= c_N3bM/parmdf$'P_3tM'
    P_3fM_Frac= (parmdf$'P_3tM'-P_3bM)/parmdf$'P_3tM'
    Total_Pt= c_F3bM_Frac+c_N3bM_Frac+P_3fM_Frac
   vent_supp= ((1+ parmdf$'F_cr') * c_F3bM_Frac)/(parmdf$'F_cr'+ c_F3bM
_Frac)
    Vent_resc= (1- vent_supp)
out4=cbind(all_outputs,c_F3bM,c_N3bM,c_F3bM_Frac,c_N3bM_Frac,P_3fM_Frac
,Total_Pt,vent_supp,Vent_resc)

df1<-data.frame(cbind(parms))
df2<-data.frame(cbind(xstart))
wb1 <- loadWorkbook("Pop_Simulation of Fentanyl and Naloxone with UIF3.
xlsx")

writeData(wb1, sheet = "Sheet 1 (4)", df1, startRow=1, startCol=37, row
Names=T, colNames = T)
writeData(wb1, sheet = "Sheet 1 (4)", df2, startRow=1, startCol=40, row
Names=T, colNames = T)
writeData(wb1, sheet = "Sheet 1 (4)", out4, startRow=1, startCol=1, col
Names = T)
saveWorkbook(wb1,"Pop_Simulation of Fentanyl and Naloxone with UIF4.xls
x",overwrite = T)
```

RESUME

Jasmin Akther Hossain

2067 Burlington Columbus Rd
Bordentown, NJ- 08505, USA
(718)-844-6619
jasmin.hossain@my.liu.edu
https://www.linkedin.com/in/jasminahossain/

Ph.D. in Pharmaceutics Science with specialization in PK/PD and physiological-based modeling and simulations. My doctoral research was a pioneering effort to develop a PBPK (physiologically based pharmacokinetic) model for intranasal naloxone and fentanyl displacement from brain receptors, all programmed using the versatile R language.

QUALIFICATIONS

- Experienced in model development and diagnostic using SimCyp, Phoenix NLME, and WinNonlin software
  - Physiological-based PKPD studies in special populations: pediatric, geriatric, and renal failure patients.
  - Simcyp online workshop- Pediatrics: Physiology and ontogeny, DDI, Pediatric drug absorption, and Preterm PBPK.
  - Drug interaction studies using Simcyp: Capstone project on Verapamil and digoxin drug interaction.
  - Noncompartmental analysis (NCA) using Phoenix WinNonlin
  - Workshop on Phoenix NLME: Continuous and Categorical covariates, Non-linear disposition, Time-dependent PK, PK transit compartments, Allometric scaling, Emax model, PD transit compartments, TMDD.
  - Basics of PML language
- Experienced in Data Science with R programming, Posit Cloud, R-Markdown
  - Physiologically based pharmacokinetic (PBPK) model development, evaluation, and programming in R using ordinary differential equation solver
  - Data analysis and visualization by R

Skills

- Excellent communication skills and capability of multitasking.
- Skilled in scientific writing and professional presenting
- Strong analytical and problem-solving skills
- Data analysis (pharmaceutical and clinical data)
- Experience in Google Data Analytics Professional Certificate Course: SQL, Tableau, Data Analysis, and Data Visualization using R.
- Data Analysis in Health Care with Marc Voorhees (ELVTR)

Research experience

Long Island University, Brooklyn, NY
Doctorate Dissertation Project Oct 2022-May2024

- Performed PBPK modeling analysis of naloxone.
- Constructed a PBPK model for intranasal naloxone.
- Modeled PBPK with opioid agonist (Fentanyl) and antagonist (Naloxone) binding and release with MOR receptors in the Brain.
- Constructed different tissue compartments involved with naloxone and fentanyl disposition, wrote and solved the system of differential equations with constraints.
- Evaluated model and equations using R and PK-Solver®
- Modeled and evaluated population simulation for fentanyl overdose and naloxone rescue.

Southern University, Bangladesh, Chittagong
Master Thesis Project

- Performed analysis of plant extracts, including pharmacological and toxicological evaluation.
- Plant extract effects on Microbes and Animals.

Education

- **Ph.D. in Pharmaceutics** (Jan 2015 – May 2024)
  Long Island University, LIU Pharmacy, Brooklyn, NY
  Doctoral Dissertation: Developing a PBPK Model for Intranasal Naloxne and Opioid Displacement from Brain Receptors

  Courses: PBPK Modeling and Simulation, Pharmacokinetics, Advanced Biopharmaceutics, Pharmacogenomics, Drug Metabolism, Polymer Science, Dosage Form Design, Solid State Characters, Pharmaceutical Analysis, Biostatistics, Physical Pharmacy, Industrial Pharmacy, Pharmaceutical Regulatory

- Master of Pharmacy (M. Pharm.):
  Southern University Bangladesh, Chittagong (2010-2011)
- Bachelor of Pharmacy (B. Pharm.):
  Southern University Bangladesh, Chittagong (2006-2009)

Work experience

- Teaching assistant, Division of Pharmaceutical Science, LIU Pharmacy, Brooklyn, NY (Summer 2015- Fall 2019)
- Lecturer, Dept. of Pharmacy, Southern University Bangladesh (Jan 2011 - Oct 2013)

References
Available upon request